GEOLOGICAL SURVEY OF CANADA
OPEN FILE 6764

Development of a GIS-based System for Assessment of Discovery Potential Using an Expert-Defined VMS Deposit Model and Digital Geological Maps

C. Chung, J.M. Franklin, and E.M. Hillary

2011

Natural Resources Canada Ressources naturelles Canada

Canada

GEOLOGICAL SURVEY OF CANADA
OPEN FILE 6764

Development of a GIS-based System for Assessment of Discovery Potential Using an Expert-Defined VMS Deposit Model and Digital Geological Maps

C. Chung, J.M. Franklin, and E.M. Hillary

2011

doi:10.4095/288205

This publication is available from the Geological Survey of Canada Bookstore (http://gsc.nrcan.gc.ca/bookstore_e.php).
It can also be downloaded free of charge from GeoPub (http://geopub.nrcan.gc.ca/).

Recommended citation:
Chung, C., Franklin, J.M., and Hillary, E.M., 2011. Development of a GIS-based System for Assessment of Discovery Potential Using an Expert-Defined VMS Deposit Model and Digital Geological Maps; Geological Survey of Canada, Open File 6764, 69 p. doi:10.4095/288205

Publications in this series have not been edited; they are released as submitted by the author.

Development of a GIS-based System for Assessment of Discovery Potential Using an Expert-Defined VMS Deposit Model and Digital Geological Maps

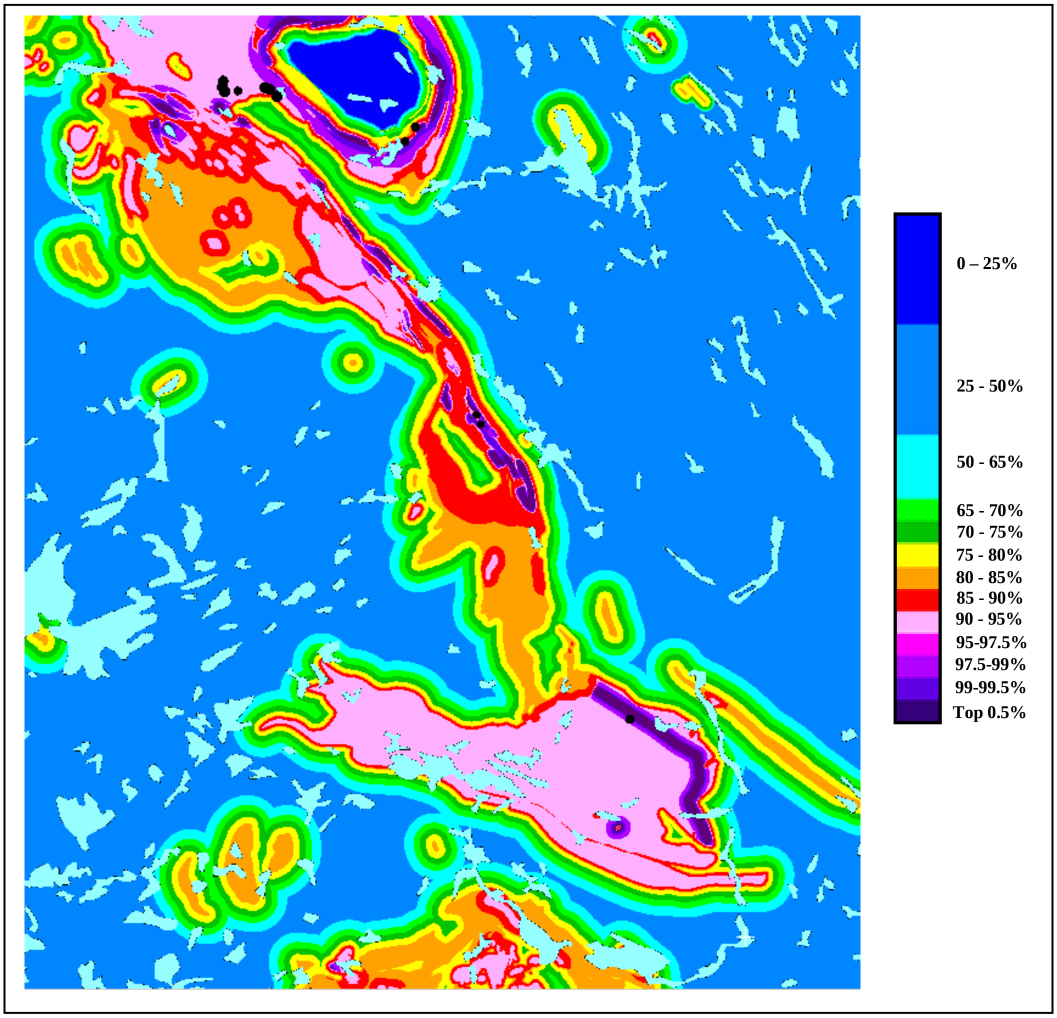

Chang-Jo Chung, James M Franklin and Elizabeth Hillary

2011

Executive Summary, Recommendations and Next Steps

This work was done under **Contracts # 35-MGM011655W and #35-MGM012081W.**

In this study, we attempt to develop a robust, digitally-based and expert-driven system for assessing the potential for discovery of new mineral resources in Canada's north.

We try to:

1) establish a *spatially*-based method for determining the potential for discovery
2) establish a *statistically robust* method for determining the uncertainty of this measure of potential.

Important factors:

1) Increasingly, newly discovered deposits are buried deeply and may not have a surface expression or "footprint".
2) Most of northern Canada has been mapped geologically at very broad scales, but little has been recently mapped, or mapped with sufficient detail to encourage exploration.
3) Much of the mapping predates the development of a modern understanding of the key criteria that are necessary to target mineral exploration.
4) Key geological processes associated with the formation of mineral deposits produced physical or chemical characteristics whose "signatures" should be geologically mappable features that may be observable on a geological map.

We used:

1) existing digital maps
2) a prioritized list of key criteria for one specific deposit type, volcanogenic massive sulfide deposits, that could be identified on these maps.

Method

1: The methodology developed for this report has successfully identified areas of highest potential for discovery of VMS deposits. It was applied without including the knowledge of the location of these deposits, and successfully "found" the majority of them. From any point on a map sheet (pixel in digital terms) we measured the distance to the nearest observation of each of the key criteria. The value of each criterion (which was already modified by our uncertainty as to the quality of it, both for its genetic criticality and "correctness" of map identification) is reduced (decayed) as a non-linear function of the distance from that observation. The reduced values of these key criteria are then summed at each point on the map, and after evaluation of all of the pixels, the values are contoured.

2: The digital geological maps that we used for this method development required some preparation. Specifically, the legends had to be parsed to identify the principal rock types. In the case of the Hackett River map, the oldest compilation that we used (Frith, 1987), all of the geological attributes were identified in the legend except for subvolcanic intrusions; these were assigned on the basis of form, stratigraphic position and composition. Newer maps (Whitehills, Slave compilation) contained information in the descriptive fields that enabled us to assign rock types quite reliably. However, these assignments still required some interaction by the user, as some of the most significant information (e.g. qualifiers for intrusions, identifiers for exhalite) was contained with text-field descriptions, and had to be manually extracted. In future, the less data manipulation required, the more objective the assessment will be.

3: The list of key criteria that we used are based on expert knowledge of the specific deposit type, both from genetic and exploration aspects. In preparing this list, we recognized that some criteria have a more uncertain relationship to the genesis of this deposit type than do others, and also that some criteria may not have a direct relationship to the deposit genesis, but are a manifestation of key genetic attributes that otherwise would not be evident on a map. For example, exhalite that is generally related to VMS deposits would rarely be specifically identified on a geological map. However, key lithotypes, such as chert, sulfidic sedimentary rocks, or banded iron formation are commonly displayed on maps. The certainty of assigning these to the potential presence of deposits is significant, so we use a higher measure of uncertainty when including their presence as par of our evaluation methodology. Also, in the case of exhalite, deposits need not occur specifically where they are observed, but generally are within a few hundred meters of them, so we established a “decay function” that reduced the value of this observation as a function of the distance from it to our observation point. In one case, major underpinning subvolcanic intrusions, the best potential for VMS deposits is at least 500m, and as much as 4 km away from them. In this case, we established a non-linear decay function that reflects that the best potential is in an “envelope” that does not coincide with the intrusion. We found that determining the best weighting factors and decay functions for each criterion was best done iteratively using a well-understood test area. However, those weighting and decay factors determined by the expert group generally were close to those used in the final evaluation method.

4: Our list of key criteria included some attributes that we did not use. Some of these, such as alteration attributes, are not uniformly noted on maps, and thus we avoided using them. These also include geophysical attributes, and lithogeochemical data. Both of these require that the data be prepare in a way in which they can be assessed using our technology. In order to do that, these data sets need to be compiled and tested in the same manner as were the geological maps.

Recommendations

1: All future digital map products should have a legend that separates information on age, primary lithology, and secondary attributes such as volcanological style, alteration or significant stratigraphic information (e.g. submarine volcanic, pyroclastic volcanic, subaerial volcanic or sedimentary, subvolcanic intrusive, syntectonic intrusive etc.) placed in separate columns. This will reduce the amount of interpretation and map preparation required prior to using any form of digital resource assessment technology. Also, linear elements in the geology (e.g. faults, with sense of motion of possible, thin bands of exhalite, dykes) need also to be included in the same data set. Currently these are commonly separated into separate files, adding steps to the process used to prepare the data for “pixel” rendering. The unified hierarchical legend system being prepared by Peter Davenport will meet these requirements.

2: Key criteria used for this evaluation must be evident on a geological map that will be used for evaluation purposes. The uncertainties assigned to the value of each criterion are best established by experts in the genetic attributes and exploration for this deposit type. <u>We</u>

recommend that the best set of criteria should be established by experts in the field, and adjusted through a testing procedure.

3: The "decay function" or way in which the presence of a criterion is decayed as a function of distance to the observation of it, was established first on an expert basis, and refined through use of a test case (with known deposits) to establish the best factors to use. We recommend that for each deposit type, one or two test areas, which contain well established deposits and most of the key criteria that will be used for evaluation, be used to develop the best set of uncertainty and decay factors.

4: In future we recommend that digital geological data sets being used for resource potential assessment include geophysical compilations and petrochemical data sets. The latter are available for many of the Provinces, but are not available in Yukon, NWT or Nunavut.

Next steps:

1: Continue to refine the methodology for assessing the potential for discovery of VMS deposits. Include additional criteria, and develop methods for integrating them into the methodology develop herein.

2: Build criteria lists and digital technology to assess the potential for discovery of other deposit types. Our priority order for assessing the Canadian Shield is:

A: Orogenic and other gold deposit types: a preliminary list of key criteria has been prepared, and will be used to test an area with established resources
B: Magmatic Cu-Ni-PGE-Cr deposits
C: All types of uranium deposits that occur in Canada
D: Sedex deposits
E: Iron oxide-copper-gold deposits
F: Silver vein deposits

Some deposit types are much more abundant in Phanerozoic orogens and cratonic covered areas. In order to apply the methodology to areas that are more typically outside of the Canadian Shield, the discovery potential for the following deposit types need to be assessed:

A: Copper ± molybdenum ± gold porphyry systems
B: Skarn deposits
C: Low- and high-sulfidation epithermal deposits
D: Mississippi-Valley Pb-Zn deposits
E: Granite-hosted tin deposits

3: Make the software developed for this assessment process more user-friendly.

1.0 Introduction

We were asked by the Geological Survey of Canada (GSC) to investigate the possibility of developing a robust, digitally-based and expert- driven system for assessing the potential for discovery of new mineral resources in Canada's north. The desired outcomes are to not only attempt to establish a *spatially*-based method for establishing the potential for discovery, but also to establish a *statistically robust* method for determining the uncertainty of this measure of potential. These outcomes will help to lay a framework for decision-making by the Geological Survey as to the priorities for obtaining new geoscience information to underpin the social and economic development of the north. Having determined that some areas have higher potential for discovery of new resources than others, decision makers in the GSC must also know the quality of the information that underpins this assessment. Areas with high potential that also have high uncertainty in the quality of their information are those that presumably will rank highest for establishing new regional geoscience initiatives.

Our team consisted of Dr Chang-Jo Chung, retired senior statistician with the Geological Survey, Dr James Franklin, retired Chief Geoscientist for Natural Resources Canada, and Ms Elizabeth Hillary, currently a resource analysis specialist at the GSC. We were assisted by Dr Jeff Harris, Ms Diane Paul, Dr Alan Galley, and members of the Mineral Deposits subdivision, including Benoit Dube, Charlie Jefferson, Suzanne Paradis, Louise Corriveau, Wayne Goodfellow, Jan Peter and retired former members of that subdivision including Drs. Don Sangster, David Sinclair, and Roger Eckstrand. Discussions with Drs. Lesley Chorlton, Marc St Onge, Chris Harrison, Simon Hanmer and others in the GSC were of considerable help, particularly in laying the framework for future gathering of geological data in a more useful format for resource assessment work by industrial as well as government agencies.

2.0 Statement of the Problem and Project Objectives

One of the key objectives of research by specialists in mineral resource geology at the GSC and Canadian Universities has been to establish precise criteria for explaining the occurrence of metallic and precious metal resources. Economically-recoverable mineral deposits have a "footprint" or surface expression of about 0.2 to 5.0 km^2. Given that Canada's landmass exceeds 10 million km^2, these are almost infinitely small targets for discovery. An added complexity to the prediction for discovery of new resources is that increasingly newly discovered deposits are buried deeply and do not have a surface expression or "footprint" at all. If Canada is to remain preeminent in the provision of high-value metals and minerals, it must continue to refine its methodology for discovery. Underpinning new discovery is the provision of high-quality geoscience information that is sufficiently robust to attract investment from the private sector into exploration and development of new resources. Canada's north has excellent potential for such discoveries. Most of it has been mapped geologically at very broad scales, but little has been recently mapped, or mapped with sufficient detail to encourage exploration. Moreover, much of the mapping predates the development of a modern understanding of the key criteria that are necessary to target mineral exploration.

The prediction of the potential for discovery of mineral deposits is based largely on the practical application of mineral deposits models. Such models are based on the interpretation of information gathered about the process, by which a particular accumulation of metals became concentrated in one place in the earth's crust. Most metals must be concentrated by a factor of at least 1000 in order to be economically recoverable. A unique set of circumstances or processes must be operating to enable this concentration process to take place. Understanding what the circumstances of these processes might have been requires a certain amount of "reverse engineering", in which the product, an ore deposit, provides information, obtained through intensive research, about the set of processes that must be coincident in order for metals to be so concentrated. To be of practical value, some of those key processes produced physical or chemical characteristics whose "signatures" should be manifest as geologically mappable features that may be observable on a geological map. The collection of the manifestations of these processes, which may include the presence of key rock types, key structures, and the mappable signatures of key paleo-thermal conditions, become the key elements of a mineral deposits model. It is these features that we will use to develop a set of prioritized geological criteria that, if observed in a regional geological data set, will indicate good potential for resource discovery.

Thus the objective of this project is to assess the possibility of establishing a statistically robust method for predicting the potential for discovery of economically-recoverable mineral deposits, using a combination of existing maps and a prioritized list of key criteria for one specific deposit type, volcanogenic massive sulfide deposits, which could be identified on these maps. A second objective is to develop a method to assess the quality or uncertainty of the resource prediction.

3.0 Background

Assessing the potential for discovery of resources has been an important component of publically funded geological surveys since most of these surveys were founded. Since the first significant discoveries of gold in the Appalachian, Shield and Cordilleran regions of Canada were made in the 1800's and early 1900's, geologists have been trying to establish sets of criteria for finding additional hidden resources. Virtually every geological report produced by the GSC and Canada's Provincial geological surveys contains a section outlining the resource heritage and important controls on mineralization in that specific region.

The Geological Survey of Canada has undertaken many exercises in determining the resource potential of various regions of Canada. Two of these, Operation September I and II, were conducted in 1972 and 1995 (Sangster, 2007), and were used primarily for planning purposes for program structure and deployment. Other assessments (Yukon, proposed National Parks) were directed at assessing the potential for discovery in regions either where alternate use strategies were under consideration or where economic stimulus was needed. In all cases these assessments were done somewhat subjectively. Mineral deposits experts were asked to indicate their assessment of the potential for discovery, based on existing resource inventories, presence of "permissive" geological attributes, and current knowledge of mineral deposits models. These were completed by examining geological maps, all available data sets (including geophysical and geochemical surveys), and lists of all deposits for which a resource estimate of some form was available. These data, combined with personal knowledge of the regions, were somewhat subjectively combined to provide an estimate of potential value for these regions. The results were provided as a series of maps, spreadsheets and reports, most of which were not public. An example of one such map is in Figure 1.

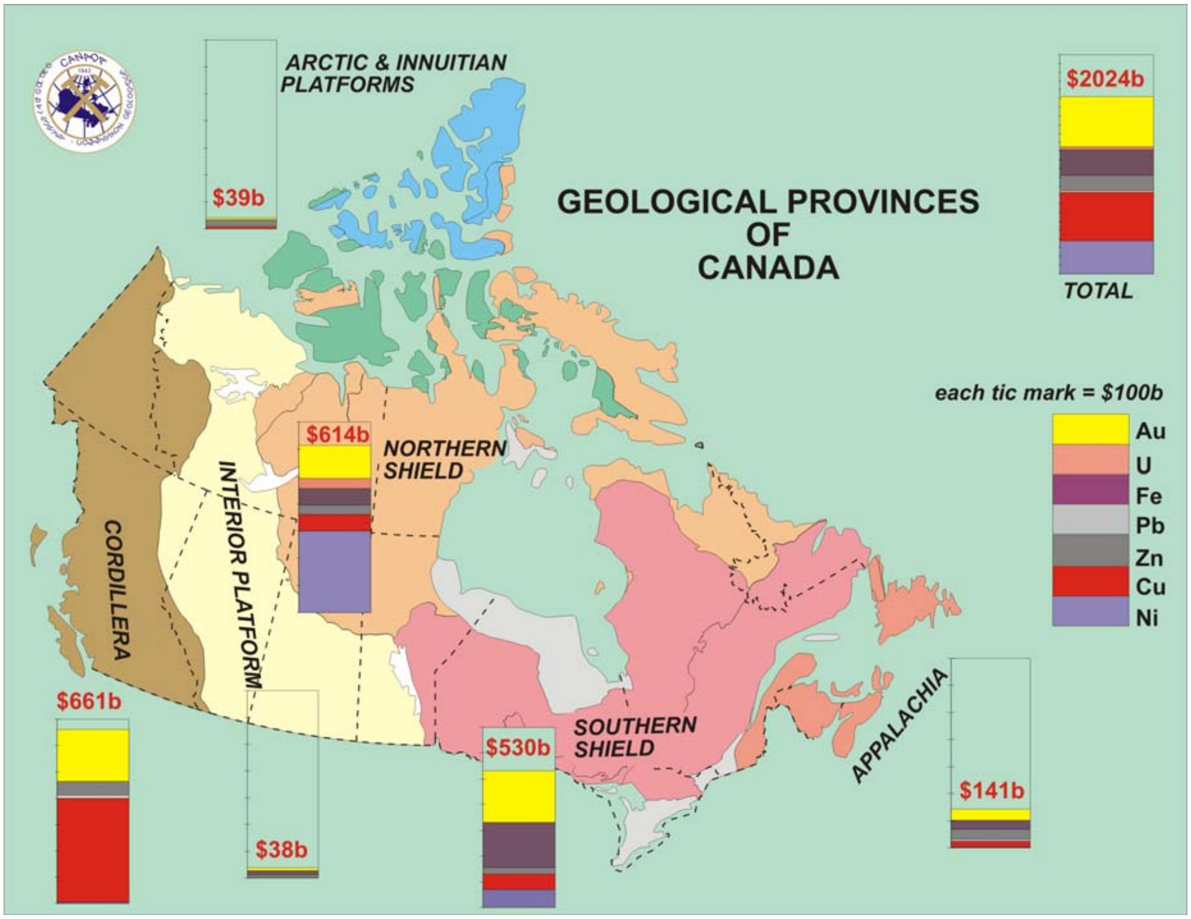

Figure 1: An estimate (in 1995 dollars) of the potential for discovery of important commodities in Canada (from Operation September II, unpublished).

Figure 1 illustrates the summary results of an expert-driven regional assessment of potential for discovery of key commodities in Canada. The experts had extensive knowledge of both the geology of various regions of Canada, and the characteristics of ore deposit types that contain these commodities; the analysis was not undertaken in a statistically rigorous manner, but rather through a somewhat more subjective approach in which permissive regions (i.e. those that had the generally correct geological characteristics to permit the possibility of discovery) were assessed for their potential by applying a priori tonnage-grade models. While these estimates have value, they are best used at a very broad scale (e.g. major geological provinces, as shown in Figure 1). We now need a more statistically robust, and more scale – independent method of approaching this type of analysis, ideally requiring less input from experts in the mineral deposits field. In addition, we are attempting to predict potential for discovery, not potential for exploitation of the existing inventory of resources. Although neither Operation September I or II were ever published, excellent summaries of them may be found in Leech, (2007) and Sangster, (2007).

Some of the earliest formalized techniques for assessing resources started with the development of the “McKelvey Box” (McKelvey, 1972), a two-dimensional scheme that combines criteria of increasing geologic assurance (undiscovered /possible/ probable/proved reserves) with those of increasing economic feasibility (sub-economic "resources" as compared with economic "reserves") for classifying resources in terms of the robustness of their resource estimates; this did not address the issue of resource potential. Resource estimation methods were further developed in the United States Geological Survey (USGS) by Singer and colleagues, as exemplified in Singer and Kouda, (2003) and references therein. The USGS then adopted a set of simplified descriptive models that described the key characteristics of many ore deposit types. Similar models were also developed by the British Columbia Geological Survey for resources in that province. More extensive models were provided for Canadian deposits in Eckstrand et al., (1995) and Goodfellow, (2007), and on a world-wide basis by Hedenquist et al., (2005). None of these attempted to prioritize the value of the criteria that explain the presence of deposits. The aforementioned examples of resource assessment were all “expert – driven”, but none were statistically based, other than to estimate tonnage-grade distribution for specific ore deposit types, and none attempted to evaluate with any statistical rigor the potential for discovery by using digital maps and prioritized, digitally represented key criteria for each deposit type.

4.0 Approach

Our first challenge was to develop a list of key criteria for a single deposit type, the VMS type, which could be reasonable expected to be observed and recorded on geological maps. We then assigned a weighting value to each criterion, which reflects the criticality of that criterion to explaining the presence of a deposit. In other words, we incorporated a value that represents the uncertainty that a particular criterion must be present in order to predict the presence of deposits. Our second challenge was to use existing digital (or digitized) geological maps on which the criteria (or at least some of them) described in the “key characteristics list” might be appropriately quantized, and thus found during some form of quantitative analysis. Once the list and the map were prepared digitally, then we planned to develop a methodology for intersecting the map with the list, and determining, from any point on a map “sheet” the distance to the presence of any one of the criteria. By applying some form of function that relates the distance to the presence of the observed criteria to the “value” of the likelihood of discovering the VMS deposit, we hoped to “integrate” the derived values for each criterion into a single value. This value indicates a measure of the likelihood of discovering the VMS deposit for a point on the map by following the description of the deposit model. At the same time, by incorporating the various uncertainties in the conversion, the model and the quality of the map information, we also planned to define the uncertainty of the integrated value, which will enable us to evaluate the quality of the resource assessment.

4.1 Prioritized List of Key Criteria for VMS deposits.

The geological model for VMS deposits is amongst the most rigorously established amongst all deposit types. This is in part because of exhaustive research into the processes attendant on the

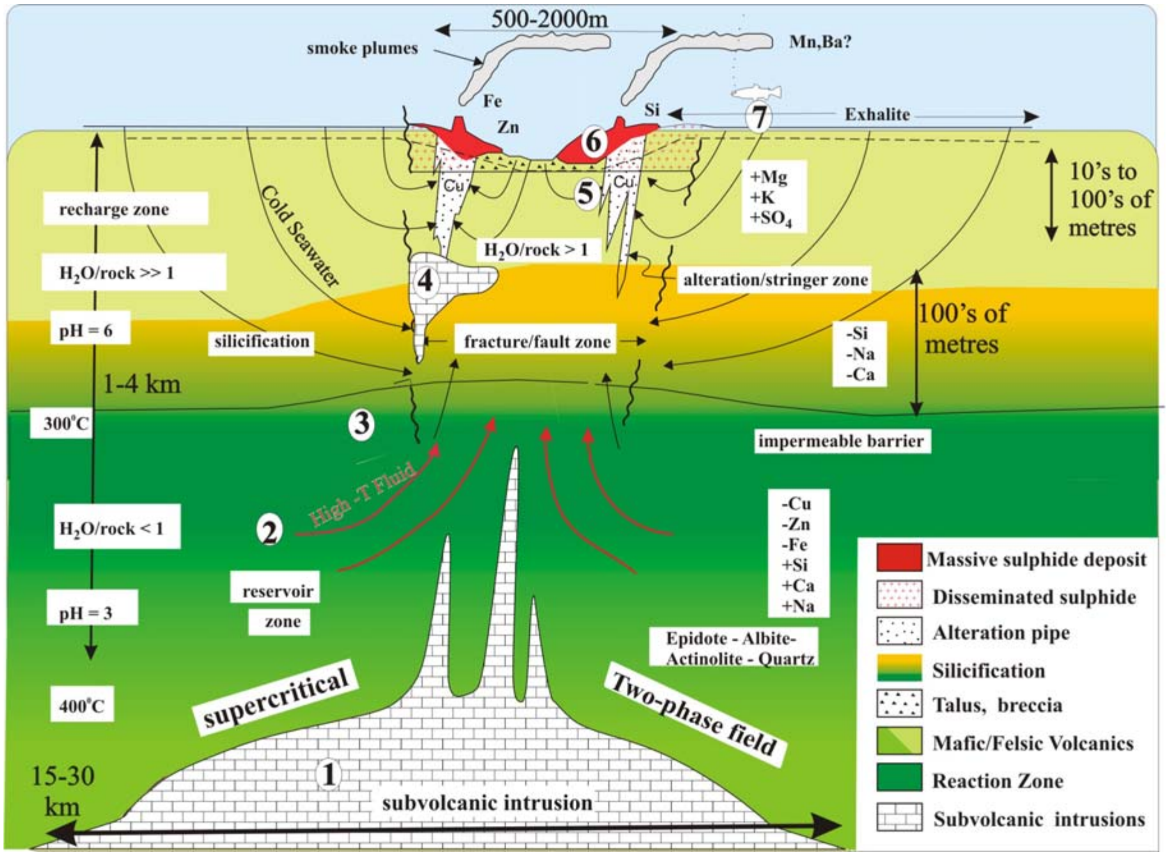

Figure 2: Hypothetical cross section of the environment of formation of VMS deposits in regions of seafloor extension. Red arrows indicate direction of flow of metalliferous high temperature fluid, black the direction of advecting cold seawater.

formation of VMS deposits, and literally hundreds of descriptive studies of example deposits. Much of this work is summarized in Franklin et al., (2005), and in earlier reviews by Lydon, (1984), Sangster and Scott, (1976) and Franklin et al., (1981). In addition, examples of this deposit type are currently forming on modern mid-ocean spreading and back-arc ridges (Hannington et al., 2005). The basic model is well accepted (Figure 2), although as with all models, there are many variants that are region-specific. For our purposes, however, it is imperative that we use those criteria that can be most generally applied to geological settings of all ages, throughout Canada.

The essential elements required to form a VMS deposit are:

1. A submarine setting: this is required because seawater is the most suitable solvent for base metals. The map evidence for this is generally clear, and is indicated by the presence of unique submarine features such as pillow lava and hyaloclastite. VMS deposits cannot form in subaerial environments.

2. An extensional setting: this is not typically evident on a geological map, but by inference, the chemical composition of the rocks will be indicative of the geological setting.
3. The presence of felsic volcanic rocks: although their presence is not a requirement, almost 90% of all VMS deposits are situated in areas where such rocks are present, typically within no more than a few hundred meters of the deposits. These rocks are a manifestation of an anomalous amount of heat that was resident at mid-crustal levels (see Vervoort et al., 1993). Their underpinning magma systems may also have contributed a minor amount of metal (specifically gold) during deposit formation.
4. The presence of major subvolcanic intrusions (#1 in figure 2): these occur typically 1.5 to 4 km below the paleoseafloor (on or near which the deposits formed) and extend parallel to the volcanic strata for 10-20 km. They are the manifestation of a focused heat source that "drove" the convective flow of seawater through fractures and void spaces in the volcanic strata. This heat helped to engender a key reaction that caused metals to be leached from the volcanic rocks (in the high temperature reaction zone, #2 in Figure 2), making these metals subsequently available to be transported to the seafloor, where rapid cooling induced metal sulfide precipitation. The reaction of leaching zone is identified by anomalous amounts of epidote, actinolite and quartz (Seyfried and Seewald, 1988), but these are not commonly identified on geological maps.
5. Exhalite horizons (#7 in Figure 2): These formed through a combination of processes attendant on the formation of the deposits, including discharge of low-temperature, silica charged fluids through fractures that surround the zone of more focused discharge (where the deposits themselves formed). Some exhalites are laterally extensive chert horizons, some include substantial amounts of iron, usually as iron oxides, forming banded iron formation (BIF), and others are comprised of volcanic detritus, cemented in silica (or less commonly, barite or carbonate) and mark the ore-bearing horizon. Some are just ferruginous mud that formed from fallout of volcanic detritus during a volcanically quiet period; these commonly contain anomalous contents of base and precious metals (tuffite), and other elements that were conserved in the hydrothermal fluid, but that became adsorbed onto the clays. Exhalite horizons occur associated with about 75% of the world's VMS districts.
6. Synvolcanic faults (#3 in figure 2), commonly occupied (in part) by very high level subvolcanic intrusions (#4 in Figure 2): Although the faults are rarely if ever mapped, the intrusions are easily identified, and usually have compositions identical to the volcanic rocks, and textures that help identify their shallow (<500m) emplacement depth.
7. Distinctive alteration ("alteration pipes, #5 on Figure 2), marked by sericite, chlorite, and /or silicification in the immediate footwall to deposits. Although these are almost always present, their size is usually not sufficient to be noted on geological maps.

In summary, seawater is locally heated by the cooling of a major subvolcanic intrusion. This fluid moves in an organized convective regime that is capped by an impermeable barrier of silicified, chloritized and epidotized volcanic rock. The fluid is focused by and discharges up extensional faults following seismic rupture events. On reaching the seafloor, rapid cooling causes the metals to precipitate. Leakage of lower temperature hydrothermal fluid causes regional silica precipitation on the seafloor, forming an exhalite unit (chert, tuffite, BIF).

In selecting the elements of this VMS model to be used in the resource evaluation exercise, we chose only those that could be expected to be shown (and coded) in to a geological map. Although the model components are somewhat scale independent, until the advent of the truly digital map, all maps are produced to be displayed at a specific scale. Much information that is observed in the field and interpretation derived from that work is not shown on most maps, but may be available in accompanying reports (and more recently in accompanying digital files). Since the objective of our project is to provide a system for assessing discovery potential without requiring in depth knowledge of the geology of any particular area to be assessed, we chose only those characteristics that are likely to be reliably depicted on a map, and that could be identified with a minimum of interpretation of the information on that map. The table of key criteria is shown in Table 1, and discussed more fully below. In addition to these criteria, it is expected that major geological districts (e.g. greenstone belts) will be classified as to the most significant attribute of their depositional environment (i.e. submarine vs. subaerial, and in Phanerozoic and some Proterozoic settings, the tectonic regime). This information is important as a first order classification criterion, but generally is not (yet) coded into map data. The coding of maps is discussed more extensively in section 4.3.

Criterion	Weighting factor	Maximum Distance (meters)	Likelihood of Correct Identification	Notes
submarine volcanic rocks	1	3000	1	Presence is a must; closeness to them (i.e., within 1 km) should be scaled steeply.
Felsic volcanic rocks	0.9	1000	0.9	Presence is highly favourable (0.9), proximity (within 500m) is very favourable (0.8), within the same belt is favourable (1-2km, 0.6). However, 11% of all VMS districts have no felsic rocks.
Exhalite horizon	0.8	1000	0.5	Usually well defined, may be an intra-volcanic sedimentary band. In felsic terrains, if it is within 200m, weighting factor is 0.8, but diminishes as a distance away from that point. For mafic terranes, there is greater uncertainty about the relationship of exhalite to the VMS process, and a lower weighting factor (0.3) is assigned.
Shallow-level subvolcanic intrusion (no more than 300m from exhalite)	0.4	1000	0.75	Not to be confused with deeper-level intrusion; compositionally similar to either mafic or felsic rocks, commonly a dyke or limited sill, best potential within 300m.
Major underpinning subvolcanic intrusion	0.7	>500<5000	0.5	Typically 1-4 km stratigraphically below the most favourable horizon. Its presence is important, the distance from the best potential area may be variable, and is usually at least 500m.

Table 1 Key criteria selected for assessing discovery potential for VMS deposits. The various columns are discussed more fully below

In Table 1, the “weighting factor” is a multiplier that is applied to this factor as a measure of its criticality to the presence of VMS deposits. The “maximum distance” value represents the maximum distance to the observation of a criterion; any greater distance than the value of that criterion is assigned a zero (0) value. The “likelihood of correct identification” is a measure of our uncertainty as to the significance of this observation in the context of the formation of VMS deposits, or also our uncertainty that the criterion is correctly assigned on the map. For example, the presence of exhalite in felsic-bearing domains is highly important, and thus has a high weighting factor. However, the correctness of assigning an observed exhalite to the generation of VMS deposits in any specific district is less certain, as discussed below. The statistical ramifications of applying uncertainty factors are discussed in section 5.6.

The “Notes” section of Table 1 includes a brief description of the rationale and some limitations on the selected criteria. Some additional factors that affect this project are:

Submarine volcanic rocks: This is the most significant element of the “Key Criteria” list (Table 1). All VMS deposits occur in submarine volcanic rocks or closely associated sedimentary horizons. Although some VMS-hosting districts also encompass subaerial strata, these are minor, In most currently available geological maps, these are not specifically identified. We use the presence of pillow lavas, well-bedded sedimentary strata and the general description of the belts to make this assignment. Thus in order to use this criterion on a large-scale compilation map (e.g. for an entire geological province, such as Slave or Superior provinces) each volcanic-dominated area must be classified as to its depositional environment. It is expected that future maps will include this factor in their coding. W give this a weighting factor of 1 (these strata are essential), and their identification is usually correct. However, their boundaries are quite commonly not well defined, and thus we have a large “maximum distance” value.

Felsic volcanic rocks: Felsic volcanic rocks, as noted above, occur in about 80% of all VMS districts. Deposits need not occur within them, but are usually within one kilometre of their occurrence. For example, many of the deposits in the Canadian Shield, Appalachian and Cordillera regions occur at the contact between felsic and mafic volcanic rocks Felsic volcanic rocks are generally correctly identified on geological maps. However, in some areas, felsic volcaniclastic rocks are classified as sedimentary strata, and in highly metamorphosed areas, they are more difficult to identify with certainty. As well, some VMS environments contain no felsic strata. Although their importance and certainty of identification are high, the slightly reduced values in Table 1 reflect their variable presence.

Exhalite horizon: These occur in the immediate hangingwall of many VMS districts, but the number of VMS districts with these is not known. For example in five major districts in the Canadian Shield (Matagami, Noranda, Manitouwadge, Bousquet, Sturgeon Lake) prominent exhalite occurs in only the first three. Usually well defined, they include intra-volcanic, ferruginous, sulfidic or siliceous sedimentary bands, chert, banded iron formation (BIF), and sulfidic volcaniclastic strata, for example. In felsic terrains, most exhalite units are within 200m of a deposit. In these terranes we assigned a weighting factor of 0.8, which diminishes in value as a distance away from that point rather quickly; hence it has a steep “decay curve” (as discussed below).

In working with available maps, we broadened permissive units to include chert, iron formation, ferruginous sedimentary rocks and carbonate-bearing sedimentary strata that are entirely enclosed within or immediately in contact with volcanic strata. Based on the experience of JMF and other experts, and following a review of the world’s VMS settings (Franklin et al., 2005), it is evident that candidates for exhalite units are much more likely to bear a genetic (temporal) relationship to the VMS-forming process if felsic volcanic rocks are present in the sequence under examination. In mafic dominated terrains, chert and iron formation are common, but much less likely to be related to the VMS-forming process. Thus we have to use a logic statement in our procedure for evaluating areas that assigns a much higher value (0.8) to the observation of a candidate exhalite if felsic rocks are present in the area under review, relative to those that are entirely mafic (0.30). For mafic terranes, there is greater uncertainty as to the relationship of exhalite to the VMS process, and a lower weighting factor (0.3) is assigned. . In all cases the genetic relationship of an observed candidate exhalite unit to the actual formational process of VMS deposits is subject to some uncertainty, and thus we maintain a low value for “likelihood of correct identification”. For purposes of developing our model, we started with an uncertainty value of 0.5. In developing our test cases for this study, we found that candidates of exhalite were rarely identified specifically as such, but permissive units as described above (chert etc) are normally recorded, even in broad-scale compilation maps.

Shallow-level subvolcanic intrusion: As noted above, these are typically emplaced along the same structures (faults) that provided the focus for discharge of hydrothermal fluids These are usually similar in composition to the volcanic rocks that have very close spatial association with the deposits. Such intrusions have been mapped only in about 40% of all districts, and thus their absence cannot be used to down-rate the potential for discovery: this is the reason for giving them a 0.4 weighting factor in assessing discovery potential. They are highly important observations, and even though they are usually small (only a few hundred meters wide, and commonly in dykes) they are observable on most maps. Unfortunately other forms of intrusion, unrelated to the VMS-forming process, may also occupy a similar map position. Although detailed work on the composition and age of suspect intrusions will generally sort out their relationships to the VMS process, this form of information is almost never available on today’s maps.   The uncertainty of the relationship of candidate intrusions to the VMS-forming process is the basis for assigning these a low (0.75) “likelihood of correct identification”.

Major underpinning subvolcanic intrusions are a manifestation of the heat source that provided the energy to form a metalliferous hydrothermal fluid. They are a highly significant feature in determining exploration potential, but unfortunately, these are commonly not present because of structural complexities. Thrust faults, for example may have caused them to be removed. As with the shallow-level intrusions, we must be careful to determine if such intrusions (which are felsic in about 75% of all districts) are actually synvolcanic. Their geological characteristics are quite well defined, however, and it is expected that, with better attention to details about their contact relations and compositional and age attributes, uncertainties will diminish. Because they are “missing” or not identified in many districts, their weighting factor is reduced to 0.75; uncertainties about their correct classification (synvolcanic vs. post-volcanic) are sufficiently high that their “likelihood of correct identification” is only 0.5. Also, because deposits rarely occur within them, and are most typically separated from them by 1 to 4 km of volcanic-related strata, their “decay curve” as explained below, is shaped to reflect an optimum distance of from 500 to 5000m form the most prospective zones. This is based on observations at several classic districts such as Noranda, Matagami and Sturgeon Lake. In reviewing the maps for the test areas (below) we noted that the term “subvolcanic” was used synonymously with “synvolcanic intrusion” When parsing data legends, we looked for these terms, and used them to classify the candidate intrusions.

Many other features, such as *alteration pipes*, *high temperature reaction zone assemblages*, and the presence of *diachronous breccia units*, were considered in our analysis, but for now were not used because of lack of identification in older maps. These, along with *key geophysical and lithogeochemical signatures* will be introduced as more robust data sets become available.

4.2 Selection of a Test Area

We selected the Hackett River district as our primary test area for several reasons. It is in NWT, and thus within the primary area of focus for the GEMS program. It was mapped in the mid 1970's (Frith, 1987). His map was recently digitized for use by the GSC for work on spectral reflectance in that area. Finally, the area contains an established VMS resource, and thus serves as an ideal test of our methodology. The quality of the map is typical of 33 year-old work; the mapping was carefully done, with good assurance of the correct identification of primary lithologies. However, the unavailability of modern geochronology , and the lack of intensive control using lithogeochemical data, mean that the interpretation is primarily restricted to field observations, and thus typifies much of the historic information available for regional compilation.

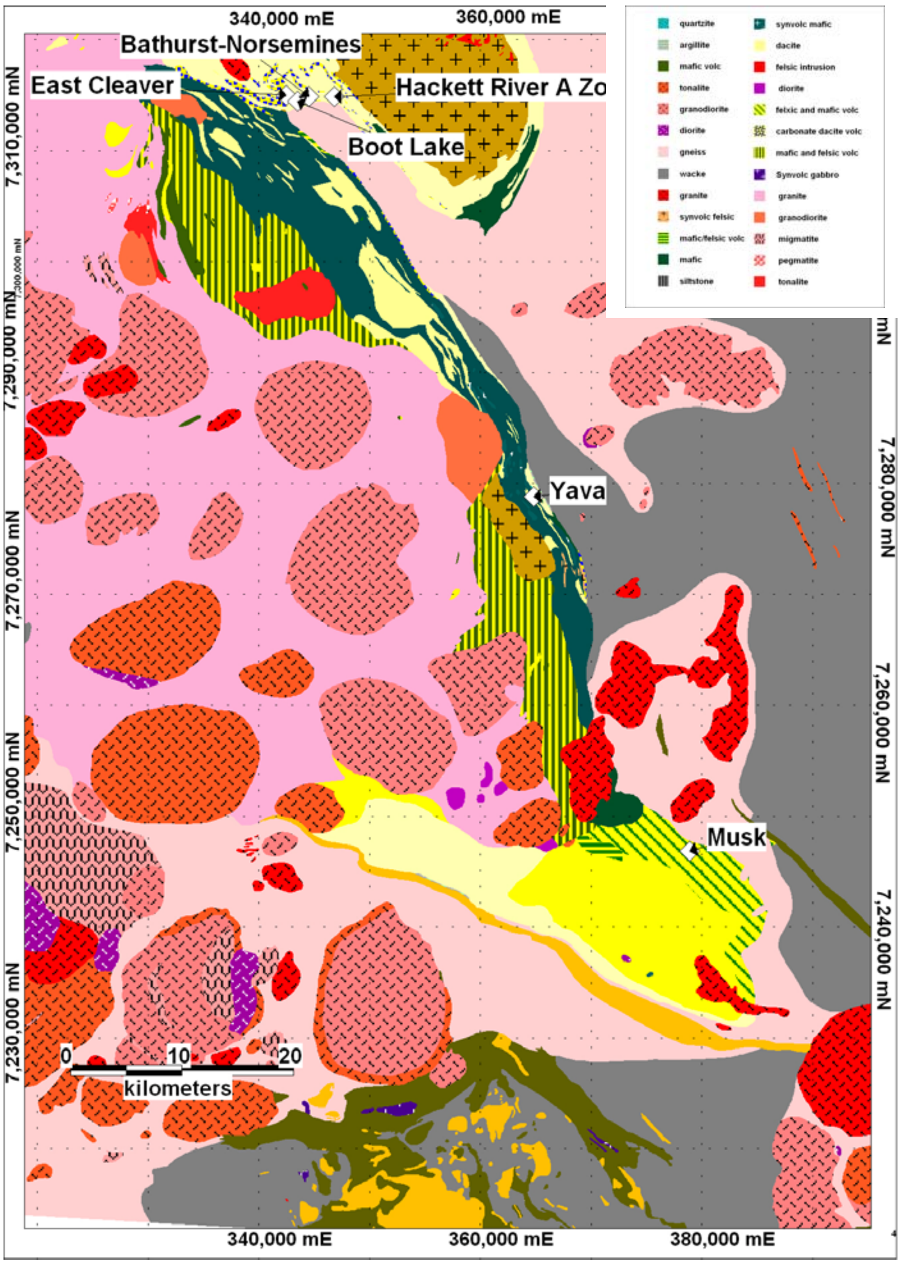

Figure 3: Geological Map of the Hackett River area, showing the locations of the 12 VMS deposits; some of these are grouped into a single deposit for this map.

Hackett River volcano-sedimentary complex is a fairly typical Archean greenstone belt, comprised of mafic and felsic volcanic strata, with a capping iron formation that may be an exhalite unit. There are several candidate subvolcanic intrusions (both mafic and felsic) along its approximately 100 km strike length. It contains 12 VMS deposits that occur in three centres, each separated by 35-40 km. These three centres may represent three separate VMS systems. The map, modified from Frith (1987), is shown in Figure 3.

A second map area, the Whitehills Lake sheet, was chosen in eastern Churchill Province. This area was much more recently mapped

(Zaleski and Pehrsson, 2005), and its qualities as a test area will be reviewed in the discussion of results for that area. Finally we used a new digital compilation map (Stubley, 2005) for the Slave Province. This compilation incorporates the Hackett River area, but the data for that area were revised to ensure overall legend consistency throughout the Slave Province. This compilation provides us with an excellent opportunity to determine if our methodology works on primary (Hackett River) and synthesized (Stubley compilation) geological data sets for the same region, and to test for similarity of results for the same area.

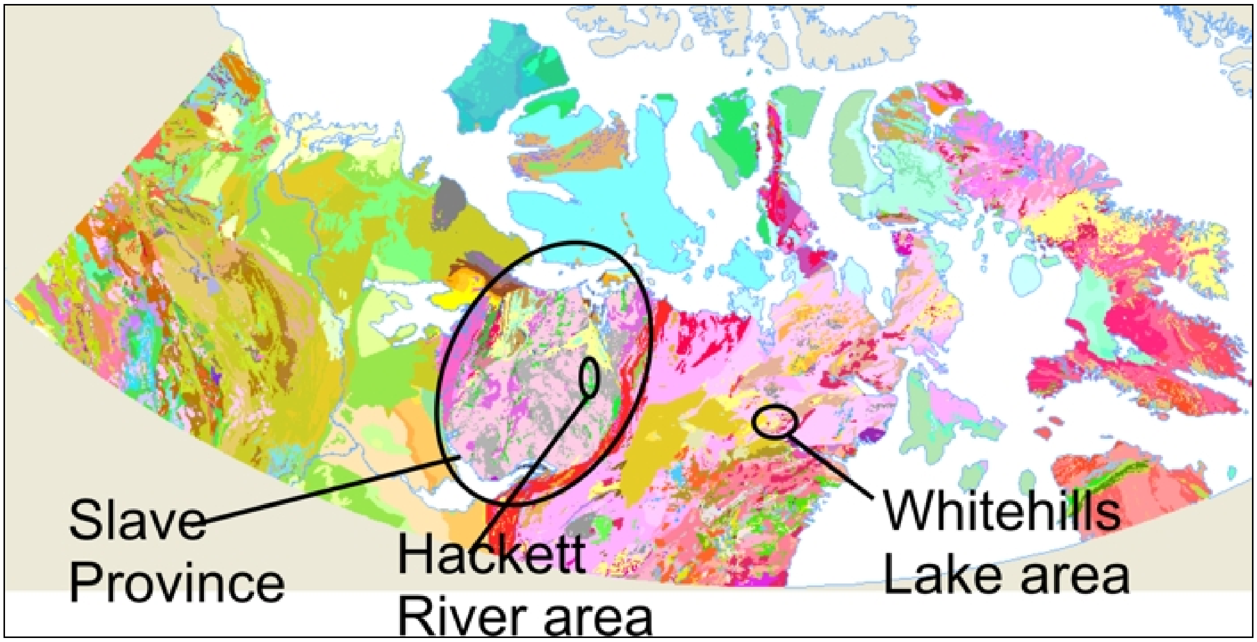

Figure 4: Geology of Canada north of 60 degrees, showing test areas used in this study.

4.3: Legend preparation

Ideally, the criteria set out in Table 1 should be coded in the maps that are to be tested, with minimal legend adjustment required. For example, felsic volcanic rocks, exhalite, and subvolcanic intrusions should be coded into the map legend. In practice, this would require the 'translation" of the criteria into legend items that reflect exactly the lithological units that are being sought. In practice, this is not so simple. The criteria that are depicted in any map legend should include age of the rocks, principal rock type, modifiers of that rock type that reflect textural or physical attributes that reflect a mapable uniqueness or key characteristic that helps define specifically a stratigraphic unit, intrusive phase or metamorphic assemblage ad texture. Added to this might be modifiers that describe alteration or a unique additional textural characteristic. For example, a mafic volcanic unit in the Hackett River area might be described as

Archean carbonatized pillow basalt. For purposes of extraction of digital information from a map, each of these four identifiers would ideally be searchable, and thus in the database that underpins the digital map, in separate database columns. Further, ideally all legends for all bedrock geological maps should be consistent.

In Canada, legends used by Provincial surveys are generally consistent. Ontario, for example, has generally used the same legend for well over 50 years, and it's easily translatable into the lithologies needed for our type of analysis. However, even if the legend clearly depicts the lithologies, there are some features that may not be easily identified, or that must be interpreted. First, "exhalite" isn't a formal lithotype; the term encompasses bedded chert, iron formation and even carbonate strata. The unifying feature is that these units are in, or at least in contact with volcanic strata or their derivatives. Thus we included all of these in the "exhalite category. Second, the assignment of an intrusion to a subvolcanic origin is also not commonly included in the digital legend. We did not, however, find that in many cases this term is found within the descriptive notes for some intrusions. Again, as with exhalite, if an intrusion is totally contained within volcanic strata, and has a composition that is similar to those strata, there is a good chance that it is subvolcanic in origin.

Legends provided with more recent maps produced by the Geological Survey of Canada present a significant challenge. In the past 20 years, the focus has been on creating a legend that contains as much litho-tectonic information as possible. This type of legend is useful for printed maps, as the legend item for each lithotype contains information about age, stratigraphic unit name, lithological group, rock type, and in some cases alteration. From the perspective of use in a digital system such as that which we are developing, these legends are concatenated in such a way as to render them unusable. As an example, Table 2 provides a few lines from the digital file that underpins the Hackett River map; Table 3 provides the same lines, but is comprised of the revised lithological assignments.

GSC COLOUR	MAPUNIT	HEADING1	HEADING2	HEADING3	UNITDESC1	LEG_ORDER
329	ABa	Archean	Yellowknife Supergroup	Back Group	massive and pillowed andesite, porphyritic andesite and andesite tuff	23
537	ABLc	Archean	Yellowknife Supergroup	Beechey Lake Group	carbonaceous mudstone	30
329	ABs	Archean	Yellowknife Supergroup	Back Group	**synvolcanic metagabbro sills and dykes**	26
419	AH	Archean	Yellowknife Supergroup	Hackett River Group	**undifferentiated volcanic rocks**	34
419	AHd	Archean	Yellowknife Supergroup	Hackett River Group	**metamorphosed dacite rocks**	36
419	AHm	Archean	Yellowknife Supergroup	Hackett River Group	migmatitic volcanic rocks	38
736	AIi	Archean	Yellowknife Supergroup		Ignerit Formation: andesite, basalt and basic tuff	41
32	AMd	Archean	Archean	Mara River Complex	quartz diorite or diorite	56
32	AMg	Archean	Archean	Mara River Complex	granodiorite	54
847	AN	Archean	Yellowknife Supergroup		Nauna Formation: undifferentiated andesite and dacite flows and pyroclastic rocks	43
847	ANd	Archean	Yellowknife Supergroup		**Nauna Formation: dacite**	44
847	ANi	Archean	Yellowknife Supergroup		Nauna Formation: andesite and basalt	45
847	ANm	Archean	Yellowknife Supergroup		**Nauna Formation: basic synvolcanic sills and plugs**	47
97	Ap	Archean	Archean		**trondhjemite pegmatite**	21
186	ARd	Archean	Archean	Regan Intrusive Suite	**diorite, quartz diorite**	18
74	ARg	Archean	Archean	Regan Intrusive Suite	**granodiorite, undifferentiated**	16
88	ARt	Archean	Archean	Regan Intrusive Suite	**tonalite**	17
535	As	Archean	Archean		**synvolcanic tonalite, granodiorite, quartz diorite, migmatite**	20
572	Pd	Proterozoic	Early Proterozoic		gabbro sill	3

Table 2: Excerpt from data file for GSC Map AS1619, after Frith 1987. This is the legend that was provided with the digital version of that map.

In Table 2, note that the lithology descriptions are in the fifth column (UNITDESC1). These are text descriptions that contain formational names (e.g. Nauna Fm), rock compositions (but as extended text, i.e. "Nauna Formation: undifferentiated andesite and dacite flows and pyroclastic rocks") and rock codes (MAPUNIT). Note that some of the rock codes have the Group and Complex name imbedded in them (e.g. ANd is Archean Nauna formation dacite), but the formation names are not in the HEADING3 column. The rock codes are not easily parsed into rock type and formation name, nor do they impart any significance as to lithological group (e.g. intrusion vs. extrusion vs. sedimentary rock). Felsic volcanic rocks, which seem to occur in several formational units (which are all informal designations) appear in three different coded units, ANd, AN, and AHd. Subvolcanic (or synvolcanic intrusive rocks) rocks are noted in two units, and mafic volcanic rocks are in five units. Several units contain "undifferentiated" mafic and felsic rocks. For purposes of our test, only the actual predominant lithology (mafic, felsic, or basalt, andesite, dacite etc) and lithotype (intrusive, subvolcanic, volcanic, sedimentary, metamorphic etc) is important. Parsing the GSC legend was a major job; interestingly, parsing legends from Provincial surveys is much easier, as they typically code less into their lithcodes. The GSC is making steady progress on reconciling its approach to legends with the needs of the emerging digital applications (Davenport et al., 2002).

In Table 3 we illustrate our simplification of the legend. We attempted, where possible, to use a single lithotype, and to place modifiers in a separate column (UnitDescJMF). Also, we placed formational units into separate columns. If the necessity arises to combine these (e.g. formational name with lithology) a simple concatenation in a separate column is all that is required (e.g. the last two columns of Table 3). We used the fifth column in Table 3, "UnitDescJMF", and acknowledge that in doing so, we arbitrarily changed the original map somewhat.

The final classification of polygons required that we add a separate layer for iron formation, which was not included with the main digital version of the map; this was an oversight on the part of the digitizers. All lithologies should be included in a single file that underpins the map polygons. One issue that caused problems was the use of a mixed lithology identifier to classify rather large areas. The areas classified as "mafic and felsic volc" should have been more clearly represented as either felsic or mafic on the map. The field mapping was completed over 30 years ago, and we only note this to suggest that such assignments should be avoided in future. In future, a single lithological designation should be assigned to each polygon, unless the presence of two or more lithologies is so intimate as to be impossible to separate.

The finalized lithology list is in Table 4. In establishing this, we created some redundancy of units (i.e. two lithology assignments for what should have been a single lithotype) that in future (and in the other two map areas) we avoided. It is critical that before finalizing the lithology assignments and integrating them back into the map database, these be listed and checked to ensure that they are unique and that the units that we intend to be included on the map are all represented and correctly identified. It's important to simplify the map to the extent that there is only one lithotype to represent a key criterion. For example, we use felsic rocks as a key criterion; "dacite", "rhyolite" and "rhyodacite" are all synonymous with "felsic volcanic", requiring that the former lithotypes be reassigned to the more general latter term.

MAP UNIT	UNITDESC1	LEGEND ORDER	Object_ ID	UnitDesc	simplified lithjology	Formation_Complex_Group	Formation_lith
ABa	massive and pillowed andesite, porphyritic andesite and andesite tuff	23	281	mafic volc	mafic volcanic	Back Group	Back Group_mafic volc
ABLc	carbonaceous mudstone	30	329	argillite	sediment	Beachey Group	Beachey Group_argillite
ABs	**synvolcanic metagabbro sills and dykes**	26	277	**Synvolc gabbro**	**synvolcanic gabbro**	Back Group	Back Group_Synvolc gabbro
AH	**undifferentiated volcanic rocks**	34	234	**mafic and felsic volc**	**mafic and felsic volc**	Hackett River Group	Hackett River Group_mafic and felsic volc
AHd	**metamorphosed dacite rocks**	36	48	**dacite**	**felsic volcanic**	Hackett River Group	Hackett River Group_dacite
AHm	migmatitic volcanic rocks	38	19	mafic and felsic volc	**mafic and felsic volc**	Hackett River Group	Hackett River Group_mafic and felsic volc
AIc	Ignerit Formation: carbonate and dacite fragmental rocks	42	102	carbonate dacite volc	felsic volcanic	Ignent Formation	Ignent Formation_carbonate dacite volc
AIi	Ignerit Formation: andesite, basalt and basic tuff	41	135	mafic	mafic volcanic	Ignent Formation	Ignent Formation_mafic
AMd	quartz diorite or diorite	56	330	diorite	mafic intrusion	Mara Complex	Mara Complex_ diorite
AMg	granodiorite	54	39	granodiorite	granitoid intrusion	Mara Complex	Mara Complex_ granodiorite
ANd	**Nauna Formation: dacite**	44	424	**dacite**	**felsic volcanic**	Nauna Formation	Nauna Formation_dacite
ANi	**Nauna Formation: andesite and basalt**	45	462	**mafic**	**mafic volcanic**	Nauna Formation	Nauna Formation_mafic
ANm	Nauna Formation: basic synvolcanic sills and plugs	47	119	synvolc mafic	subvolcanic mafic	Nauna Formation	Nauna Formation_synvolc mafic
Ap	trondhjemitic pegmatite	21	82	felsic intrusion	subvolcanic felsic	Basement?	Basement?_felsic intrusion
ARd	diorite, quartz diorite	18	226	diorite	mafic intrusion	Regan Complex	Regan Complex_diorite
ARg	granodiorite, undifferentiated	16	70	granodiorite	granitoid intrusion	Regan Complex	Regan Complex_granodiorite
ARt	tonalite	17	393	tonalite	granitoid intrusion	Regan Complex	Regan Complex_tonalite
As	synvolcanic tonalite, granodiorite, quartz diorite, migmatite	20	402	wacke		Siorak Formation	Siorak Formation_wacke
Pd	gabbro sill	3	173	gabbro	mafic intrusion	Goulburn Group	Goulburn Group_gabbro

Table 3: Simplification of the legend for the Frith (1987) map. Only the Archean portion is shown here, and the original numbers assigned to the map table are retained.

Unit number	Simplified map unit name	Key model unit
20	Iron Formation	exhalite
3	andesite. dacite/pyroclastic	felsic
19	carbonate, dacite/fragmental	felsic
1	andesite/pillow	mafic
2	andesite. basalt/flow or tuff	mafic
17	volcanic/undifferentiated	mafic
4	argillite. mudstone. quartzite, siltstone or turbidite/seds	sediments
5	basic intrusive/synvolcanic	subvolcanic intrusions
7	felsic intrusive/synvolcanic	subvolcanic intrusions

Table 4: Cross tabulation of simplified map unit names and key VMS model components (right column)

Ideally, assignment of simplified lithologies should not require inspection of the map, but in the case of Hackett River, we checked our assignments interactively with the GIS-based map. Assigning specific intrusions to the "subvolcanic" category was fairly easy, as the term "synvolcanic" was used with various types of intrusive rock, and we took these to all be subvolcanic. However, since Frith was not necessarily considering the importance of subvolcanic intrusions when he was mapping (the VMS model was relatively immature at that time) we may have under-represented this category.

All of the preparative work for assigning the simplified lithologies to their respective polygons was done in either ArcGIS® or MapInfo®. Once we finalized the lithology list, the map was transferred into a registered raster image. Each pixel has an assigned lithology, and in the Hackett River test area, pixel sizes for all lithologies are $20m^{2.}$ Pixel sizes for exhalite are $3m^2$, because of the narrowness of the units (most are represented only as lines in the original data file).

In summary, we recommend that the GSC undertake a major revision of the way in which it presents legends for its maps. These must become much more "digital-friendly". In doing so, industrial and academic users will be able to make much broader use of the map products.

5.0 Methodology: Analysis of Effectiveness

5.1. Generating decay (favourability) functions based on expert's knowledge

The ***Key criteria to discover VMS deposits*** in any selected area are summarized in Table 1. Using the criteria alone, it would not be possible to estimate an absolute measure of the "***probability (or certainty)***" of the next VMS discovery for any specific map area. However, the criteria will provide a measure of the "***relative significance or favourability***" with respect to the existence of VMS deposits in an area. An attempt has been made here to convert the key criteria to a mathematical function such that, for any given area, we can generate a measure of the relative significance or favourability with respect to the existence of the VMS deposits in the area.

The conversion to a mathematical form can be achieved in three steps. The first two steps are of transferring each key criterion into a mathematical function: Having already generated a raster map in which each pixel is assigned a lithology, we then, on a pixel-by pixel basis, evaluate the distance from any pixel to the nearest occurrence of a pixel that contains a key criterion.

(Step.1) to generate a *data layer* where each value at a pixel (pixel value) is a value for the distance to a specific criterion on the geological map, and

(Step.2) to develop a mathematical model that estimates the relative significance or favourability for the discovery of the VMS deposits as a function of the distance from an observation point (pixel) to the nearest pixel that contains that criterion (as generated in Step.1). This function usually describes the non-linear relationship between the value of the likelihood of discovery of the VMS deposit and its distance away from that key criterion.

The mathematical function in (Step.2) is termed the "***decay function***" of the key criterion for VMS deposits, and it is determined for each criterion. Its values range from 0 to 1. Through the decay function, each pixel value in the data layer (map) generated in (Step.1) is converted to a value between 0 and 1 depending on the relative significance (or favourability) for VMS deposits. For example, as noted in Table 1, proximity to submarine volcanic rocks does significantly but not directly relate to the presence of VMS deposits. If a pixel is greater than 3000 m from the nearest submarine volcanic rocks, its value representing the relative significance (or favourability) for VMS deposits for that criterion will be 0. For each key criterion, one decay function is generated. In the final Step.3, the decayed values generated in the first two steps (one for each of the key criteria) for each pixel are integrated into one mathematical function, termed the "***favourability function***" for VMS deposits.

We will illustrate these steps in the Hackett River area, NWT. Let us take the first criterion – the presence of submarine volcanic rocks in Table 1. In (Step.1), we generated the first data layer (map). It is named "submarine volcanic data layer", and was constructed by computing the distance to the nearest submarine volcanic rocks from each pixel. It is shown in Figure 5, with the 12 VMS deposits in the Hackett River area, NWT. The pixel values in the data layer represent the minimum distance to the presence of submarine volcanic rocks, shown as black in Figure 5, and these distance values range from 0 (presence of submarine volcanic rocks) to 46.4 km, shown as magenta. The pixel values ranging from 0 to 46.4 km will be used to calculate the relative significance or favourability with respect to the existence of the VMS deposits in the next step.

The "decay function" to be established for the "submarine volcanic rocks" criterion would estimate the "favourability score" characterizing the "relative significance (or favourability)" for VMS deposits as a function of the distances from submarine volcanic rocks, decayed by a function that we establish that is represented by a decay curve. To establish the decay function, we combine the distance measured and a multiplier that is determined by using the corresponding note in Table 1 (maximum distance (meters)) to set a limit, beyond which the value for this function goes to 0. This "maximum distance" is a limiting guideline, but there is no unique way to generate the decay function from this value. From the description in the last column of Table 1 containing the "*Presence is a must; closeness to them (i.e. within 1 km) should be scaled steeply*", and "*3000*" as the maximum distance, a decay function has been

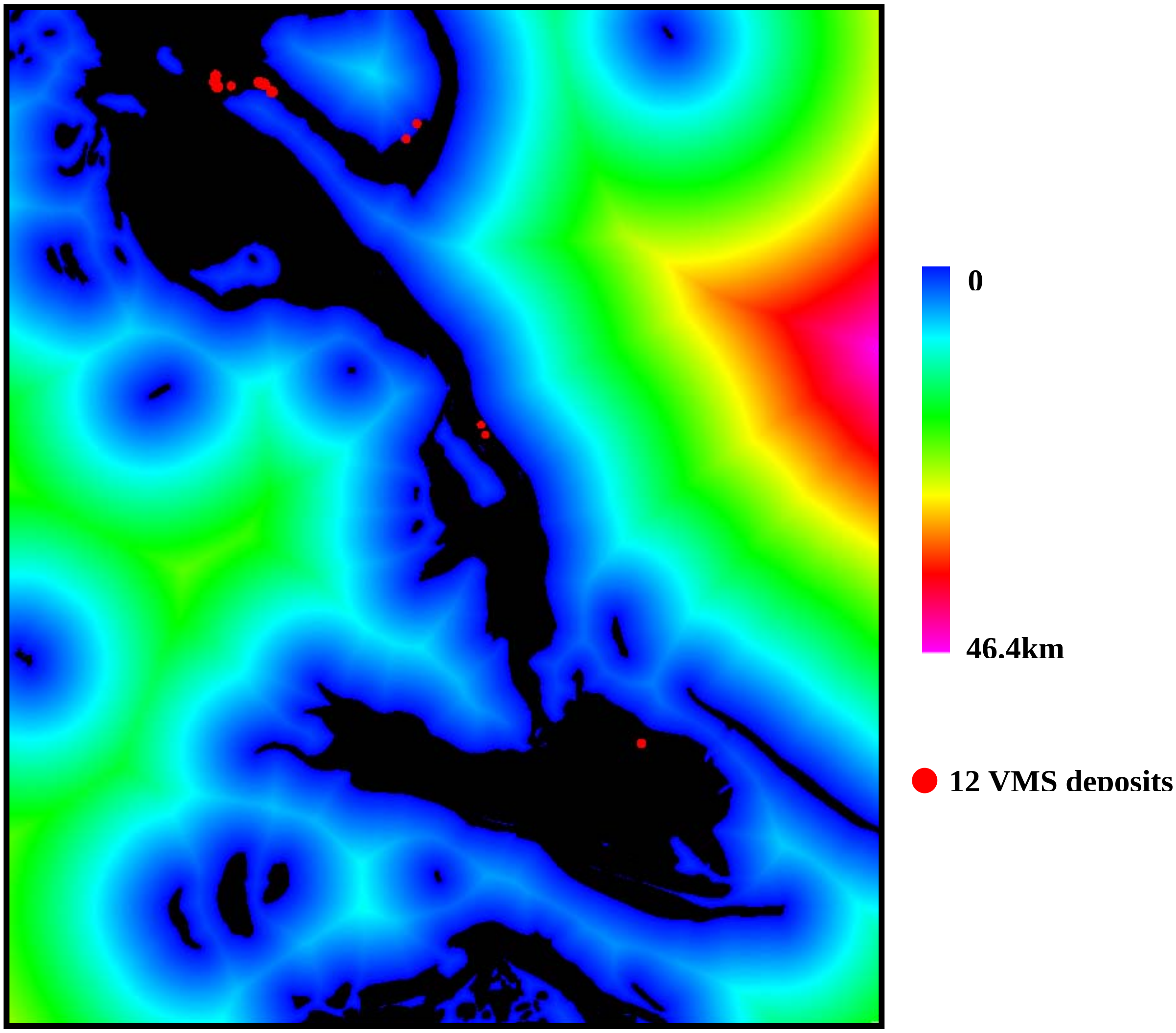

Figure 5. Distance from submarine volcanic rocks in Hackett River area, NWT, Canada. 12 known VMS deposits are plotted as red dots.

established and it is shown in Figure 6 as a black curve. The steep scaling directs us to form a curve that decays the value of the distance measured very quickly.

In Figure 6, the X-axis represents the distance from submarine volcanic rocks, and the Y-axis shows a “measure (value from 0 to 1)” representing the relative significance or favourability for VMS deposits. Following the black decay function in Figure 6, the measure for the areas within the submarine volcanic rocks is 1. However, the measure for the areas near (approximately 500m) the submarine volcanic rocks is reduced to 0.35. The distant areas (farther than 1000 m) have scores less than 0.15. The measure for the areas farther than 3000m from submarine volcanic rocks is 0, suggesting no prospect of VMS deposits, based on the criterion of submarine volcanic rocks from Table 1. The representation of the relative significance or favourability for

VMS deposits by the decay function is based on the assumption that the boundary of submarine volcanic rocks is fixed.

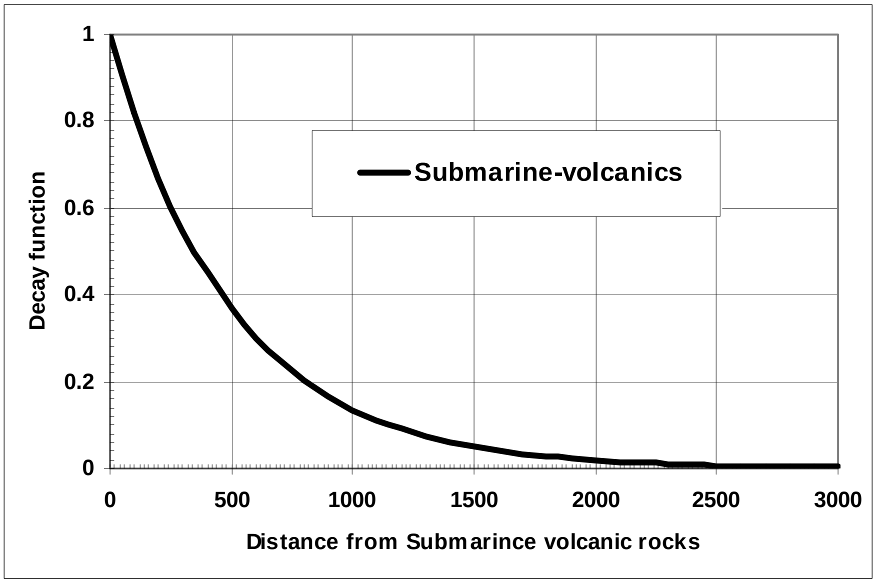

Figure 6. Decay functions for the first criterion, "presence of submarine volcanic rocks for VMS deposits." The black curve was established as the decay function by following the description in the second row of the last column in Table 1.

In reality, the assumption that a boundary for submarine volcanic rocks (or any other unit that we use for assessing the likelihood of occurrence of VMS deposits) as shown on a map or contained in the digital file may not to be true, and its accuracy depends to some extent on the scale of the geological map used, as well as the interpretation of the geologist who mapped the area. The uncertainty or dependence on the accuracy of this boundary is represented in part by the number shown in the fourth column under the heading of "likelihood of correct identification" in Table 1. We will use it to determine our uncertainty of the representation of a specific type of unit (e.g. submarine volcanic rocks, or for other criteria, such as felsic volcanic strata or subvolcanic intrusions), which will in turn affect our estimation of the favourability for occurrence of VMS deposits, based on the first criterion, the presence of submarine volcanic rocks.

5.2. Types of decay (favourability) functions, reflecting expert knowledge

For each criterion, the accompanying description usually provides guideline to establish the decay function but there is no unique way to generate that function. Five mathematical functions have been developed to adapt five different scenarios of the decay functions: (1) Steep decay function; (2) Medium decay function, (3) Slow decay function; (4) Humped decay function; and

(5) Linear decay function. They are shown in Figure 7. The basis for determining the shape of the curve is the judgement of the expert who built Table 1, based on knowledge of the ore deposit type. Such curves can be easily adjusted, but they generally reflect the uncertainty of the precise location of a geological boundary, and also that the potential presence of an orebody is commonly related to proximity of these characteristics. However, the deposit need not be located within or immediately adjacent to any one of the boundaries. For some criteria (e.g. the presence of subvolcanic intrusions) the deposit will not be in the intrusion, but the likelihood of a deposit occurring is best at some distance (usually 2-4km) from its upper contact. Thus for this criterion, we use a "humped" curve, with its maximum indicating the most likely distance that a deposit might occur from such an intrusion.

A decay function is a normalized function of the distance from a geologic unit related to the key criterion and the value of a decay function diminishes (becomes 0) after some distance, termed the "maximum distance". In Figure 7, all the five normalized decay functions are shown. The X-axis represents the "relative distance" from the geologic units related to the key criteria and it is assumed that "1" is the maximum distance

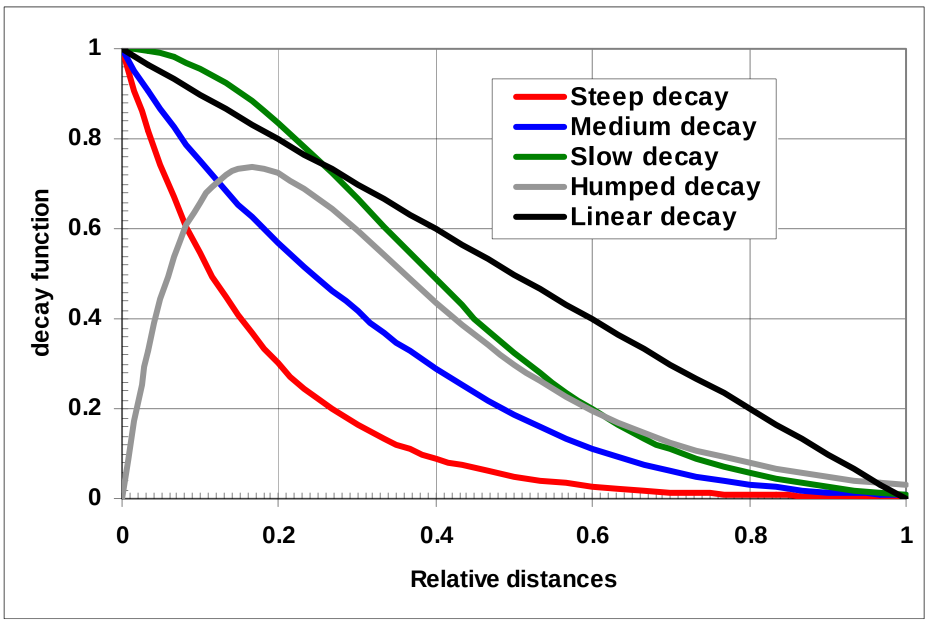

Figure 7. Five different types of decay function. The X-axis represents the relative distance from the geologic units related to the key criteria, with the maximum distance from the geologic unit being 1; the Y-axis shows the "scores" representing the relative significance or favourability for VMS deposits.

For the decay function for submarine volcanic rocks shown in Figure 6, the steep decay function shown as a red curve in Figure 7 was selected and modified, with 3000m being the maximum distance. Although most of the decay functions are monotonically decreasing, the humped decay function as a grey curve in Figure 7 was also added to represent the last key criterion in Table 1 for "Major underpinning submarine volcanic intrusion". It suggests that the likelihood of the existence of VMS deposits is neither very near nor very far away from the intrusion, but at some distance (which we fixed, from observation of many districts, as > 500m but less than 5000m from the intrusion, Table 1) from the intrusion.

5.3. Five key criteria, five decay functions and corresponding potential maps

As we discussed for submarine volcanic rocks, for each criterion we generated a data layer by computing the distance from the corresponding geologic unit at each pixel. Similar to Figure 6, the pixel values in four additional data layers (not shown here) represent the minimum distances from the presence of (1) felsic volcanic rocks, (2) exhalite horizon / iron formation; (3) shallow level subvolcanic intrusions, and (4) major underpinning subvolcanic intrusions.

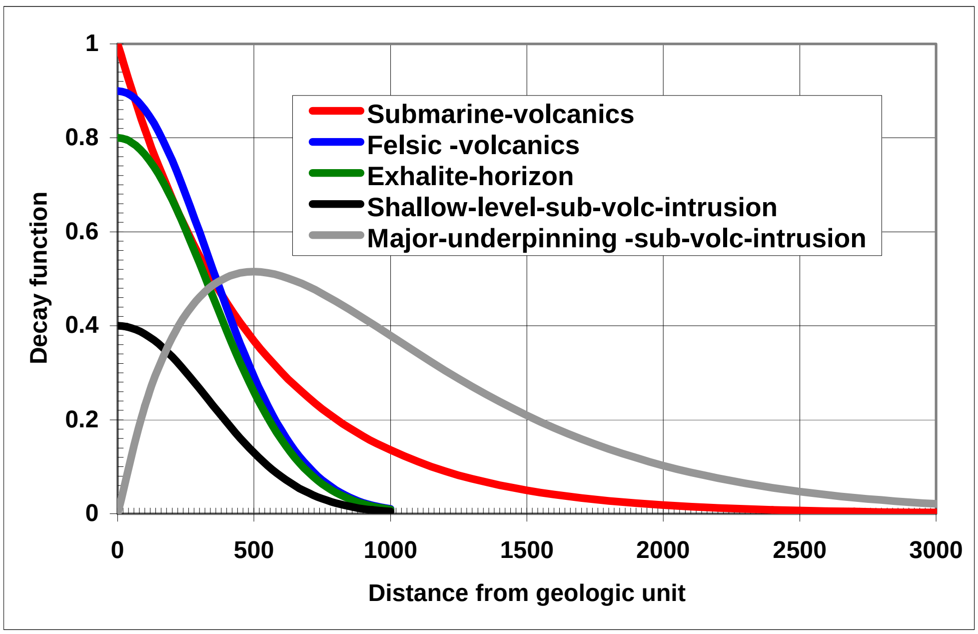

Figure 8. Five weighted decay functions for the five key criteria in Table 1. The X-axis represents the distances from the corresponding geologic units related to the key criteria and the Y-axis shows the "measure" expressing the relative significance or favourability for VMS deposits.

For each criterion, in addition to the accompanying description in the last column, the "weighting factor" in the second column in Table 1 is also included to express the relative importance of the corresponding decay function. We incorporated the weighting factor in the construction of the decay function as a multiplicative factor to that function, such that its maximum value is limited by the weighting factor. The five weighted decay functions include the decay function for submarine volcanic rocks criterion as shown in Figure 6. The functions for all five key criteria are shown in Figure 8. After the decay function is established, it is weighted by multiplying the weighting factors (second column and the second row in Table 1). However, for the weighted decay function for submarine volcanic rocks, the weighted decay function has not been changed because its weighting factor is 1.

The next step is to integrate these five weighted decay functions into one mathematical function, termed the "favourability function" for VMS deposits.

5.4. Integration of five decay functions into a favourability function

Suppose that we have only the first key criterion of submarine volcanic rocks for VMS deposits. Then the decay function in Figure 6 can be used to estimate the "***favourability score***" measuring the "relative significance or favourability" for VMS deposits as a function of the distances from submarine volcanic rocks. Every pixel value measuring the distance from submarine volcanic rocks in Figure 5 can be converted into a favourability score for VMS deposits. Figure 9 was constructed by using the decay function shown in Figure 6 in the Hackett River area, NWT, as

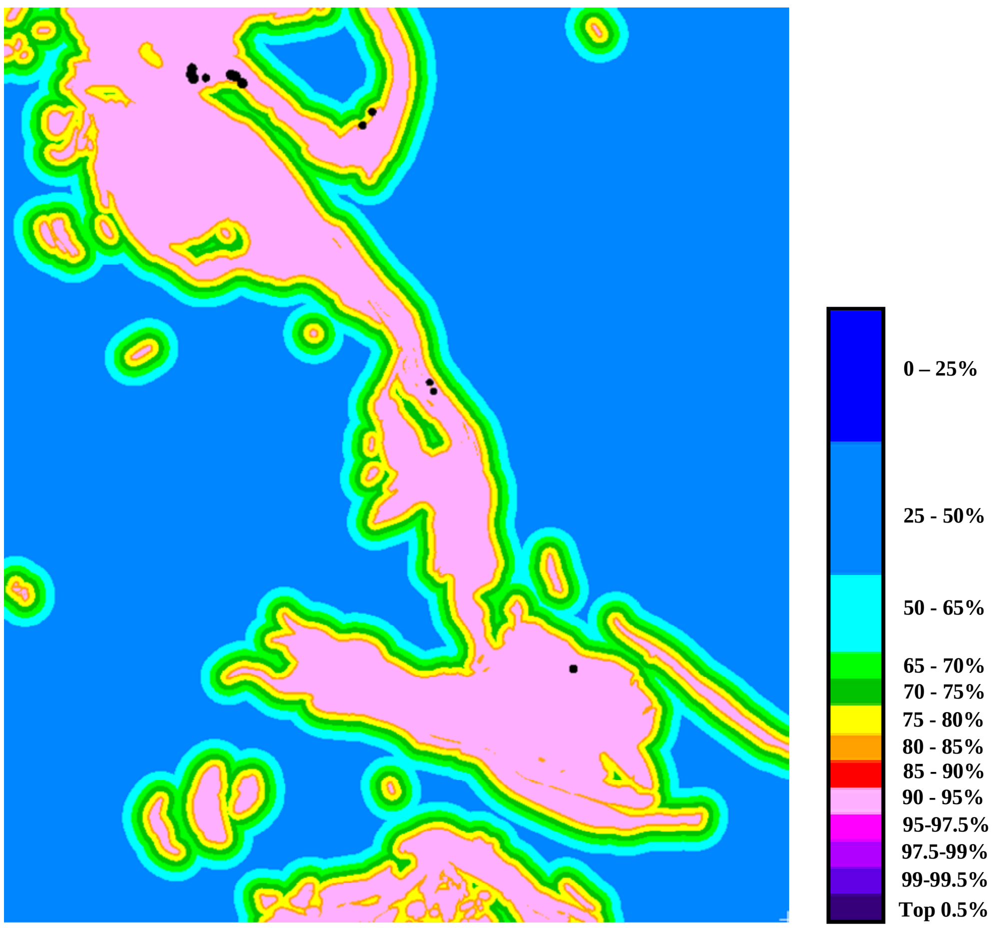

Figure 9. VMS potential map based on only one criterion of submarine volcanic rocks in the Hackett River area, NWT, Canada. The 12 known VMS deposits are plotted as black dots.

the favourability scores for VMS deposits. It can be considered a VMS potential map, assuming that there is only this one available key criterion of submarine volcanic rocks for VMS deposits.

However, for a given deposit type such as VMS deposits, several key criterion are always available. Suppose that we have "**k**" key criteria for a deposit type. For example for VMS deposits as discussed, five key criteria were provided. In general, for the i^{th} key criterion (i = 1, … , k), we generated the corresponding data layer, D_i and decay function, f_i (d_{ij}) where d_{ij} is the j^{th} pixel value representing the distance from the corresponding geologic unit in the i^{th} data layer D_i . Using mathematical notation, for the j^{th} pixel, we have **k** pixel values, (d_{1j}, … , d_{kj}).

There is neither a unique nor an optimal (or best) way to integrate the k decay functions into one mathematical function. Four simple mathematical integration procedures for integrating the k decay functions into one favourability function, $\boldsymbol{f}$ are: (1) additive procedure; (2) multiplicative procedure; (3) minimum procedure; and (4) maximum procedure by following formulas, for the j^{th} pixel with k pixel values, (d_{1j}, … , d_{kj}),

$$\boldsymbol{f}(d_{1j}, \ldots , d_{kj}) = \begin{cases} \frac{1}{k}\sum_{i=1}^{k} \boldsymbol{f}_i\left(d_{ij}\right) \text{ for the additive procedure} \\ \prod_{i=1}^{k} \boldsymbol{f}_i\left(d_{ij}\right) \text{ for the multiplicative procedure} \\ \text{Minimum}\left(\boldsymbol{f}_1\left(d_{1j}\right), \cdots, \boldsymbol{f}_k\left(d_{kj}\right)\right) \text{ for the minimum procedure} \\ \text{Maximum}\left(\boldsymbol{f}_1\left(d_{1j}\right), \cdots, \boldsymbol{f}_k\left(d_{kj}\right)\right) \text{ for the maximum procedure} \end{cases} \quad \text{(Eq. 5.1)}$$

We can also integrate the decay functions by the following "fuzzy gamma" procedure,

$$\boldsymbol{f}(d_{1j}, \ldots , d_{kj}) = \left(\prod_{i=1}^{k} \boldsymbol{f}_i\left(d_{ij}\right)\right)^{1-\gamma} \left(1-\prod_{i=1}^{k}\left(1 - \boldsymbol{f}_i\left(d_{ij}\right)\right)\right)^{\gamma} \quad \text{(Eq. 5.2)}$$

where the gamma value, γ, is a given value between 0 and 1. In this gamma procedure, not only the favourability scores f_i (d_{ij}) but also the "negative favourability scores" 1 - f_i (d_{ij}) have contributed significantly to the final favourability function, $\boldsymbol{f}$.

In addition to the five procedures in (5.1) and (5.2), we can integrate the decay functions by the following the expert-driven procedure for selecting weighting and decay values for VMS deposits. For the five key criteria in Table 1 for VMS deposits, the expert has provided the following procedure to integrate the five decay functions:

$$f(d_{1j}, \ldots ,d_{kj}) = \begin{cases} \frac{1}{5}\sum_{i=1}^{5} \boldsymbol{f}_i\left(d_{ij}\right) \textbf{(}\text{additive proced}\textbf{)} \text{ if } d_{2j}\textbf{,} \text{ distance from Felsic v}\textbf{.} \le 1000\text{m} \\ \frac{1}{5}\left(\boldsymbol{f}_1\left(d_{1j}\right) + \boldsymbol{f}_3\left(d_{3j}\right) + \boldsymbol{f}_5\left(d_{5j}\right)\right) \text{ if } d_{2j}\textbf{,} \text{ distance from Felsic v}\textbf{.} > 1000\text{m} \end{cases} \quad \text{(Eq.5.3)}$$

The above procedure in (5.3) is termed "**Expert's VMS integration**" procedure for the five key criteria for VMS deposits. <u>We will use it extensively in generating the VMS potential maps</u>.

By using one of the integration procedures in (5.1), (5.2) and (5.3), the weighted decay functions are integrated into one favourability function. The favourability scores of any favourability functions generated from the integration procedures in (5.1), (5.2) and (5.3) range from 0 to 1, and the potential maps are constructed by slicing these favourability scores into a number of "potential classes". How to slice the favourability scores, i.e., how to generate the potential classes from the scores, is discussed in the next section.

For every pixel (d_{1j}, … , d_{kj}) in the study area, we compute the score of the favourability function, $\boldsymbol{f}$(d_{1j}, … , d_{kj}). To display these favourability scores, $\boldsymbol{f}$(d_{1j}, … , d_{kj})'s on a map, instead of the original favourability scores, we use their **rankings**.

If two pixels with two favourability scores are considered, the pixel with higher score is more likely to host a VMS deposit than the other pixel with lower score. This is because the favourability score measures only relative significance for VMS deposits. Identically, the ranks also measure relative significance for VMS. The only difference between the ranks and the scores is their distribution, that is, the ranks are always evenly distributed (normalized to range from ~0 to 1) but the distribution of the scores fluctuates vastly from case to case. The distributions are dependent on the integration procedures in (5.1), (5.2) and (5.3) and on how the decay functions have been established. The principal reason for using the ranks instead of the favourability scores is the even distribution of the ranks (the heights of the intervals in the histogram of the ranks are all identical).

To illustrate how to obtain a rank of a favourability score, consider the case study of the Hackett River area, NWT. From the expert's VMS integration procedure in (5.3) using the five weighted decay functions in Figure 8, 21,500,000 favourability scores (one at each pixel) were computed for the 21,500,000 pixels in the study area. We sort the 21,500,000 scores in decreasing order. Then the **rank** of the pixel with the largest score is 21,500,000 and the rank of the pixel with the smallest score is 1. The **normalized rank** of a pixel is obtained by dividing the rank of the pixel by the number of pixels in study area, 21,500,000. The normalized ranks range from 1 to 0.0000000465 (=1/21,500,000).

The normalized ranks of the pixels are used to assign the pixels to the "**potential**" classes. For convenience, the normalized ranks are simply referred to as "ranks" and the process is referred to as "ranking procedure." It is also referred to as "histogram equalization procedure" because the heights (i.e. the number of pixels in each class or the size of each class) of the intervals in the histogram of the ranks are all identical.

An advantage of the use of ranks is that they are easily interpretable. Consider a pixel with rank 0.998 in the Hackett River study area as an example. There are only 0.2% (=1-0.998) of the 21,500,000 pixels (i.e., 43,000 pixels) that have higher scores than that of the pixel. Suppose that we wish to select an area consisting of about 0.3% of the study area for further exploration, then we may select all pixels with the ranks higher than 0.997. On the other hand, if we suppose that there is sufficient funding to explore the best 50 km^2 in the study area, then all the pixels with rank higher than 0.994186 (=1-50/8600), consisting of 125,000 pixels, would be selected as the exploration target.

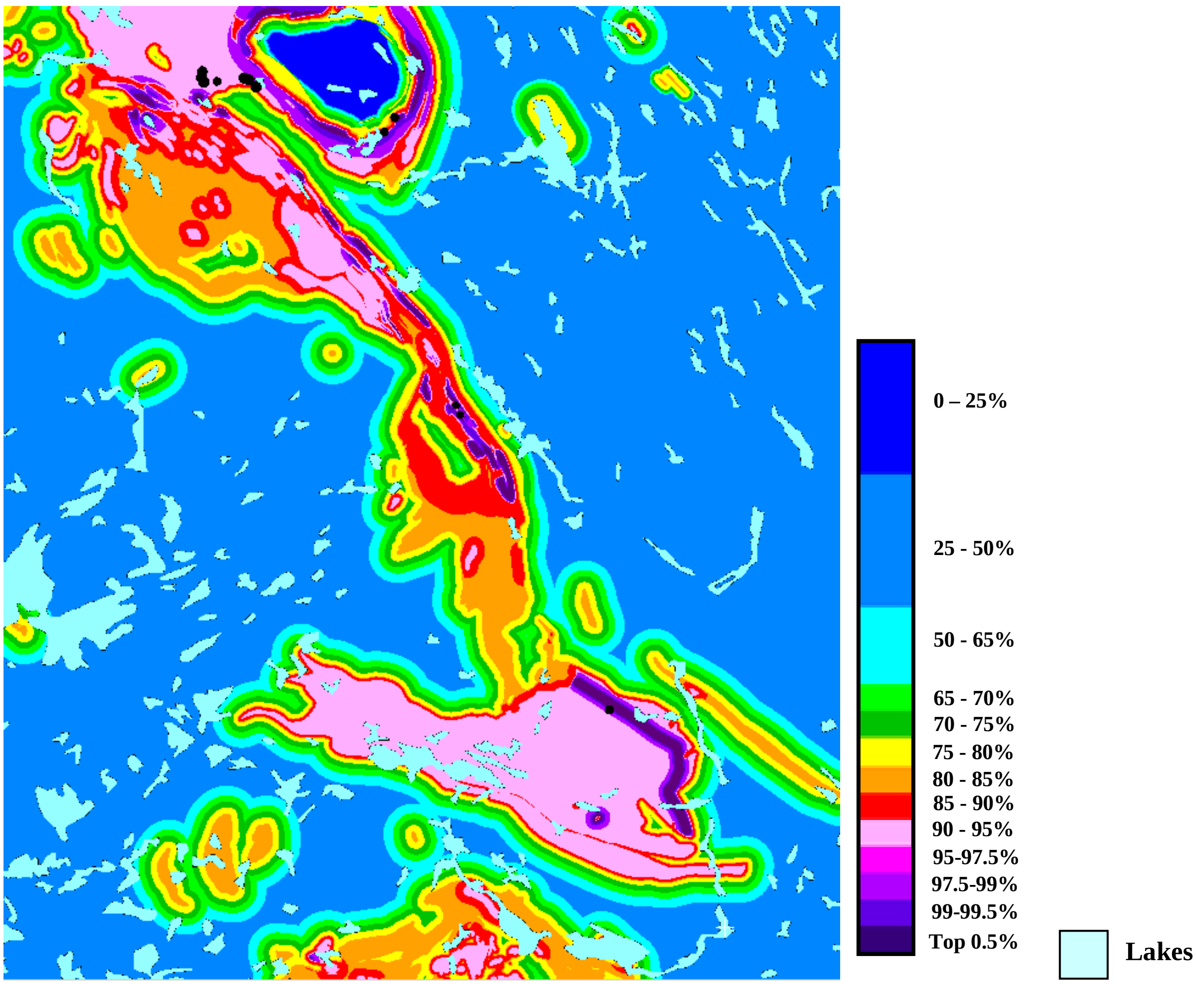

Figure 10. VMS potential map using the expert's VMS integration procedure in section 5.3, based on the five weighted decay functions in Figure 8 for the five key criteria in the Hackett River area, NWT, Canada. The 12 known VMS deposits are plotted as black dots.

For Figure 10, the potential classes were assigned by slicing the ranks. The "Top 0.5%" class, the class most likely to contain VMS deposits, consists of the pixels with the ranks higher than 0.995. The next highest potential class, "99-99.5%", contains the pixels with the ranks between 0.99 and 0.995. Each of these two highest potential classes occupies 43 km^2 of the 8,600 km^2 in the study area (0.5% of the study area of 21,500,000 pixels of 400m^2 (=20m x 20m)). Similarly the other 11 potential classes are established by slicing the ranks instead of the favourability scores.

It is extremely difficult (if not impossible) to compare two potential maps generated directly from these two sets of favourability scores. However, if the **ranks** instead of the favourability scores are used for generating potential maps, the potential maps are standardized and hence they can be compared with each other. For example, instead of using the Expert's VMS integration procedure in (5.3), we used the minimum procedure in (5.1) to generate the favourability function based on the same five weighted decay functions in Figure 8. We computed 21,500,000 favourability scores and generated the 13 potential classes using the ranks as we did for Figure 10. This is shown in Figure 11.

The "Top 0.5%" classes in the two potential maps in Figures 10 and 11, both occupy 43 km^2.

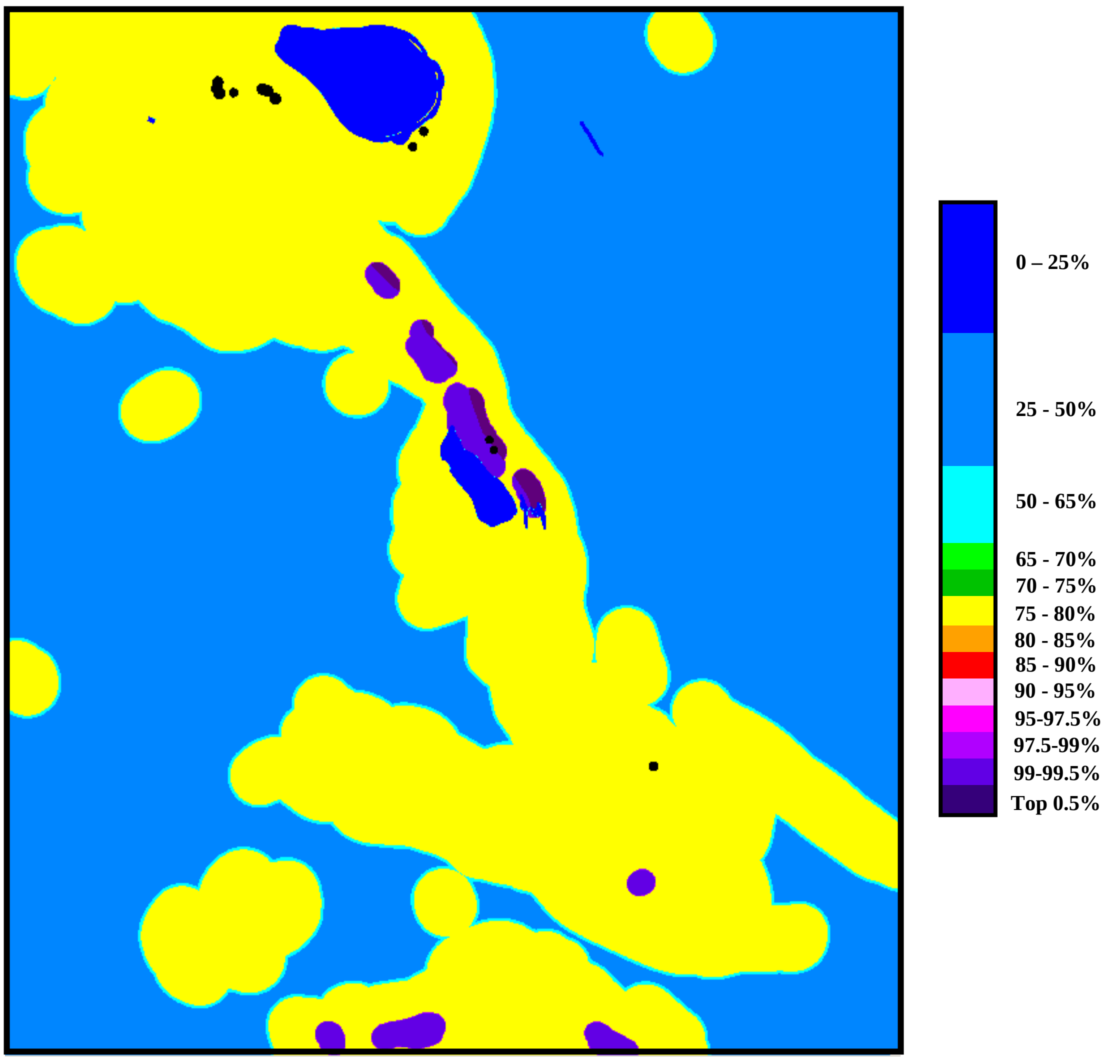

Figure 11. VMS potential map using the minimum integration procedure in section 5.1, based on the five weighted decay functions in Figure 8 for the five key criteria in the Hackett River area, NWT, Canada. The 12 known VMS deposits are plotted as black dots.

5.6. Evaluation of a potential map from a favourability function

In Figures 9, 10 and 11, we have three potential maps for VMS deposits in the Hackett River area, NWT. The next obvious question to ask is: "*how well do these three approaches work to "discover" the VMS deposits?*" There are 12 discovered VMS deposits in the Hackett River area and we will use them to evaluate the potential maps. Considering that the ranks were obtained by ordering the favourability scores of a potential map, we expect that the ranks of the pixels containing (or very close to) the deposits are very high (near "1" the maximum rank) and we will use them to obtain a measure of effectiveness of the potential map for the next discovery. The ranks of the pixels containing the deposits are termed the "**prediction rates**" of the potential map.

Obviously, the number of prediction rates of a potential map is the same as the number of discovered deposits in the map. Table 5 contains three sets of 12 prediction rates of three potential maps shown in Figures 9, 10 and 11. To examine a set of 12 prediction rates simultaneously, we use the empirical frequency distribution function (histogram) and its cumulative distribution function. Three blue, red and green histograms and cumulative frequency distributions corresponding to the three columns in Table 5 are shown in Figures 12.A and 12.B, respectively.

Table 5. 12 VMS deposits in Hackett River area, NWT. A deposit number was assigned to each deposit, and shown in the first column (Deposit #). The ranks at the pixels corresponding with the 12 deposits in Figures 9, 10 and 11 are included in the 2nd, 3rd and 4th columns, respectively.

Deposit #	Ranks in Figure 9	Ranks in Figure 10	Ranks in Figure 11
1	0.912	0.986	0.796
2	0.912	0.936	0.796
3	0.806	0.981	0.796
4	0.912	0.936	0.796
5	0.912	0.936	0.796
6	0.912	0.936	0.796
7	0.912	0.936	0.796
8	0.816	0.992	0.796
9	0.912	0.936	0.796
10	0.912	0.995	0.999
11	0.912	0.936	0.796
12	0.912	0.997	0.993

For the potential map shown in Figure 10, based on the integration procedure in (Eq. 5.3) and the five decay functions (shown in Figure 8), all 12 prediction rates (ranks of all 12 deposits) are greater than 0.936. However, only two deposits (#10, 12) have prediction rates that are greater than 0.936 for the potential map shown in Figure 11, based on the minimum integration procedure in (Eq. 5.1) and the same five decay functions (shown in Figure 8). There is no deposit whose prediction rates are greater than 0.936 for Figure 9. It suggests that the potential map in Figure 10 is the most useful to "find" the deposits, and therefore it is the best for evaluating the potential for discovery of new deposits.

To generate the histograms in Figure 12A, the prediction rates were divided into 50 potential classes of equal size of 172 km^2 (each of 2% of the whole study area consisting of 8600 km^2). The class with the highest discovery potential, or "Top 2%" (consisting of all pixels with the ranks greater than 0.98) contains the five deposits (#1, 3, 8, 10, 12) in Figure 10 (See the 3rd column in Table 5). However, only two deposits (#10, 12) are contained in the "Top 2%" for Figure 11. Again, it implies that Figure 10 is a "better" potential map than Figure 11. If we compare one potential map with another potential map, the empirical cumulative distribution functions shown in Figure 12B become particularly useful.

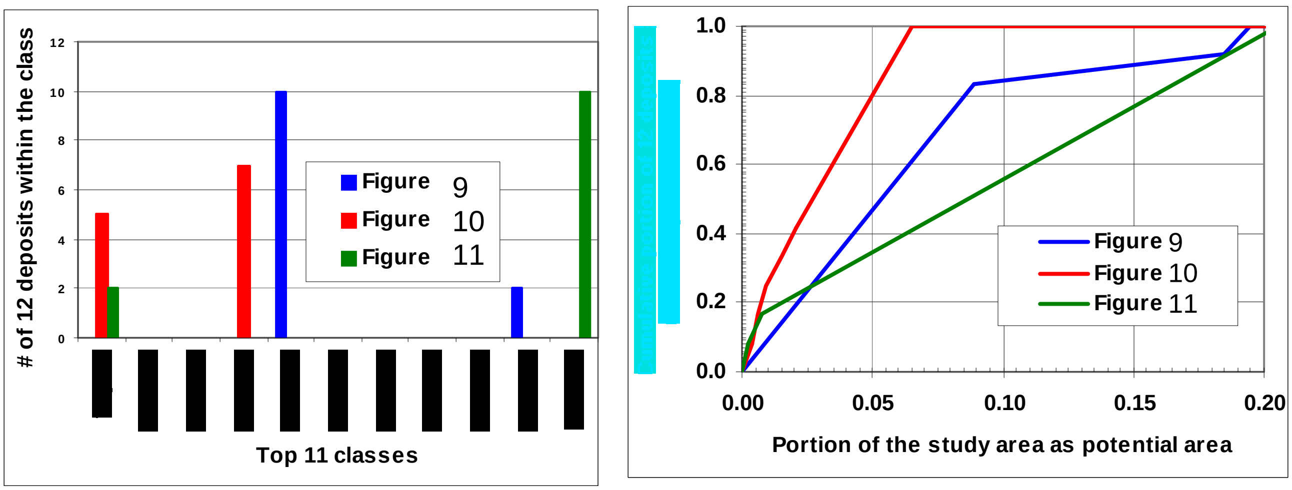

A B

Figure 12. A. Histograms of the three columns in Table 5. B. The corresponding cumulative frequency distribution functions.

5.7. Uncertainty of a potential map from a favourability function – Use of "Likelihood of correct identification" – MODEL I

In a potential map such as the one shown in Figure 10, the level of reliability is not expected to be the same for every pixel. In the study area, some sub-areas are more reliable than other sub-areas. In the previous section, for a VMS deposit potential map, we studied the issue of establishing "how good/useful is the whole potential map for "discovering" a VMS deposit." A solution was obtained by looking at the ranks of the discovered deposits in the study area. In this section, we are evaluating at every pixel the *reliability* (or *confidence*) of the potential map.

As discussed, two components, (i) the favourability function integrating five decay functions and (ii) the five data layers based on five criteria, were generated to obtain the potential map in Figure 10. At every pixel, using the pixel values of the five data layers, the favourability function computes the favourability score. The scores were used to generate that potential map. If the pixel values of the five data layers are adjusted, then the scores are altered, and consequently the potential map will also be altered.

In Table 1, the column entitled “likelihood of correct identification” is related to the “***confidence***” that units that we have identified on the map as matching one of the five key criteria is correctly identified, or at least related to the VMS-forming process in some way. The confidence in each criterion is quantized as a number between 0 and 1, where 1 represents “*absolutely confidence*” and 0 being “*no confidence*.” For example, while the likelihood of correct identification of “submarine volcanic rocks” is 1, the likelihood of correct identification of “exhalite horizon” is 0.5. This suggests a probability of 50% that the data layer identified on the map as “exhalite horizon” is, in fact an exhalite unit that really is related in some genetic way to the VMS-forming process, while the probability for “submarine volcanic rocks” in the Hackett river map sheet, shown in Figure 5, is “absolutely correct.” In other words, a unit identified as “exhalite” on the map has only a 50% chance of having a direct genetic tie to the presence of deposits; alternatives include exhalite-like horizons such as banded iron formation that may bear no genetic relationship to VMS deposits. We can reduce this uncertainty by determining if the exhalite is in the same district as felsic volcanic rocks, because in this case, there is a much better chance (based on observations in many districts) that such exhalite is related to the VMS-forming process. This type of “feedback loop” can be built into our model. When a measure of confidence of a data layer as being correctly assigned to the genetic process related to the presence of deposits is about 50%, as is the case in the exhalite horizon data layer, any pixel value should be considered a “*random variable.*” That means that we do not have a fixed value, but that the pixel value should have a distribution function with a range. Consequently we need to establish how much such a measure of confidence influences the final potential map.

As a first attempt to understand such influences in the potential map, let us consider (1) a hypothetical data layer with the confidence 0.5, and (2) the corresponding slow decay function with the maximum distance of 3000m, shown in Figures 13 and 14, respectively. The middle black circle represents the geologic unit. However, because of the confidence 0.5, the black circle possibly is as small as the white circle inside or as large as the white circle outside. Consider a pixel, 1000m from the rock type shown as a white dot in Figure 13. According to Figure 13, the pixel is 1000m from the boundary of the rock type. Considering the confidence being 50% only, the distance is likely to be 1000m but it could be anywhere between 1000 $\pm$ the distance-range “**m**”. Of course, the distance-range depends on the level of confidence; the higher the level, the narrower the range. To illustrate, let us assume that the distance-range is 500m for 50% confidence. Under that assumption, the distance could be any value between 500m to 1500m instead of a fixed 1000m. Using the decay function as the black curve in Figure 14, the pixel with 1000m should have the score of 0.6, but it could have a value between 0.32 (blue curve at 1000m) and 0.88 (red curve at 1000m), because of the 50% confidence. The red curve in Figure 14 was generated by shifting the black decay function by 500m to the right and the blue curve was generated by shifting the function by 500m to the left. The example illustrates that we may be able to modify the decay function to accommodate the confidence of the data layer (through the Likelihood of correct identification) instead of modifying the data layer itself.

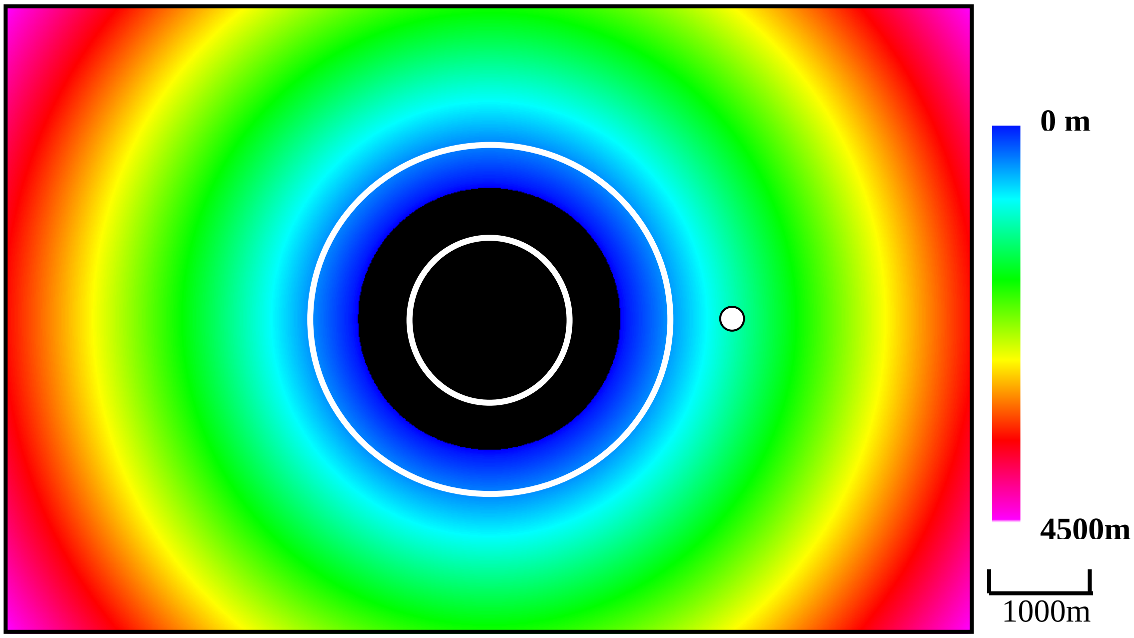

Figure 13. A hypothetical data layer with the black solid circle representing the geologic unit. The white dot represents a pixel at the distance 1000m from the unit.

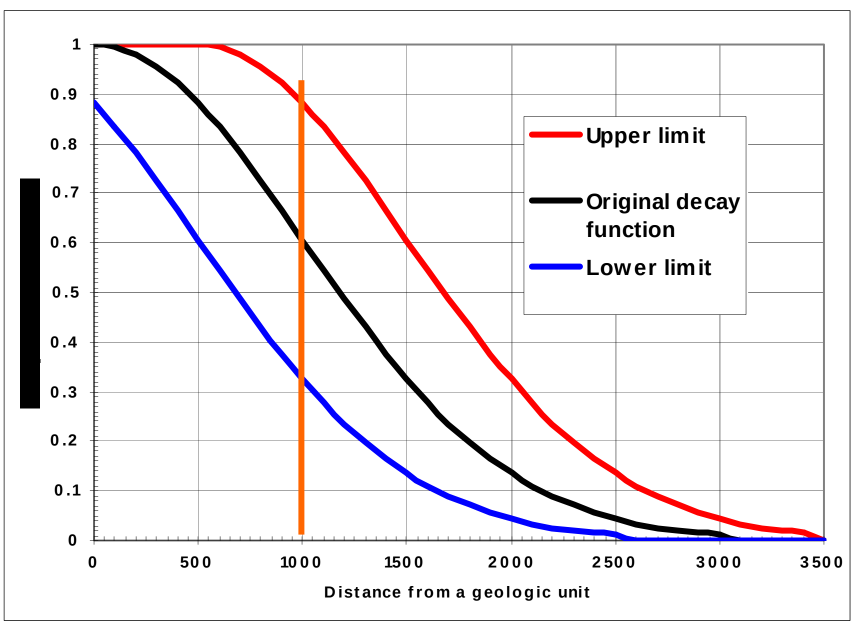

Figure 14. A hypothetical slow decay function with the maximum distance 3000m shown in black curve with the upper limit (in red curve) and the lower limit (in blue curve) obtained by shifting the decay function by 500m to each side. The vertical orange line at 1000m represents the situation of the pixel at the distance of 1000m, such as the white dot in Figure 13.

For example, under the assumption that the distance-range is 500m for the 50% confidence, instead of the value 0.6 of the decay function (black curve), the value of the decay function should be a number in the decay-function-range [0.32, 0.88], i.e., the crossing points of the orange line and three decay functions. If we make an additional assumption that the frequency of the values to be assigned is the triangular frequency distribution function illustrated in Figure 15A, with mode d = 0.6 and decay-function-range [a = 0.32, b = 0.88], the frequency of the value 0.6 is the highest. Hence, 0.6 has the highest probability to be selected as the decay function value representing the pixel with the distance between 500m to 1500m instead of a fixed 1000m. However, it should be noted here that it is not necessary that 0.6 be selected, but any number between 0.32 and 0.88 can be selected according to the triangular frequency distribution function. If we were to make an assumption of the uniform frequency distribution function illustrated in Figure 15B with the range [0.32, 0.88], the frequencies of any values in [0.32, 0.88] are all equal and hence any value has an equal probability to be selected as the decay function value representing the pixel with the distance between 500m to 1500m instead of a fixed 1000m.

In summary, to make this idea workable for each key criterion, we made two additional assumptions: (1) about the relationship setting the distance-range for a level of confidence in the "likelihood of correct identification" (in the above example, 500m for 0.5), and (2) about a frequency distribution function with the decay-function-range obtained by shifting the decay function by the distance-range for selecting a decay function value.

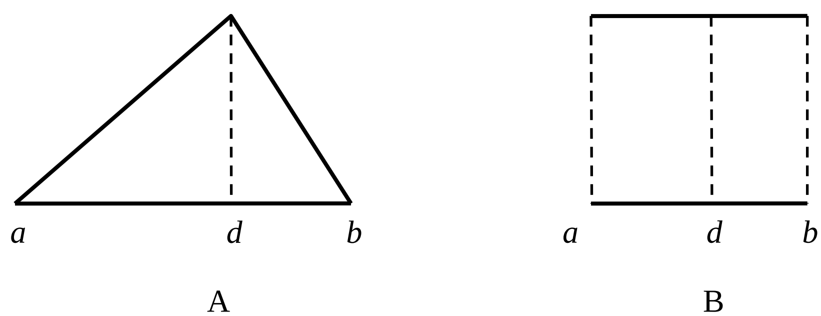

Figure 15. A. Triangular frequency distribution function with mode d and the decay-function-range [a, b]. B. Uniform frequency distribution function with the decay-function-range [a, b].

To evaluate the reliability at every pixel in the VMS potential map in the Hackett River area shown in Figure 10, we assumed: (1) the maximum distance range is 1000m; (2) a simple rule that the distance range t can be computed by:

$$t = 1000\,(1 - v); \qquad \text{(Eq. 5.4)}$$

where v (between 0 and 1) is the level of confidence is the value shown in "likelihood of correct identification" and (3) a decay function value is selected by using the triangular frequency distribution function shown in Figure 15A with the decay-function-range obtained by shifting it by the distance-range, t.

For the VMS potential map in the Hackett River area, the distance-ranges for all five criteria were computed using (Eq.5.4) with the above three assumptions. They are shown in Table 6. Figures 16A and 16B provide the five weighted decay functions shown in Figure 7 and the corresponding upper and lower limits of the decay function by shifting the functions by the distance-ranges.

Because of the likelihood of correct identification for submarine volcanic rocks being 1, absolute confidence, 0 is assigned for the distance-range, and consequently the lower and upper limits of decay function are the same as the decay function itself. However, the weighted decay function (green curve) for exhalite has been shifted by 500m to the left for the lower limits and 500, to the right for the upper limits, shown in Figure 16A as a green curve with circles and a green curve with * symbols, respectively. In contrast, the shifting of the humped decay function for the major underpinning subvolcanic intrusion is not a simple procedure because of the non-monotonic property of the humped decay function. The lower and upper limits of the decay function are shown as a grey curve with circles and with *, respectively.

Criterion (Legend unit in Fig. 16)	**Likelihood of Correct Identification**	**Distance-range using (Eq.5.4)**	**Weighted Decay Function at 500m**	**Lower Limit of Decay Function at 500m**	**Upper Limit of Decay Function at 500m**
submarine volcanic rocks (Sub.-volcanics)	1	0	0.37	0.37	0.37
felsic volcanic rocks (F.V.)	0.9	100	0.29	0.18	0.44
exhalite horizon (E.H.)	0.5	500	0.26	0.01	0.80
shallow-level subvolcanic intrusion (S.S.I.)	0.75	250	0.13	0.03	0.29
major underpinning subvolcanic intrusion (M.S.I.)	0.5	500	0.52	0.23	0.52

Table 6. The distance-ranges, the values of the weighted decay function at 500m and the corresponding lower limits and upper limits of the decay functions from Figures 16A and 16B for the five key criteria for VMS deposits. The values of the last three columns were obtained from the crossing points with the orange lines represent all pixels with the distance 500m from the corresponding geologic units in Figures 16A and 16B.

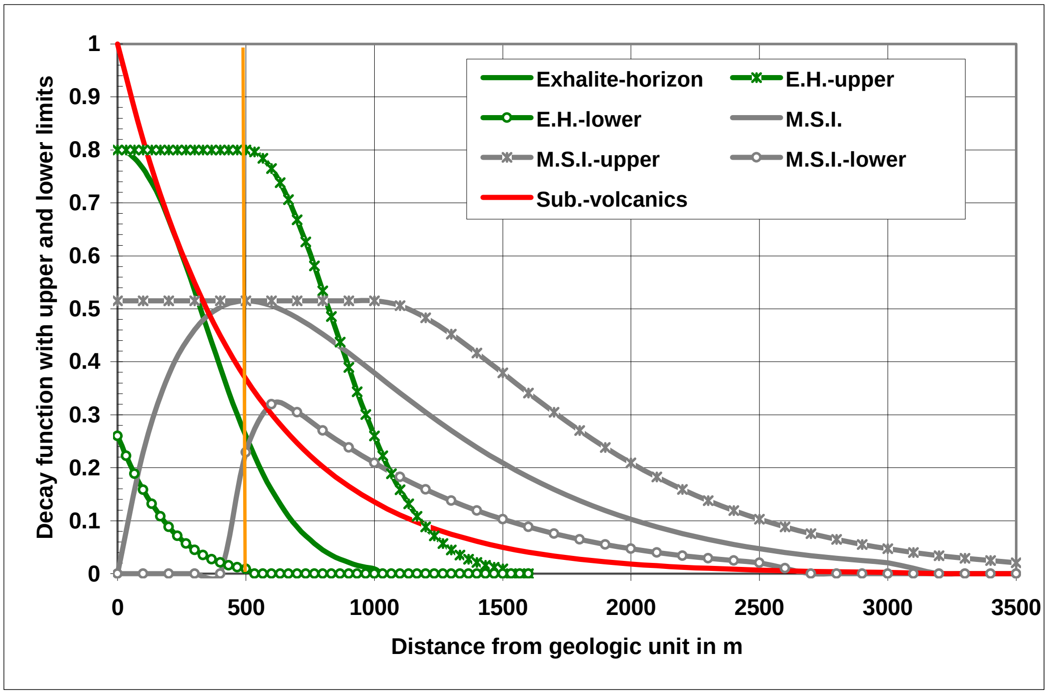

A

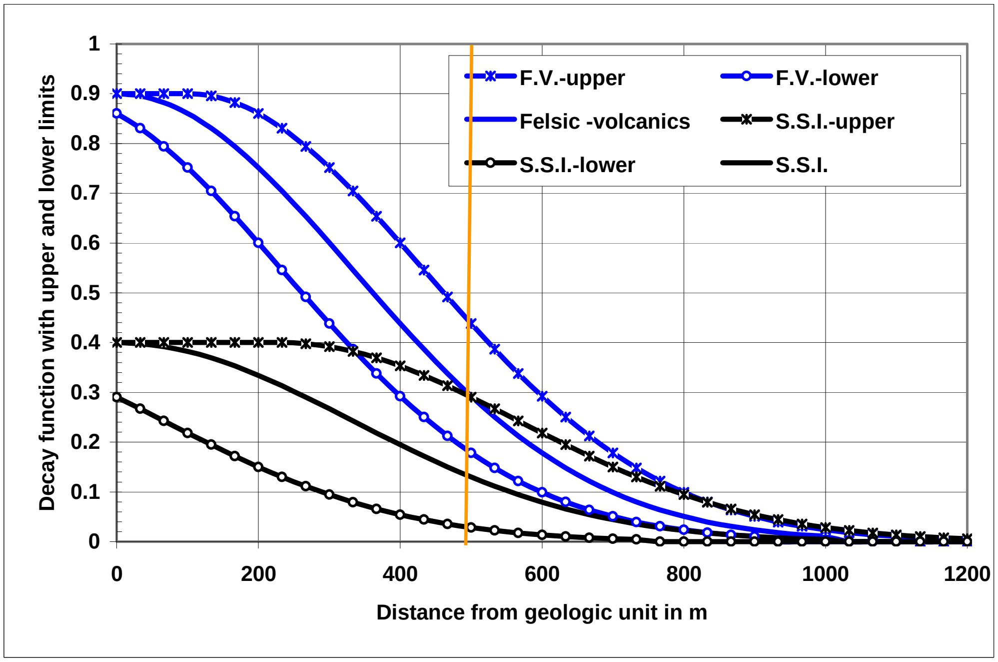

B

Figure 16. Five weighted decay functions and the corresponding upper and lower limits of the decay functions obtained by shifting the functions by the distance-ranges in Table 6. The crossing points with the orange lines represent all pixels at the distance of 500m from the corresponding geologic units and they indicate how the values of the last three columns in Table 6 were obtained.

Three integration rules were discussed earlier in (Eq. 5.1), (Eq. 5.2) and (Eq. 5.3), for a given pixel with values ($d_{1j}, \ldots, d_{5j}$). The favourability function $f(d_{1j}, \ldots, d_{5j})$ was computed using the five fixed values ($f_1(d_{1j})$, $f_2(d_{2j})$, $f_3(d_{3j})$, $f_4(d_{4j})$, $f_5(d_{5j})$) from the decay functions. However, except for $f_1(d_{1j})$ for the first criterion with the confidence being 1, the remaining four values, $f_2(d_{2j})$, $f_3(d_{3j})$, $f_4(d_{4j})$ and $f_5(d_{5j})$ are no longer fixed values: each is a random variable, determined by following the triangular frequency distribution functions with the corresponding decay-distance-range. The final favourability function $f(d_{1j}, \ldots, d_{5j})$ is also a random variable with some unknown frequency distribution function at each pixel.

To generate the unknown frequency distribution function of the favourability score of a pixel, we carried out a *simulation experiment* consisting of four steps, at each pixel with ($d_{1j}, \ldots, d_{5j}$);

(Step.1) Compute the five fixed values ($\boldsymbol{f}_1(d_{1j})$, $\boldsymbol{f}_2(d_{2j})$, $\boldsymbol{f}_3(d_{3j})$, $\boldsymbol{f}_4(d_{4j})$, $\boldsymbol{f}_5(d_{5j})$) from the decay functions shown in Figure 8;

(Step.2) For $\boldsymbol{f}_2(d_{2j})$, generate the corresponding decay-distance range [a, b] using Figure 16B. For example, if d_{2j} is 500m, then $\boldsymbol{f}_2(d_{2j}) = 0.29$ and the range is [0.18, 0.44] as shown in Table 6. Select a random number, g_2 from the triangular distribution function with the mode $\boldsymbol{f}_2(d_{2j})$ with the range [a, b]. Similarly, for the remaining three values, $\boldsymbol{f}_3(d_{3j})$, $\boldsymbol{f}_4(d_{4j})$ and $\boldsymbol{f}_5(d_{5j})$, generate the corresponding random numbers, g_3, g_4 and g_5;

(Step.3) Follow the integration rule based on (Eq. 5.3):

$$\hat{\boldsymbol{f}}\,(d_{1j},\cdots,d_{5j}) = \begin{cases} \frac{1}{5}\left(\boldsymbol{f}_1\left(d_{1j}\right) + \boldsymbol{g}_2 + \boldsymbol{g}_3 + \boldsymbol{g}_4 + \boldsymbol{g}_5 \right) \text{ if } d_{2j}\text{, distance from Felsic v.} \le 1000\text{m} \\ \frac{1}{5}\left(\boldsymbol{f}_1\left(d_{1j}\right) + \boldsymbol{g}_3 + \boldsymbol{g}_5 \right) \text{ if } d_{2j}\text{, distance from Felsic v.} > 1000\text{m} \end{cases}$$

(Step.4) Repeat Step.2 and Step.3 ***n*** times (e.g., at least 1000 times).

From each repetition, we generate a potential map based on $\hat{\boldsymbol{f}}$ ($d_{1j}, \ldots, d_{5j}$) at each pixel and a potential map similar to that in Figure 10 was generated by using the ranking procedure discussed earlier. One thousand (1000) potential maps are generated from the simulation experiment. At every pixel, 1000 ranks from these 1000 simulated potential maps are examined. From the 1000 ranks at each pixel, we compute the *90 percentile-range* defined by:

90 percentile-range=950th highest rank – 50th lowest rank.

The 90 percentile-ranges are shown in Figure 17, coloured in 10 classes only. The class ">0.01" consists of all pixels whose 90 percentile-range is less than 0.01. It means that the ranks of the pixels in these class change less than 0.01 and the potential map covering the pixels in this class is the most reliable and trustworthy.

On the other hand, the pixels from the classes "0.04-0.05" change their ranks more than 0.04 (4% - 5%), and the potential map covering the pixels in this class is somewhat questionable and not reliable. We are going to use Figure 17, based on the 90 percentile-ranges, as the "uncertainty" map for the VMS potential map shown in Figure 10.

By selecting the pixels with the top three classes "> 0.01", "0.01-0.02", "0.02-0.03" in Figure 17, the potential map in Figure 10 is obtained covering the pixels selected, as shown in Figure 18. In it the remaining pixels are coloured as grey representing "high uncertainty area" and therefore somewhat not reliable and not-predictable areas in the potential map.

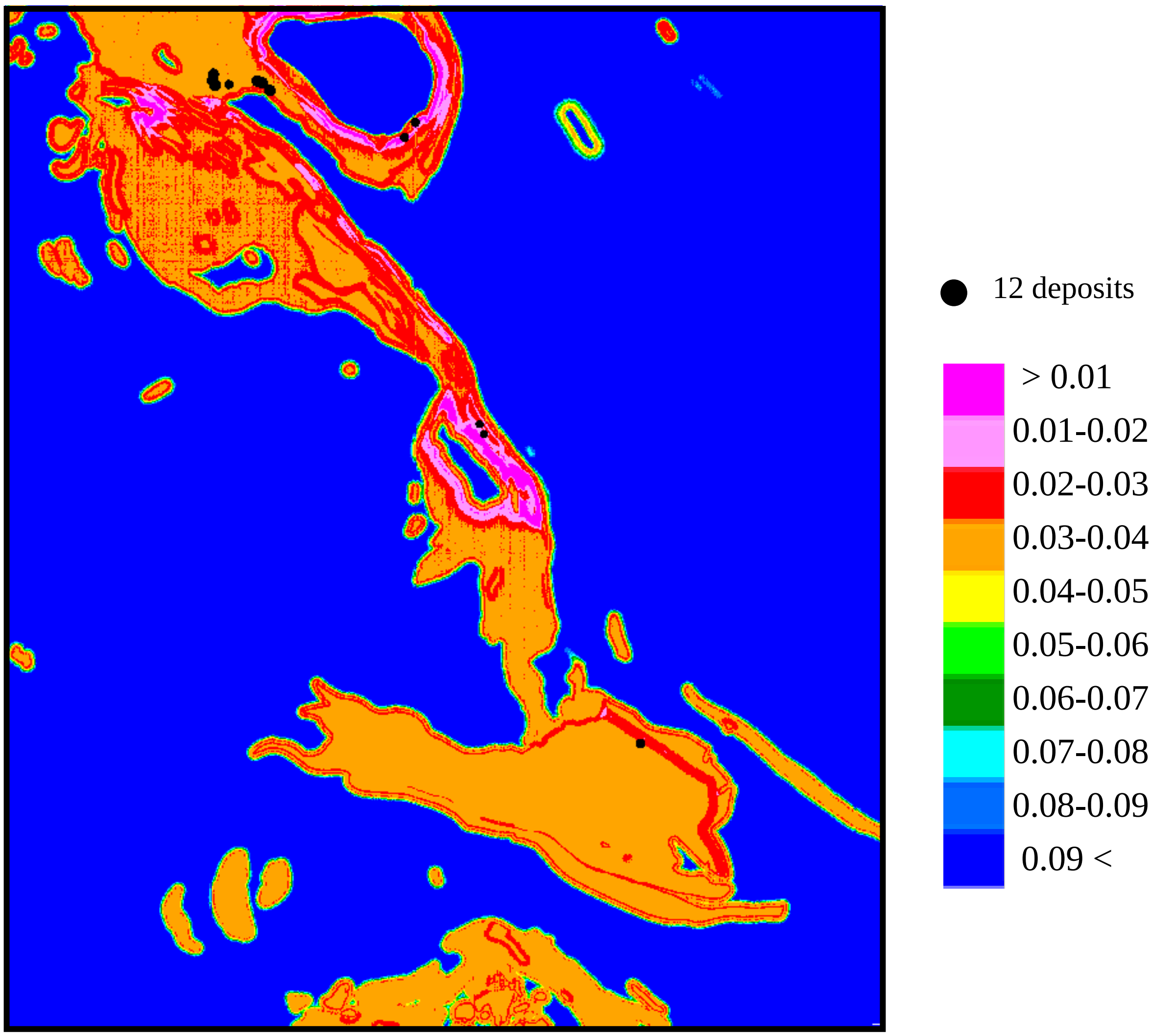

Figure 17 Uncertainty map for the VMS potential map shown in Figure 10 using 1000 simulation experiments based on the column "likelihood of correct identification" in Table 1.

As expected, the potential map will change as the conditions in the key criteria fluctuate. Each of the five weighted decay functions shown in Figure 9 directly depends on three factors in Table 1: (1) weighting factor; (2) maximum distance; and (3) the note containing the description. If any number or any description in the table should be changed, the favourability function also changes and consequently the favourability scores change. Obviously, the numbers and the descriptions are based on the best knowledge of the VMS system available, but none of them is an "*absolute* *truth*". Given that there are at least five sub-types of VMS (Franklin et al, 2005), some of the key characteristics may be less applicable in some of the districts to be surveyed. Therefore these numbers and descriptions and/or the key criteria themselves are expected to change as we better comprehend the VMS deposit-processes. Additionally these numbers and descriptions can be significantly different from one study area to another. If we can quantify the *variation* (or *uncertainty*) of these numbers in the key criteria, then we have made some progress in the simulation experiment.

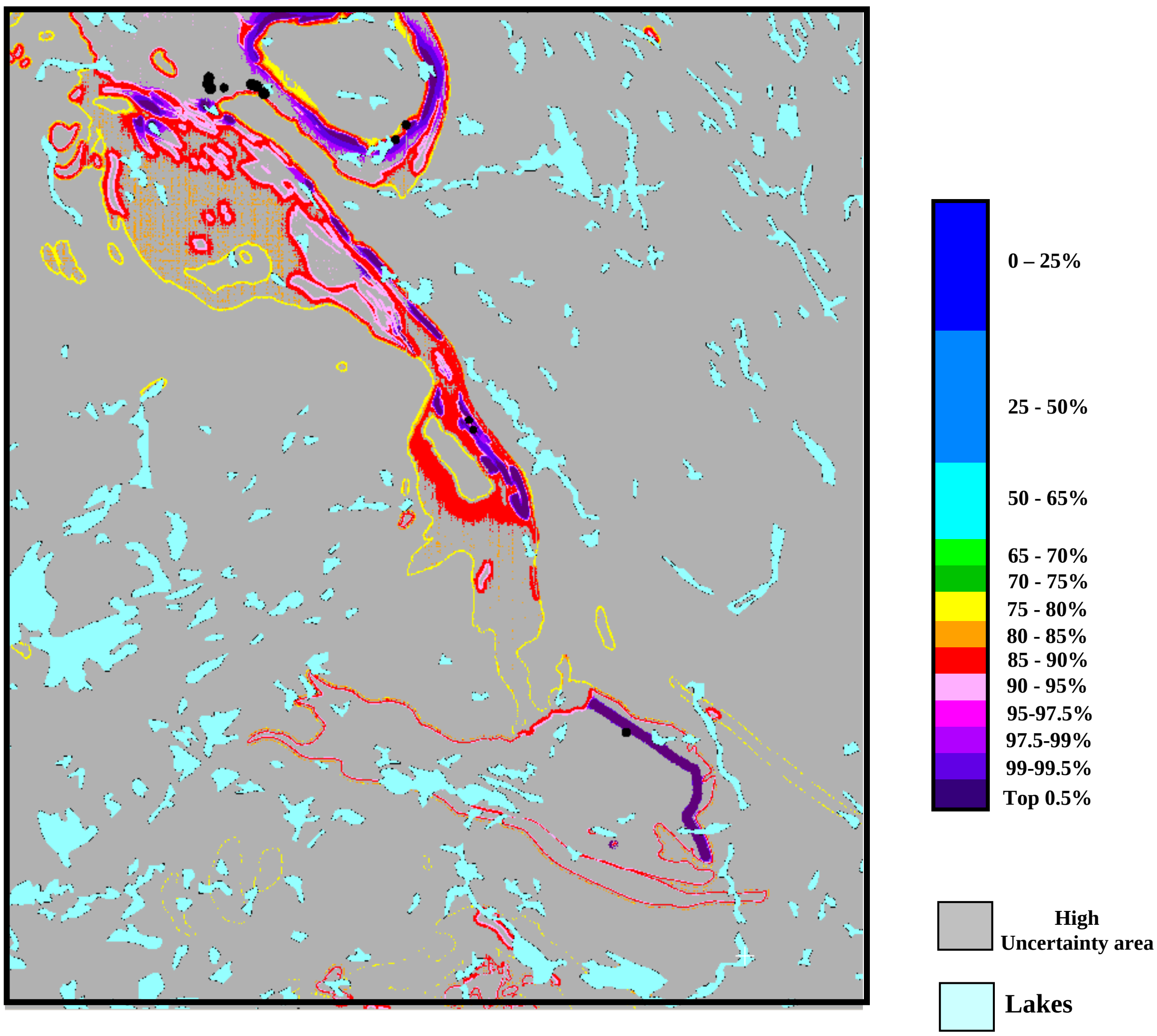

Figure 18. VMS potential map using the expert-based VMS integration procedure in section 5.3, based on the five weighted decay functions in Figure 8 for the five key criteria in the Hackett River area, NWT, Canada. The pixels with the top three classes "> 0.01", "0.01-0.02", "0.02-0.03" in Figure 17 are shown in colors, the remaining pixels are coloured as grey representing "high uncertainty area" and therefore they are considered somewhat not reliable and not-predictable areas in the potential map. 12 known VMS deposits are plotted as black dots.

5.8. Uncertainty of a potential map from a favourability function – Use of "Likelihood of correct identification" - MODEL II

We made a second attempt to understand the use of "likelihood of correct identification". Let us again consider the hypothetical data layer shown in Figure 13 with the confidence 0.5 and the same slow decay function in Figures 14 with the maximum distance of 3000m, also shown in Figure 19. Consider a pixel, 1000m from the rock type shown as a white dot in Figure 13. Instead of establishing the upper and lower limits shown in Figure 14 of the decay function by shifting the decay function by ± the distance-range, where the distance-range was computed by using Eq. 5.4, let us modify the upper and lower limits directly by computing the range [vd, $1-v+vd$], where d is the value of the decay function and v (between 0 and 1) is the value of "likelihood of correct identification." As discussed before, the value of the decay function for the pixels with 1000m from the rock type d = 0.6. Considering the confidence being only 50%, the range is [0.3(=vd=0.5*0.6), 0.8(=1-v+vd=1-0.5+0.3)]. It is somewhat similar to the range [0.32, 0.88] computed by shifting the decay function by 500m as discussed before. The upper and lower limits, as shown in Figure 19, are distinctly different from the upper and lower limits in Figure 14 by shifting the decay function by 500m. Using the decay function as a black curve in Figure 19, the pixel with 1000m should have the score of 0.6, but it could have a value between 0.3 (blue curve at 1000m) and 0.8 (red curve at 1000m) instead, because of the 50% confidence under the assumption imposed here.

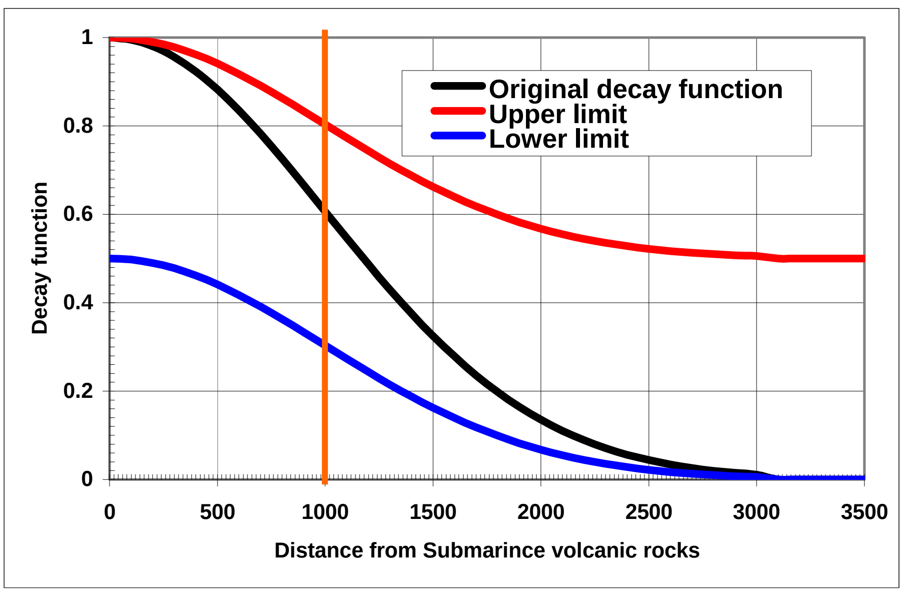

Figure 19. A. A hypothetical slow decay function with the maximum distance 3000m shown in black curve with the upper limit (in red curve) and the lower limit (in blue curve) obtained by computing the upper limit = $1- d + dv$ and the lower limit = dv where d is the value of the decay function and v (between 0 and 1) is the value of "likelihood of correct identification." The intersection points with the orange line represent pixels that are 1000m from the geologic units.

To evaluate the reliability at every pixel in the VMS potential map in the Hackett River area shown in Figure 10, we now assume: (1) a simple rule that the upper and lower limits for the level, v (between 0 and 1) of confidence in “likelihood of correct identification” at the value of decay function d, is:

$$\text{Lower limits} = vd \text{ and Upper limit} = 1 - v + vd \qquad \text{(Eq. 5.5)}$$

and (2) the triangular frequency distribution function shown in Figure 15A has the range $[vd, 1-v+vd]$.

For the VMS potential map in the Hackett River area, under the above two assumptions, the ranges for all five criteria were computed using (Eq.5.5). They are shown in Table 7. Figures 20A and 20.B provide the five weighted decay functions shown in Figure 7 and the corresponding upper and lower limits of the decay function by computing the ranges using (Eq. 5.5).

Because of the likelihood of correct identification for submarine volcanic rocks being 1 (absolute confidence), the lower and upper limits of decay function are the same as the decay function itself. However, the weighted decay function (green curve) for the criterion “exhalite horizon” has the lower limit as a green curve with circles and the upper limit as a green curve with * symbols.

Table 7. Values of the weighted decay function at 500m, and the corresponding lower limits and upper limits of the decay functions from Figures 20A and 20B, for the five key criteria for VMS deposits. The values of the last three columns were obtained from the intersection points of the curves with the orange lines, representing all pixels at a distance of 500m from the corresponding geologic units in Figures 20A and 20B.

Criterion (Legend unit in Fig. 20)	**Likelihood of correct identification**	**Weighted decay function at 500m**	**Lower limit of decay function at 500m**	**Upper limit of decay function at 500m**
submarine volcanic rocks (Sub.-volcanics)	1	0.37	0.37	0.37
felsic volcanic rocks (F.V.)	0.9	0.29	0.25	0.36
exhalite horizon (E.H.)	0.5	0.26	0.12	0.62
shallow-level subvolcanic intrusion (S.S.I.)	0.75	0.13	0.10	0.35
major underpinning subvolcanic intrusion (M.S.I.)	0.5	0.52	0.27	0.76

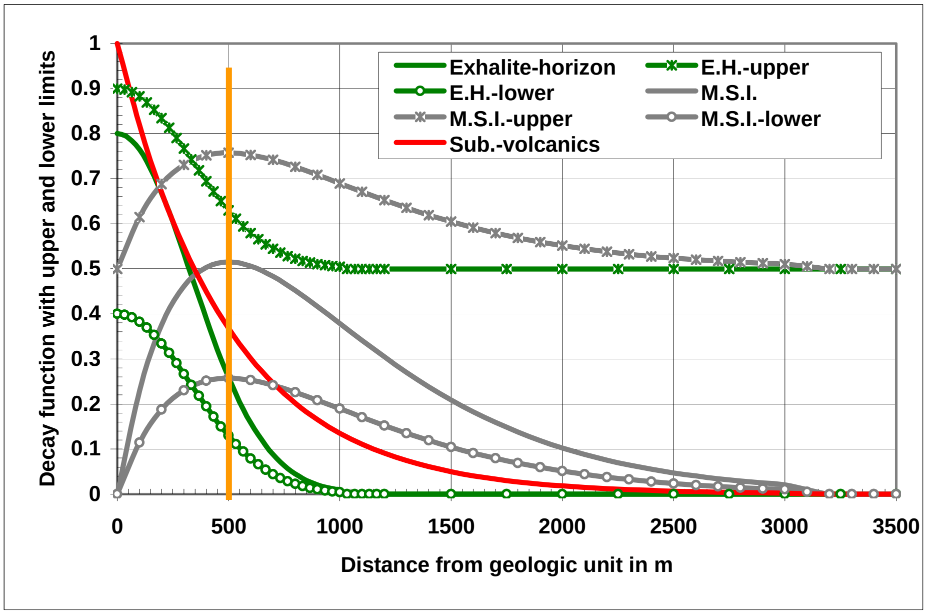

A

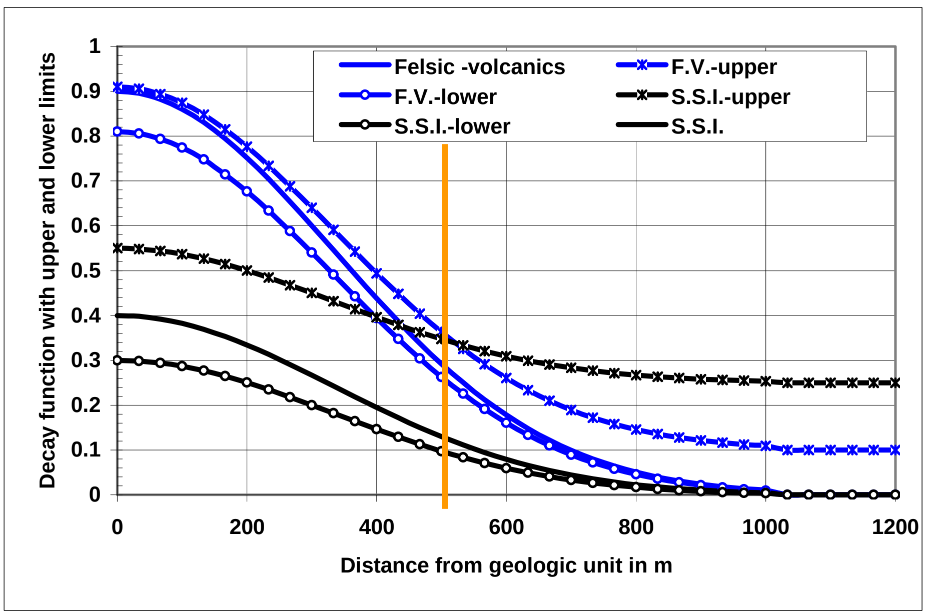

B

Figure 20. Five weighted decay functions and the corresponding upper and lower limits of the decay functions obtained by shifting the functions by the distance-ranges in Table 7. The intersection points with the orange lines represent all pixels at the distance of 500m from the corresponding geologic units.

As before, to generate the unknown frequency distribution function of the favourability score of a pixel, we carried out a *simulation experiment* consisting of four steps, at each pixel with (d_{1j}, … ,d_{5j});

(Step.1) Compute the five fixed values ($\boldsymbol{f}_1(d_{1j})$, $\boldsymbol{f}_2(d_{2j})$, $\boldsymbol{f}_3(d_{3j})$, $\boldsymbol{f}_4(d_{4j})$, $\boldsymbol{f}_5(d_{5j})$) from the decay functions shown in Figure 8;

(Step.2) For $\boldsymbol{f}_2(d_{2j})$, generate the corresponding decay-distance range [a, b] using Figure 20B. For example, if d_{2j} is 500m, then $\boldsymbol{f}_2(d_{2j}) = 0.29$ and the range is [0.25, 0.36] as shown in Table 7

. Select a random number, g_2 from the triangular distribution function with the mode $\boldsymbol{f}_2(d_{2j})$ with the range [a, b]. Similarly, for the remaining three values, $\boldsymbol{f}_3(d_{3j})$, $\boldsymbol{f}_4(d_{4j})$ and $\boldsymbol{f}_5(d_{5j})$, generate the corresponding random numbers, g_3, g_4 and g_5;

(Step.3) Follow the integration rule based on (Eq. 5.3):

$$\hat{\boldsymbol{f}}\,(d_{1j}, \ldots ,d_{5j}) = \begin{cases} \frac{1}{5}\left(\boldsymbol{f}_1\left(d_{1j}\right) + \boldsymbol{g}_2 + \boldsymbol{g}_3 + \boldsymbol{g}_4 + \boldsymbol{g}_5 \right) \text{ if } d_{2j}\text{, distance from Felsic v.} \le 1000\text{m} \\ \frac{1}{5}\left(\boldsymbol{f}_1\left(d_{1j}\right) + \boldsymbol{g}_3 + \boldsymbol{g}_5 \right) \text{ if } d_{2j}\text{, distance from Felsic v.} > 1000\text{m} \end{cases}$$

(Step.4) Repeat Step.2 and Step.3 ***n*** times (e.g., at least 1000 times).

From each repetition, we generate a potential map based on $\tilde{\boldsymbol{f}}$ (d_{1j}, … ,d_{5j}) at each pixel and a potential map similar to that in Figure 10 was generated by using the ranking procedure discussed earlier. The 1000 potential maps are generated from the simulation experiment. At every pixel, 1000 ranks from these 1000 simulated potential maps are examined. From the 1000 ranks at each pixel, we compute the *90 percentile-range* defined by:

90 percentile-range=950th highest rank – 50th lowest rank.

The 90 percentile-ranges are shown in Figure 21 coloured in 10 classes only. The class “>0.01” consists of all pixels whose 90 percentile-range is less than 0.01. It means that the ranks of the pixels in these class change less than 0.01, and that the potential map covering the pixels in this class is the most reliable and trustworthy.

On the other hand, the pixels from the classes “0.04-0.05” change their ranks more than 0.04 (4% - 5%), and the potential map covering the pixels in this class is somewhat questionable and not reliable. We are going to use Figure 22, based on the 90 percentile-ranges, as an “uncertainty” map for the VMS potential map shown in Figure 10.

By selecting the pixels with the top three classes “> 0.01”, “0.01-0.02”, “0.02-0.03” in Figure 17, the potential map in Figure 10 is obtained covering the pixels selected, as shown in Figure 22. In it the remaining pixels are coloured as grey representing “high uncertainty area” and therefore somewhat not reliable and not-predictable areas in the potential map.

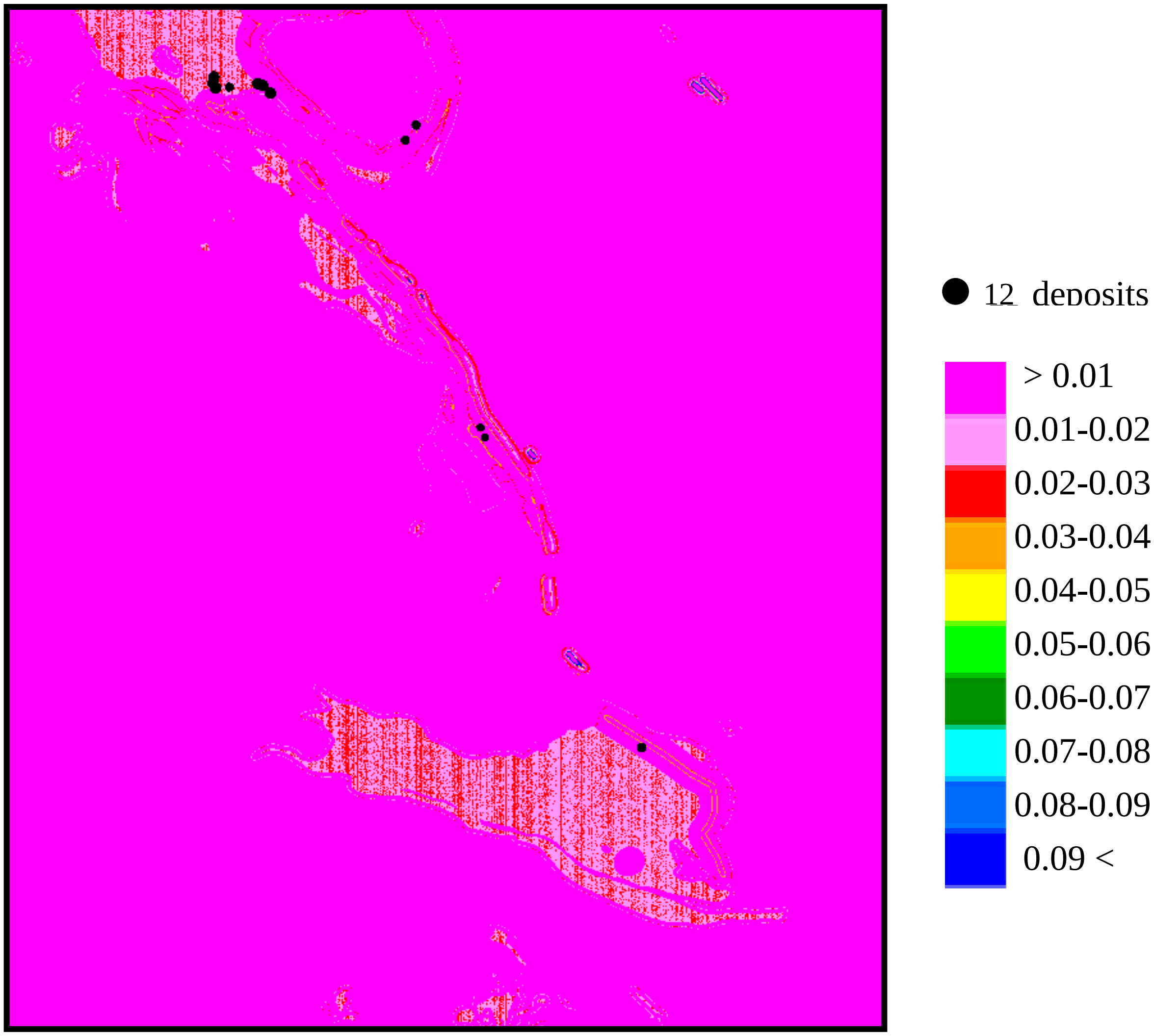

Figure 21 Uncertainty map for the VMS potential map shown in Figure 10 using 1000 simulation experiments based on the column "Likelihood of correct identification" in Table 1.

As expected, the potential map will change as the conditions in the key criteria fluctuate. Each of the five weighted decay functions shown in Figure 9 directly depends on three factors in Table 1: (1) weighting factor; (2) maximum distance; and (3) the note containing the description. As any number or any description in the table change, the favourability function also changes and consequently the favourability scores change. Obviously, the numbers and the descriptions are based on the best geological knowledge on the VMS deposits that we can obtain, but each has some measure of uncertainty attached to it. Therefore these numbers and descriptions and/or the key criteria themselves are expected to change as we better comprehend the VMS deposit-forming processes. Additionally these numbers and descriptions may be significantly different from one study area to another. If we can quantize and specify the *variation* (or *uncertainty*) of these numbers in the key criteria, then we have made some progress in the simulation experiment.

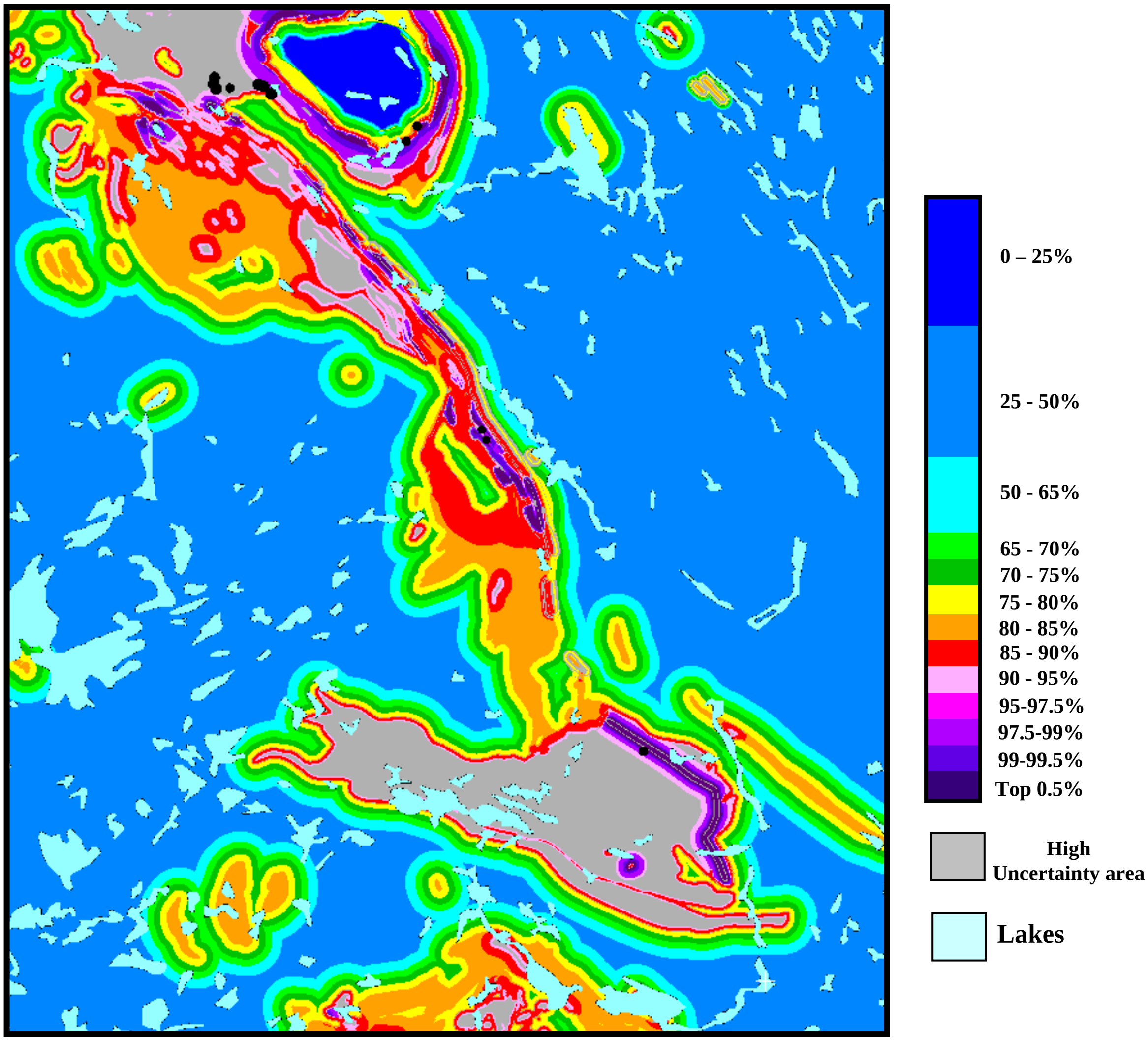

Figure 22. VMS potential map using the expert's VMS integration procedure in section 5.3, based on the five weighted decay functions in Figure 8 for the five key criteria in the Hackett River area, NWT, Canada. The pixels with the top three classes "> 0.01", "0.01-0.02", "0.02-0.03" in Figure 21 are shown in colors, the remaining pixels are coloured as grey representing "high uncertainty area" and therefore they are considered somewhat not reliable and not-predictable areas in the potential map. 12 known VMS deposits are plotted as black dots.

6.0 Assessment of the Whitehills Lake area, Nunavut

We selected this area because it is in the western Churchill (Northern Rae) province, and was recently mapped by (Zaleski and Pehrsson 2005) . This provided us with the opportunity to examine the application of the method to an area where a robust digital data set was developed. The geological setting is more complicated than that for the Hackett River area, in that both Archean and Proterozoic strata are present. The area (Figure 23) consists of a typical greenstone belt, with abundant felsic volcanic strata, a major capping exhalite unit, and an excellent candidate for a subvolcanic intrusive complex.

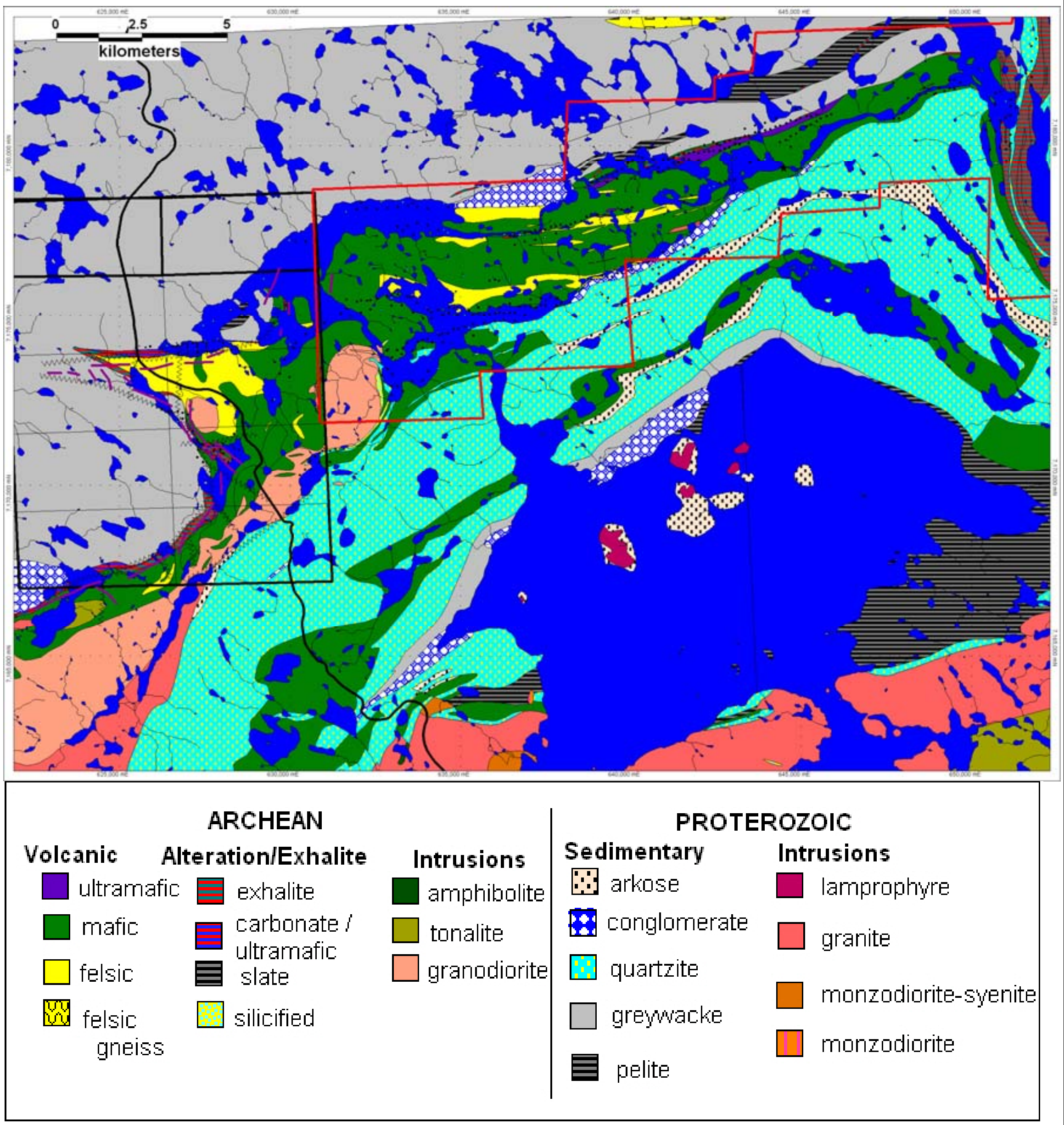

Figure 23: Geology of the Whitehills Lake area (After Zaleski and Pehrsson, 2005). The legend was simplified as per the description below (UTM NAD 83 Zone 14).

The Whitehills Lake map was accompanied by an extensive spreadsheet of point data, which included data on structure, key mineral assemblages and geochronology. Although these data were not used in the current assessment, some of the data, particularly the mineral assemblage information, could be very valuable in improving our approach in future. For example, Zaleski and Pehrsson (2005) noted the presence of epidote-actinolite-quartz alteration in the mafic volcanic rocks. This is a key assemblage that indicates the zone of high-temperature reaction (see Figure 2, #2) that would provide an even stronger indication of VMS potential.

The legend accompanying the map was similarly challenging to "parse" into usable form. Each legend item combines the age (Archean), the formational unit name (as a single letter), the major rock type and its rock series modifier (e.g. volcanic, felsic), and in some cases, additional information such as alteration. These are all concatenated into a single, variable-length legend item that was somewhat difficult to parse into the most important information that we required, that is the rock type (e.g. felsic volcanic). Furthermore, in the point data, as well as the text description for each polygon, it was apparent that a significant intrusive complex (granodiorite on the map) at the base of the Archean volcanic assemblage, was possibly a subvolcanic intrusion, and that a small intrusion of a similar composition that occurs within the basal part of the felsic complex was a high-level subvolcanic intrusion. We thus, in simplifying the legend, assigned these (with appropriate uncertainty) to these lithologies.

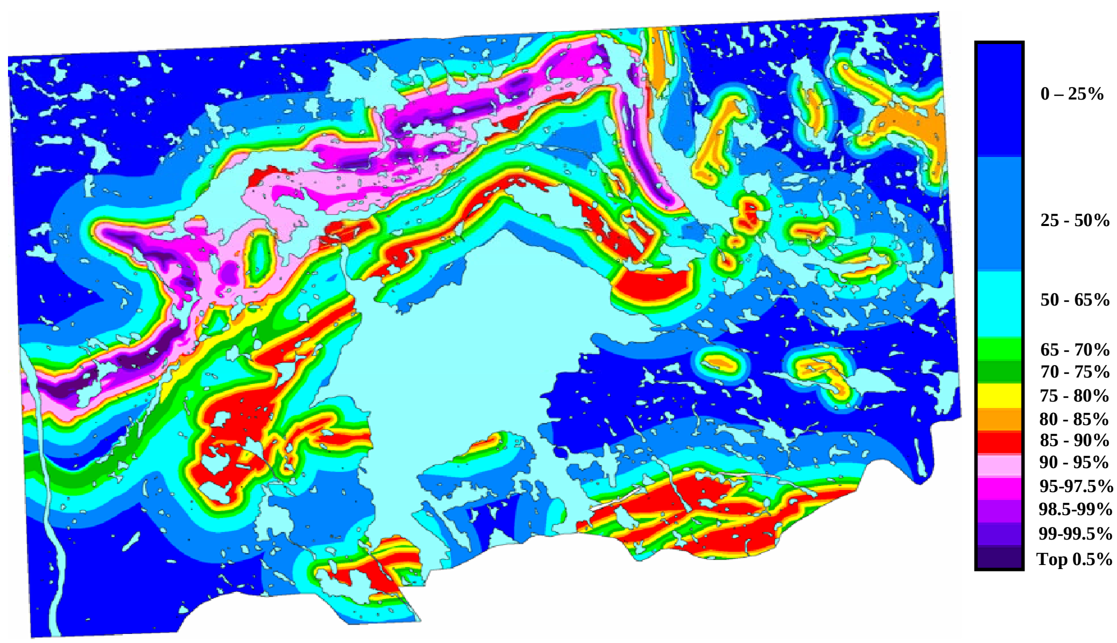

Figure 24: Potential for discovery of VMS deposits, Whitehills Lake area, Nunavut.

We used the same key criteria as for Hackett River, including the five criteria to establish five "layers" or maps depicting the potential for VMS deposits for each criterion. The criteria were weighed according to Table 1, and we applied the same "decay" curves to modify the weighting as a function of distance from the "key criteria" as were used for the Hackett River case (above). The results from the five "layers" were added to make the prediction map in Figure 24.

Figure 24 llustrates that the best potential for VMS deposits is within the northwestern-most part of the volcanic sequence, and generally corresponds to the units of felsic volcanic rock and immediately adjacent mafic volcanic strata. These generally correspond well to recent discoveries made in this area (Aura Resources Ltd. Press Release # 09-01, February 9, 2009).

The second step is to create an uncertainty map, following the same procedures in section 5.7 as outlined for Hackett River. As in Hackett River, the reliability of our estimate at each pixel is not equal. Following this procedure, the majority of the pixels are too sensitive to changes in the certainty of our lithological classification to be useful. We keep only those pixels that change by less than 10% during the simulation experiment. This method provides a more tightly constrained set of "high potential" pixels, which have more certainty as to their potential. The maps derived from this uncertainty analysis are shown in Figures 25 and 26.

Having removed the pixels with <90% uncertainty, we obtain a much better definition of the areas of highest potential (Figure 25). By then selecting only the uppermost three classes from

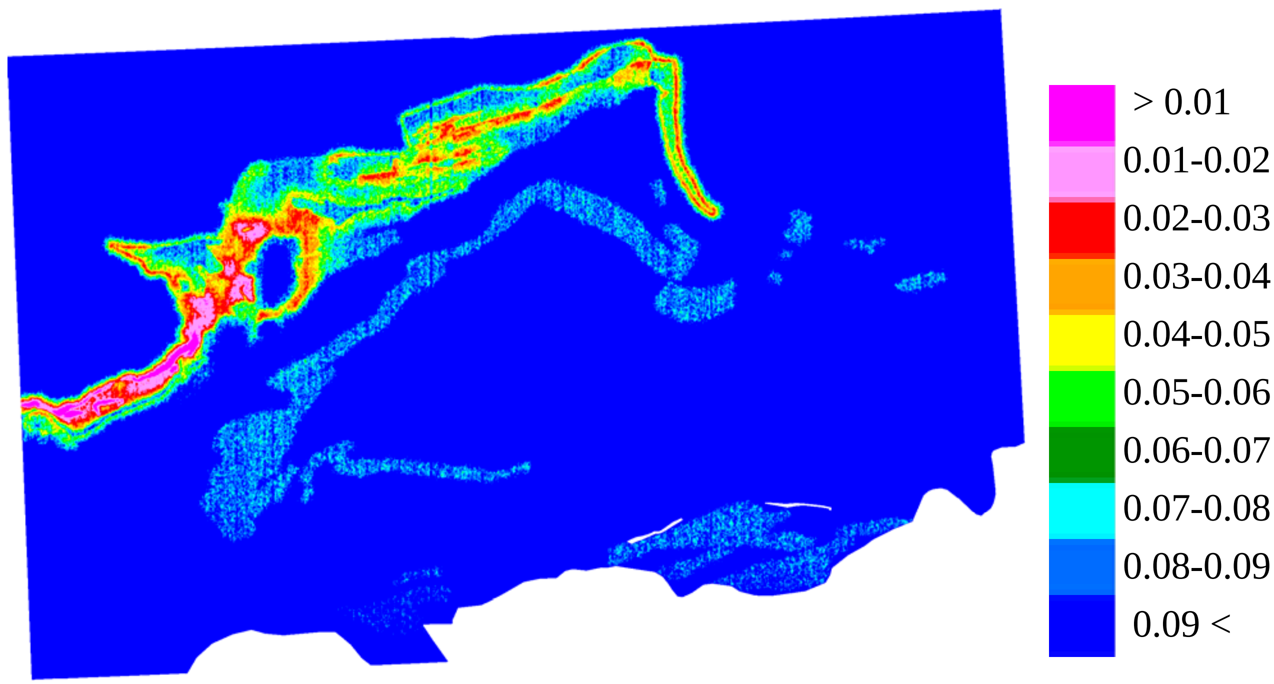

Figure 25: Uncertainty map for the VMS potential map shown in Figure 24 using 100 simulation experiments based on the column "Likelihood of correct identification" in Table 5

Figure 25, i.e. those with ranges > 0.01 (1%), 0.01-0.02 (1-2%), 0.02-0.03 (2-3%) , we obtain a map that shows only the areas of highest certainty of the highest potential (Figure 26). This is our most robust assessment of the potential for the Whitehills lake area.

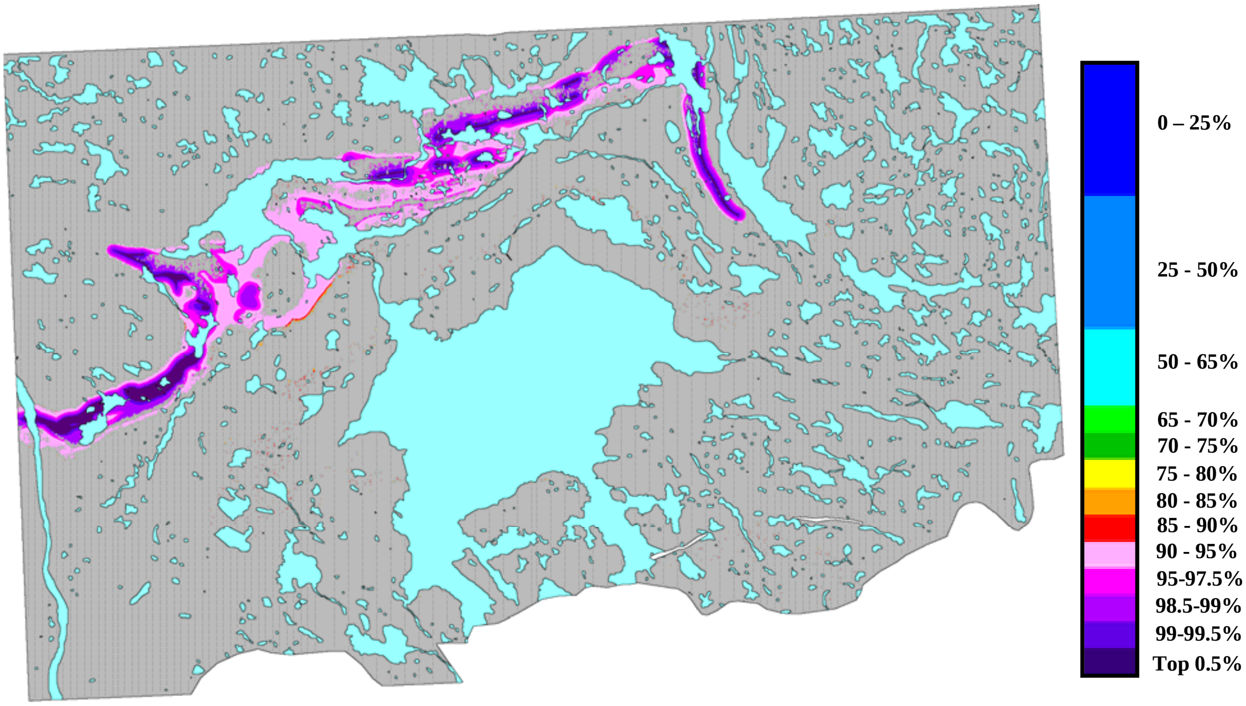

Figure 26: VMS potential map using the integration procedure in (section 5.3) based on the five weighted decay functions in Figure 16 for the five key criteria in the Whitehills Lake area, Nunavut, Canada. The pixels with the top three classes "> 0.01", "0.01-0.02", "0.02-0.03" in Figure 25 are shown in colors, the remaining pixels are coloured as grey representing "High uncertainty area" and therefore they are considered less reliable and not-predictable areas in the potential map.

In comparison with the geological map (Figure 23) , it is evident that the best potential for discovery of VMS deposits is confined to a relatively narrow set of areas that correspond to the uppermost part of the geological sequence in that area. Recent discoveries by Aura Silver Resources Ltd are all in that zone indicating that the methodology that we applied has promise as a tool for selection of high-priority targets for exploration and development (http://www.aurasilver.com/s/NewsReleases.asp).

7.0 Assessment of VMS potential of Slave Province: using the recent Stubley compilation

As a final test of the methodology that we have developed to establish a more quantitative approach to assessing resource potential, we undertook to assess the entire Slave Province, using a recent compilation by Mike Stubley (Stubley 2005). The Slave Province consists of an assemblage of Archean volcano-sedimentary and granitic terrains (Figure 27), many of which contain volcanogenic massive sulfide deposits.

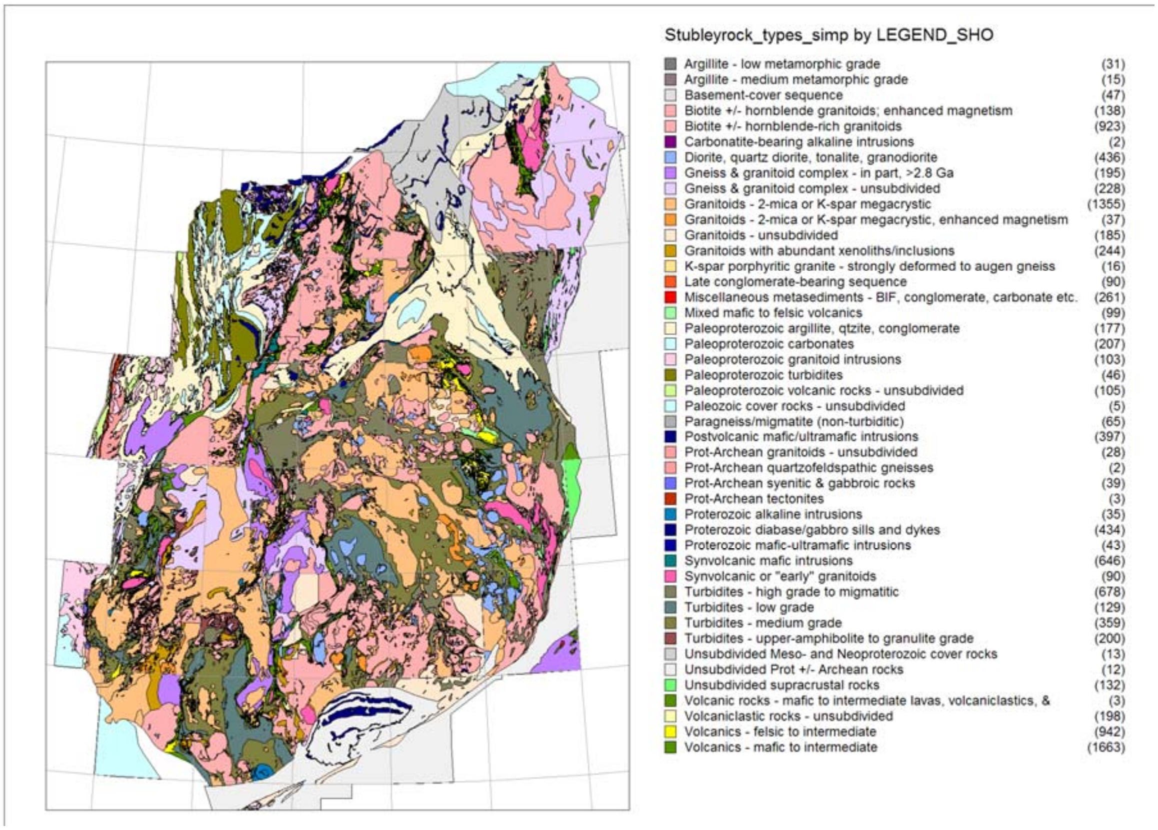

Figure 27: Geology of Slave Province, after Stubley, 2005. Legend taken from codes provided in the digital data set.

The legend for this new digital compilation was translated into the criteria for which we are searching (Table 1). The primary data included most of the information that we required, but it was in some cases, buried in a text line. The steps that were used are:

1) To the list of rock types assigned to the polygons in original Stubley map, (UNIT_CODE, EON, ROCK_CLASS, ROCK_SUBCL, Rx_simp, Ind Mins, POLYGON_DE, LEGEND, LEGEND_SHO, RECNO) 3 columns were added ("Rx_simp", "Rx_syn_volc", and "Ind Mins/metam_grade").

Added temporary columns for shorter "Eon" and "Polygon_De" terms to concatenate into ("Rx_simp"); to do this, a second table, with the shorter names and their longer equivalents, was created and the new shorter names created in a new Mapinfo® table.

2) Searched for any mention of "synvolcanic" and noted it in the new column "Rx_syn_volc".
3) Copied some metamorphic or indicator mineral info into "Ind Mins/metam_grade
4) Deleted extra columns used to form “Stubley_simpler.csv”.
5) Finalized this by simplifying the map to only 19 units (13 Archean and 6 Proterozoic or undefined). This simplified legend is used to assign a "raster val" value in the legend (1 to 19), that is then assigned to each pixel in the raster map supplied to the program that was developed to undertake the evaluation procedure.

The procedure to convert the information from the original map to something that may be used for assessment purposes is lengthy and, in future, hopefully unnecessary.

Following the procedures used in Section 5 (above) a series of maps were prepared, using the same protocols as for the Hackett River and Whitehills assessments, thus providing an opportunity to test the method and see if the results are comparable. Although the Hackett River map was used in part as a base for the Stubley compilation, the latter brought all of the existing maps in Slave Province to a common, simplified base. The compilation map is the result of the author’s best judgement to represent all of the litho-stratigraphic units in the Slave province on a common basis.

The first map (Figure 28) is a basic assessment of the potential for discovery of VMS deposits using the basic criteria described in Table 1. This only measures the distance to the key criteria and uses the decay curves to modify the value of these criteria. The uncertainties assigned to each criterion are not used for this map.

The second map (Figure 29) uses the same methodology as the first, but is an enlargement of the Hackett River map area. Note that for this map we used the same approach as was used in developing the methodology, except that the map is derived (without modification) from the Stubley compilation.

Figures 30 and 31 are a more robust determination of VMS potential (same regions as for Figures 28 and 29), using the uncertainty values that we assigned to each of the criteria (see section 5.7 for an explanation of the methodology used to obtain this map). This provides a measure of the certainty of the identification of areas of high potential, and lowers the estimation of certainty for those areas identified using criteria for which we have less confidence, either in their identification, (i.e. they may have been assigned incorrectly to a particular criterion) or for those criteria in which we have less confidence as to their significance relative to the presence of potential deposits.

Figures 32 and 33 are derived from 30 and 31 and scale the estimated potential value as a percentage of the total area assessed. It is evident on these maps that they predict the presence of the known deposits (shown as circles) very well.

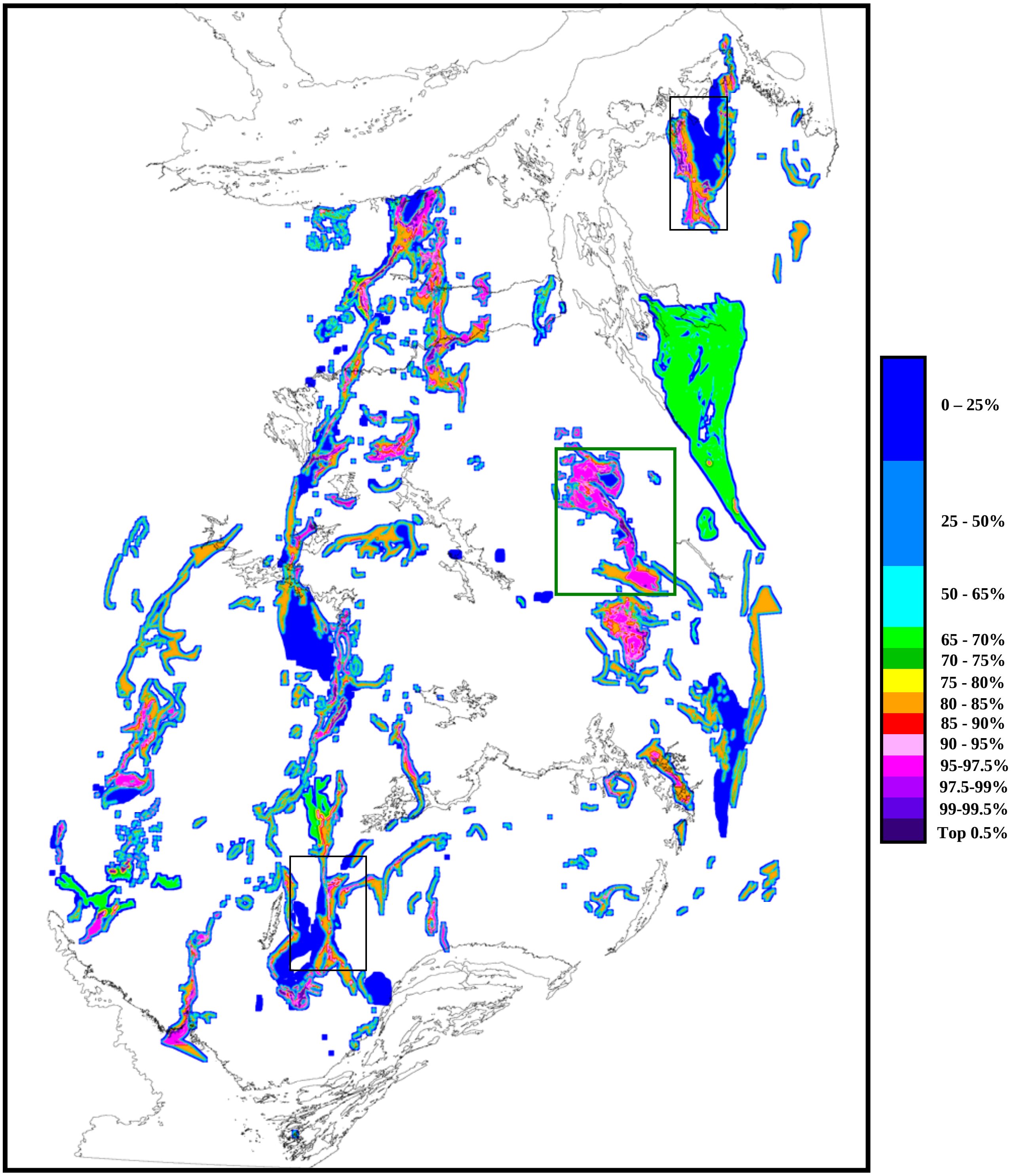

Figure 28. VMS potential map in Slave Province. The prediction was based on four key criteria for VMS deposits proposed in Table 1. Green rectangle area is the outline of Hackett River area and the enlargement of Hackett River area is shown in Figure 29.

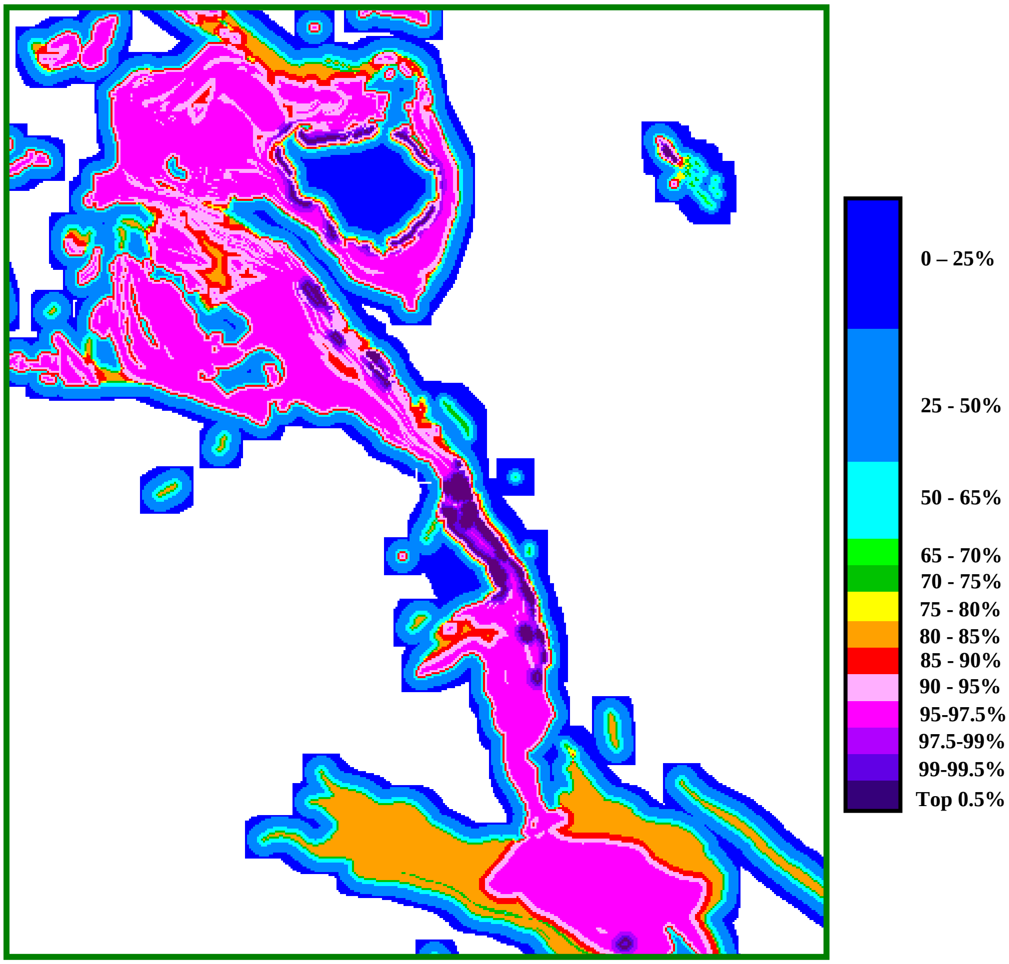

Figure 29. Basic assessment of VMS potential map in Hackett River area – enlargement of the area from VMS potential map in Slave in Figure 28.

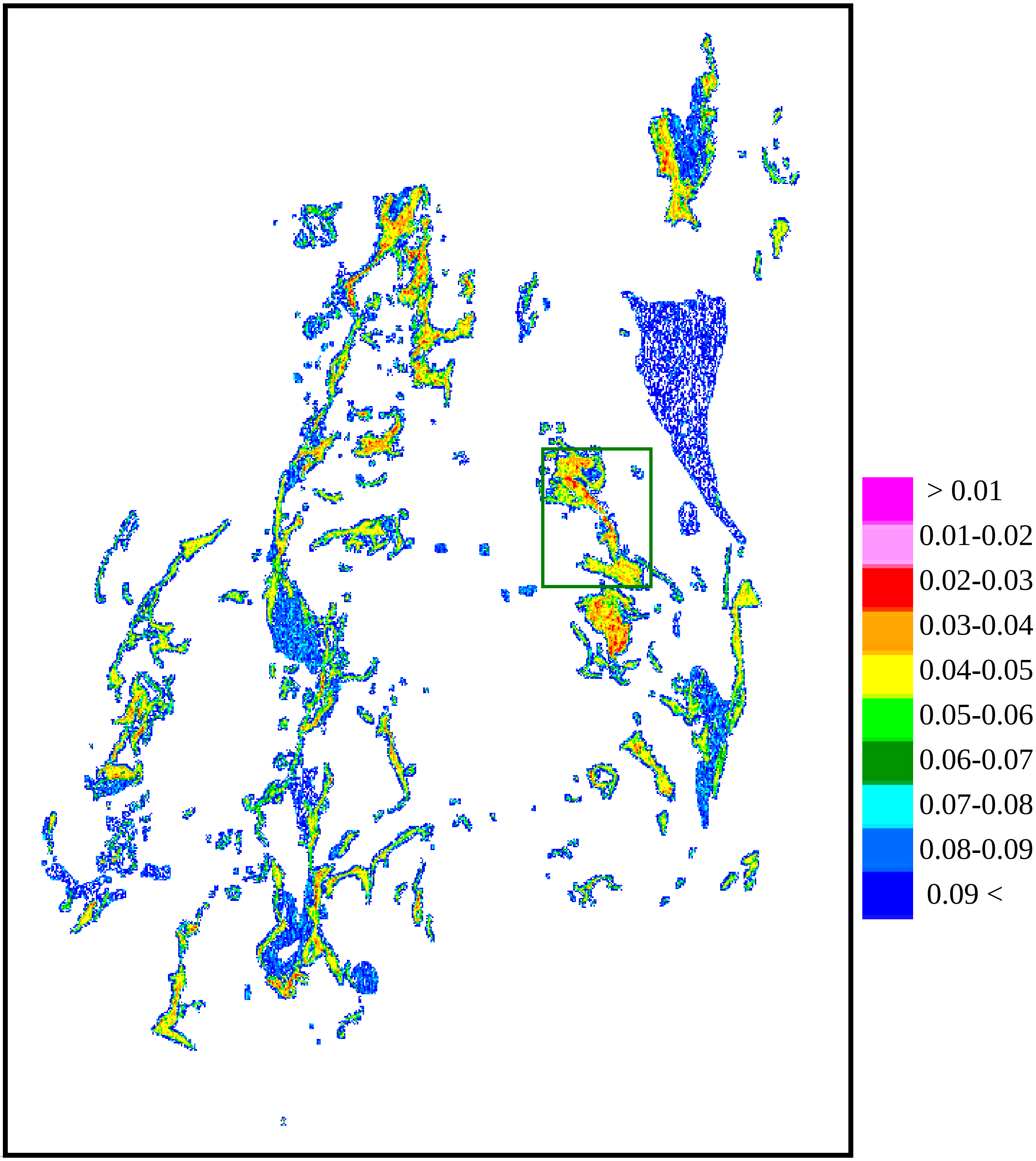

Figure 30. Uncertainty map for VMS potential map in Slave Provinces using the geological map compiled by Stubley (2005). The prediction was based on four key criteria for VMS deposits from Table 1. “Uncertainty” was estimated by 100 simulation experiments using “likelihood of correct identification.” Green rectangle area is the outline of Hackett River area and the enlargement of Hackett River area is shown in Figure 31.

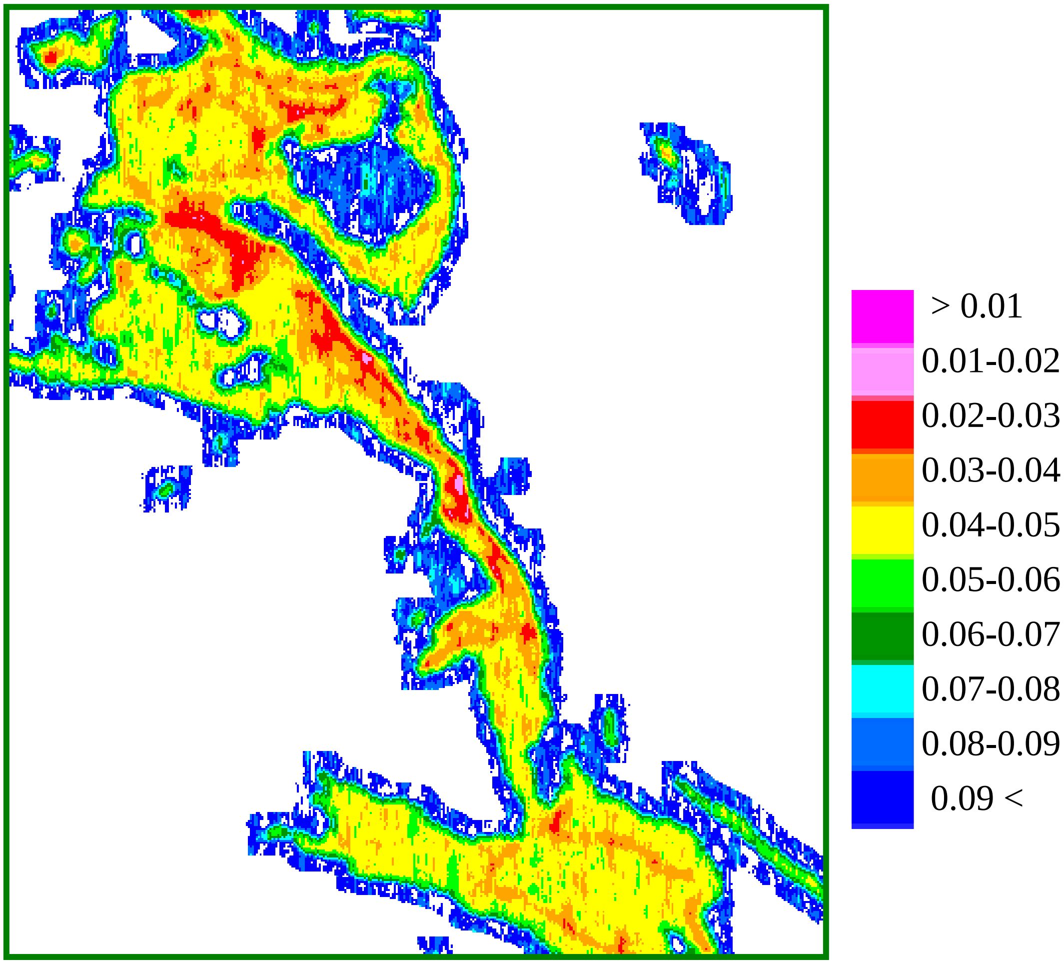

Figure 31. Uncertainty map in Hackett River area – enlargement of the area from uncertainty map of Slave Province in Figure 30.

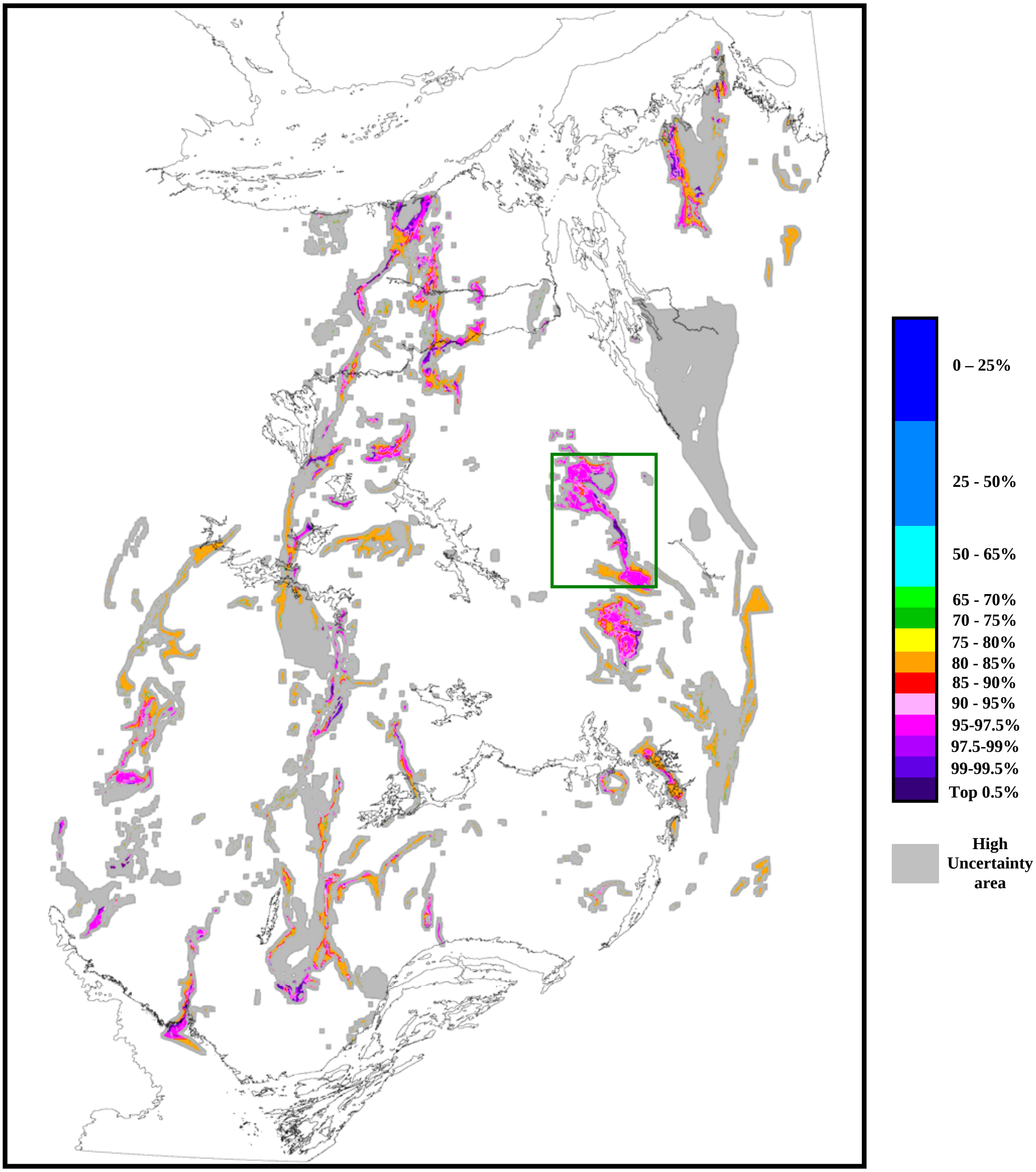

Figure 32: Uncertainty map for VMS potential map in Slave Provinces using the geological map compiled by Stubley (2005). The prediction was based on the four key criteria for VMS deposits in Table 1. "Uncertainty" was estimated by 100 simulation experiments using the "likelihood of correct identification" method described in Section 5.7. Green rectangle is the outline of Hackett River area. The enlargement of Hackett River area is shown in Figure 33.

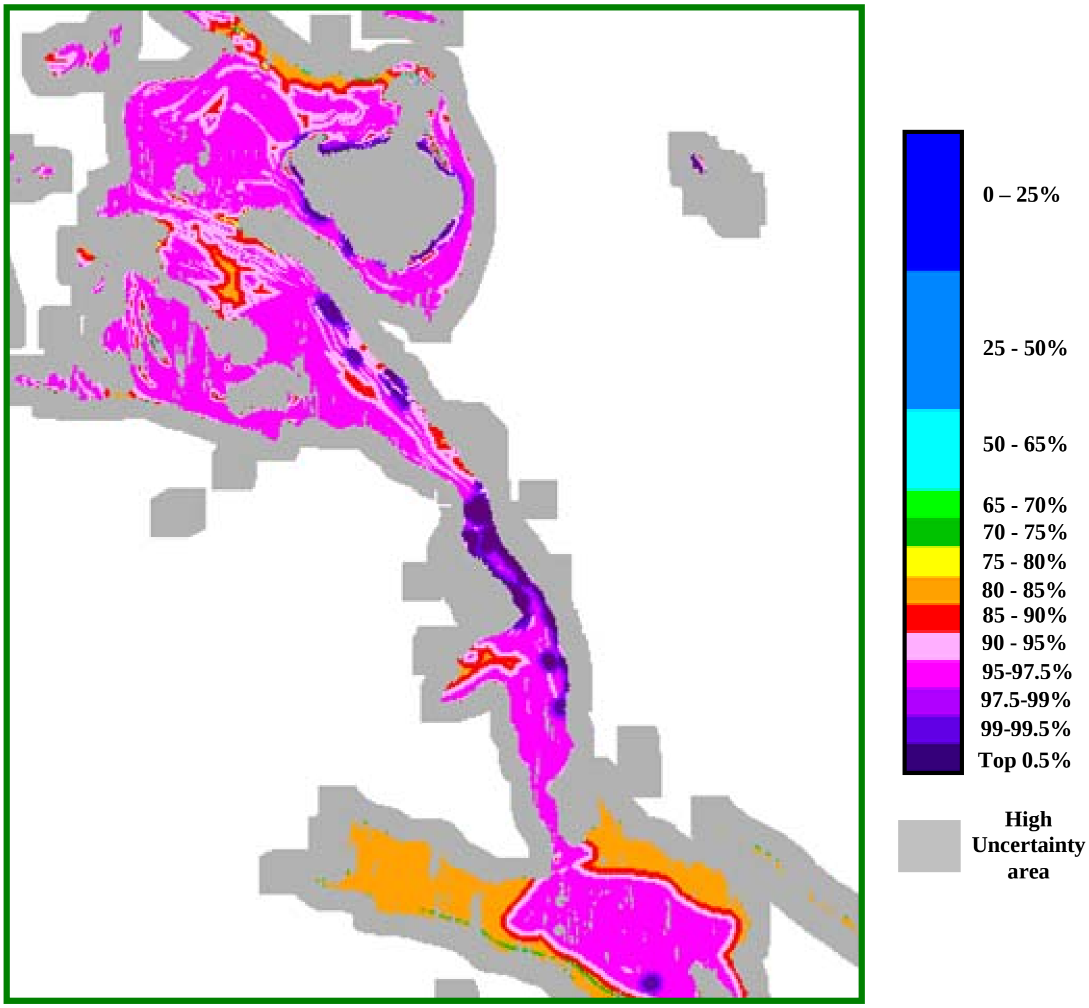

Figure 33. Combination map in Hackett River area – enlargement of the area from uncertainty map of Slave Province in Figure 32. This is based on the geology from Stubley (2005) map.

This map may be compared to Figure 18 in section 5.7 (reproduced below as Figure 34). The areas of highest potential show excellent correspondence with the assessment in Figure 18, which was based on the Frith (1987) map. Note that these assessments are not entirely independent of each other, as Stubley based his compilation map on Frith's (1987) map as well as other information.

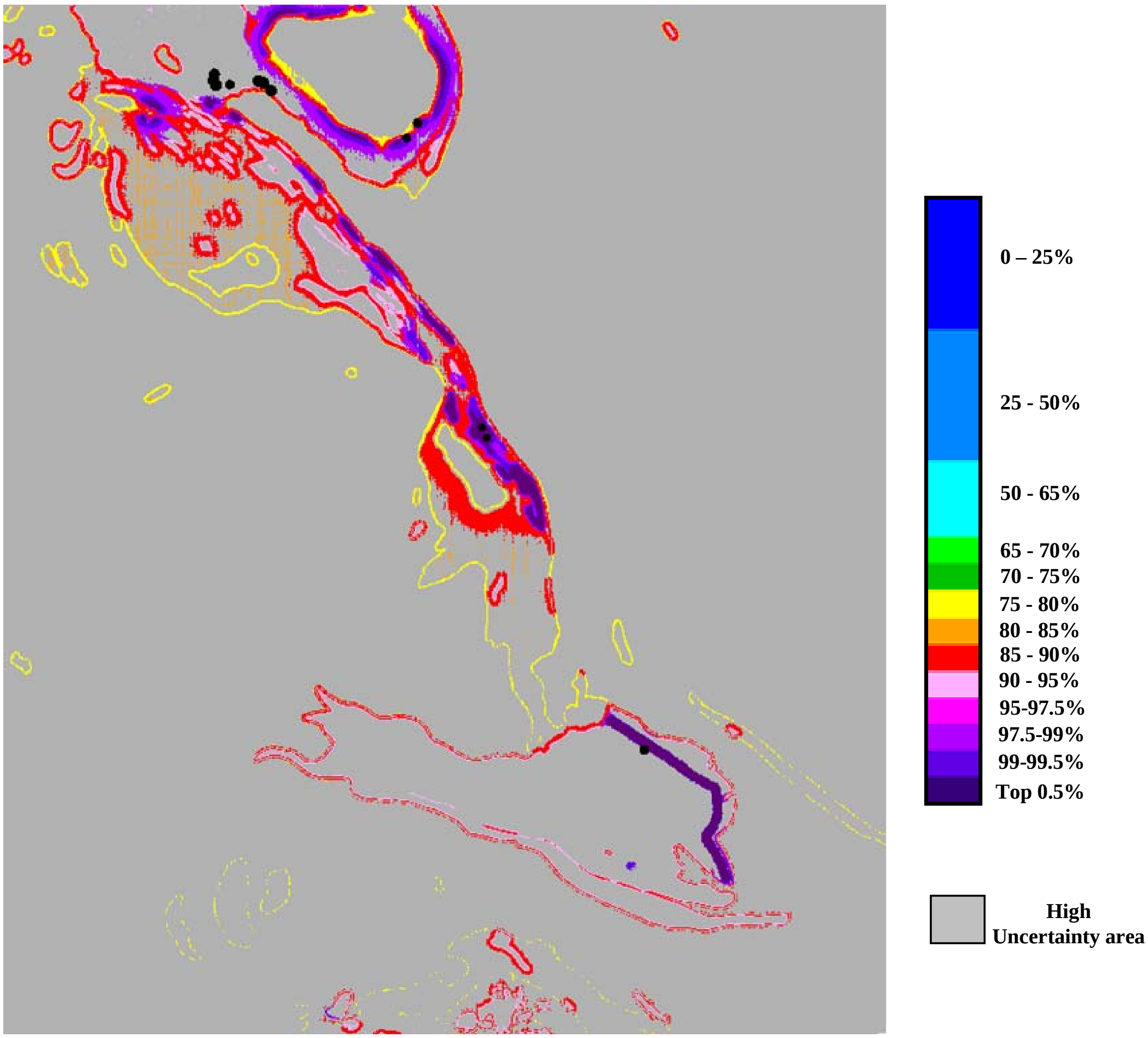

Figure 34 (same as Figure 18). VMS potential map using the VMS integration procedure in described in section 5.7 based on the five weighted decay functions for the five key criteria in Hackett River area, NWT, Canada. 12 known VMS deposits are plotted as black dots. This map is based on the geology in the Frith (1987) report and map.

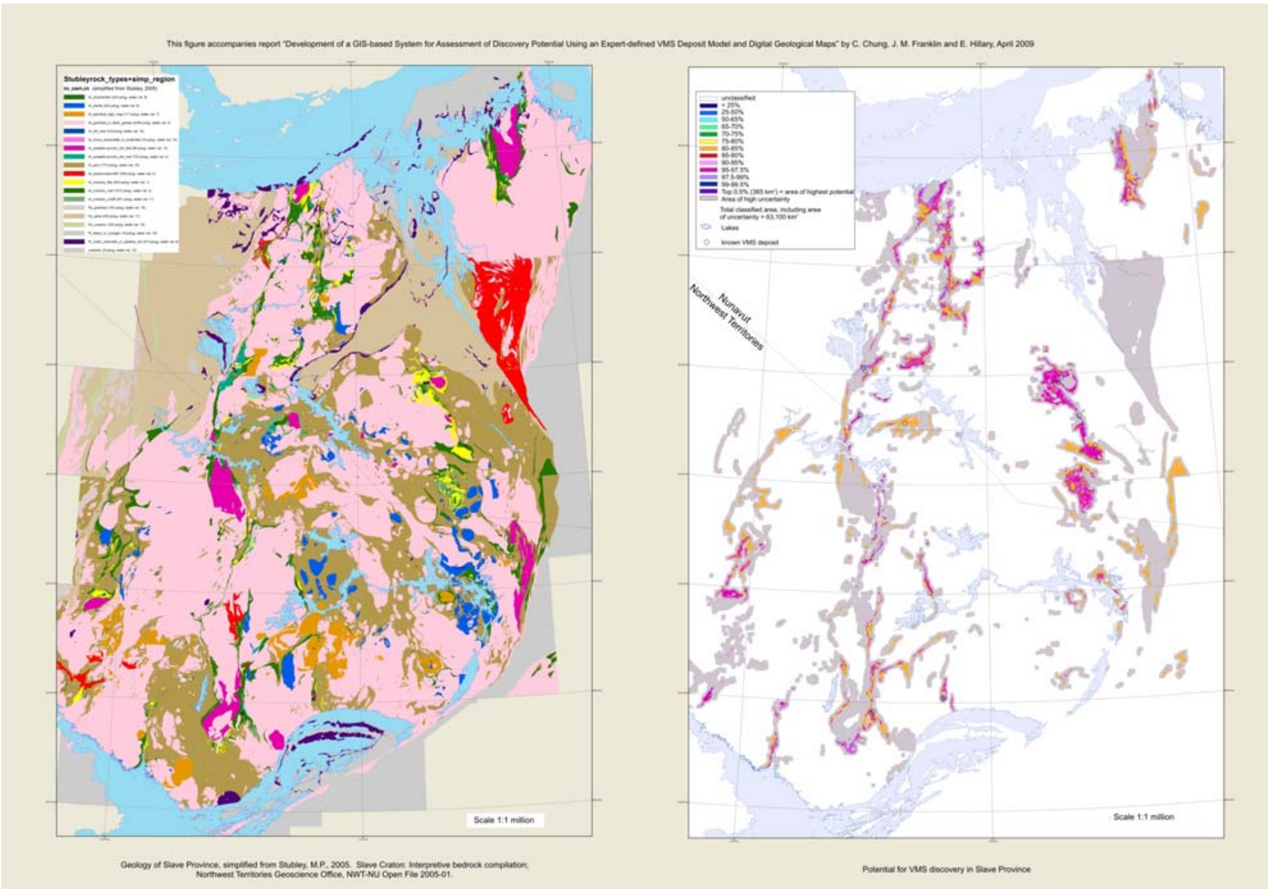

Figure 35. Summary map of the VMS potential for Slave Province (right), based on the geology map of Stubley (2005) (left). Parts of these maps are reproduced in Figure 36.

Finally, we examined the distribution of deposits in the finalized assessment map for Slave Province (Figures 35 and 36).

Virtually all of the deposits occur in the top 5% of the areas of highest potential, and many are within the top 0.5% of the high potential areas. The overall area of Slave Province is approximately 340,000km^2. The total area of the greenstone belts within that area is about 24% (82,000 km^2) of the overall area. Of that, 63,100 km^2 is estimated to have some VMS potential (about 18% of Slave Province), but that includes areas where the geological information is highly uncertain (grey in the summary figure). About 3,650km^2 has excellent potential (top 5% of areas of highest potential, which contain most of the know occurrences). This amounts to about 4% of the total greenstone belt area in the Province. Using the statistical methodology developed herein, those areas with the highest potential for the discovery of VMS deposits has been determined. These are the areas that should now be assessed for the quality of information pertaining to them, as part of the process in establishing prioritized for mapping over the next decade.

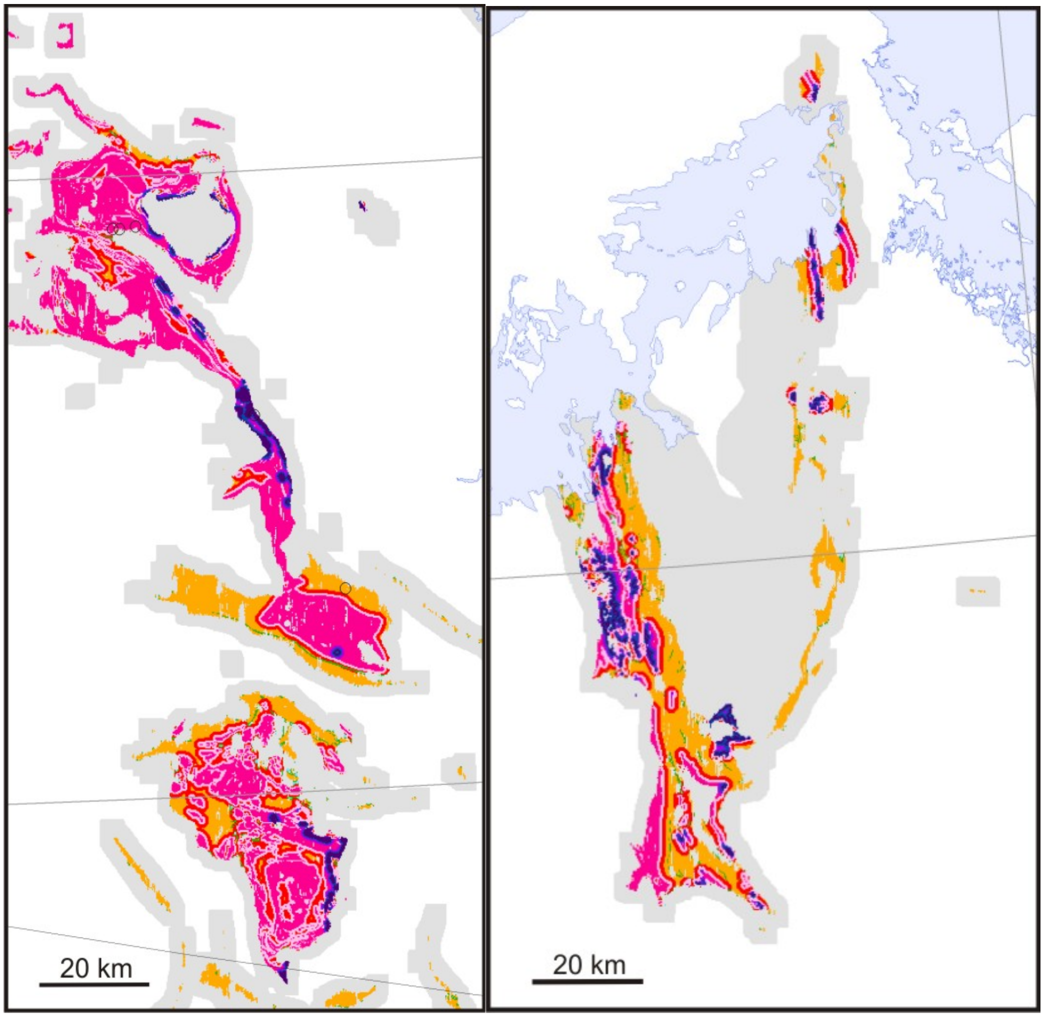

Figure 36. Close-up of Hackett River belt (left) and Hope Bay belt (right) from Figure 35.

8.0 Summary, Recommendations and Next Steps

1: The methodology developed for this report has successfully identified areas of highest potential for discovery of VMS deposits. It was applied without including the knowledge of the location of these deposits, and successfully "found" the majority of them. From any point on a map sheet (pixel in digital terms) we measured the distance to the nearest observation of each of the key criteria. The value of each criterion (which was already modified by our uncertainty as to the quality of it, both for its genetic criticality and "correctness" of map identification) is reduced (decayed) as a non-linear function of the distance from that observation. The reduced values of these key criteria are then summed at each point on the map, and after evaluation of all of the pixels, the values are contoured.

2: The digital geological maps that we used for this method development required some preparation. Specifically, the legends had to be parsed to identify the principal rock types. In the case of the Hackett River map, the oldest compilation that we used (Frith, 1987) all of the geological attributes were identified in the legend except for subvolcanic intrusions; these were assigned on the basis of form, stratigraphic position and composition. Newer maps (Whitehills, Slave compilation) contained information in the descriptive fields that enabled us to assign rock types quite reliably. However, these assignments still required some interaction by the user, as some of the most significant information (e.g. qualifiers for intrusions, identifiers for exhalite) was contained with text-field descriptions, and had to be manually extracted. The less data manipulation required, the more objective the assessment.

> **Recommendation 1:** All future digital map products have a legend that separates information on age, primary lithology, and secondary attributes such as volcanological style, alteration or significant stratigraphic information (e.g. submarine volcanic, pyroclastic volcanic, subaerial volcanic or sedimentary, subvolcanic intrusive, syntectonic intrusive etc.) placed in separate columns. This will reduce the required amount of interpretation and map preparation required prior to using any form of digital resource assessment technology. Also, linear elements in the geology (e.g. faults, with sense of motion of possible, thin bands of exhalite, dykes) need also to be included in the same data set. Currently these are commonly separated into separate files, adding steps to the process used to prepare the data for "pixel" rendering. The unified hierarchical legend system being developed within the GSC will meet these requirements.

3: The list of key criteria that we used are based on expert knowledge of the specific deposit type, both from genetic and exploration aspects. In preparing this list, we recognized that some criteria have a more uncertain relationship to the genesis of this deposit type than do others, and that also that some criteria may not have a direct relationship to the deposit genesis, but are a manifestation of key genetic attributes that otherwise would not be evident on a map. For example, exhalite that is generally related to VMS deposits would rarely be specifically identified on a geological map. However, key lithotypes, such as chert, sulfidic sedimentary rocks, or banded iron formation are commonly displayed on maps. The certainty of assigning these to the potential presence of deposits is significant, so we use a higher measure of uncertainty when including their presence as par of our evaluation methodology. Also, in the case of exhalite, deposits need not occur specifically where they are observed, but generally are within a few hundred meters of them, so we established a "decay function" that reduced the value of this observation as a function of the distance from it to our observation point. In one case, major underpinning subvolcanic intrusions, the best potential for VMS deposits is at least 500m, and as much as 4 km away from them In this case, we established a non-linear decay function that reflects that the best potential is in an 'envelope" that does not coincide with the intrusion. We found that determining the best weighting factors and decay functions for each criterion was best done iteratively using a well-understood test area. However, those weighting and decay factors determined by the expert group generally were close to those used in the final evaluation method.

> **Recommendation 2**: Key criteria used for this evaluation must be evident on a geological map that will be used for evaluation purposes. The uncertainties assigned to the value of each criterion are best established by experts in the genetic attributes and exploration for this deposit type. We recommend that the best set of criteria should be established by experts in the field, and adjusted through a testing procedure.

> **Recommendation 3:** The "decay function" or way in which the presence of a criterion is decayed as a function of distance to the observation of it, was established first on an expert basis, and refined through use of a test case (with known deposits) to establish the best factors to use. We recommend that for each deposit type, one or two test areas, which contain well established deposits and most of the key criteria that will be used for evaluation, be used to develop the best set of uncertainty and decay factors.

4: Our list of key criteria included some attributes that we did not use. Some of these, such as alteration attributes, are not uniformly noted on maps, and thus we avoided using them. These also include geophysical attributes, and lithogeochemical data. Both of these require that the data be prepare in a way in which they can be assessed using our technology. In order to do that, these data sets need to be compiled and tested in the same manor as were the geological maps.

> **Recommendation 4:** In future we recommend that digital geological data sets being used for resource potential assessment include geophysical compilations and petrochemical data sets. The latter are available for many of the Provinces, but are not available in Yukon, NWT or Nunavut.

Next steps:

1: Continue to refine the methodology for assessing the potential for discovery of VMS deposits. Include additional criteria, and develop methods for integrating them into the methodology develop herein.

2: Build criteria lists and digital technology to assess the potential for discovery of other deposit types. Our priority order for assessing the Canadian Shield, is:

A: Orogenic and other gold deposit types

B: Magmatic Cu-Ni-PGE-Cr deposits
C: All types of uranium deposits
D: Sedex deposits
E: Iron oxide-copper-gold deposits:
F: Silver vein deposits

Some deposit types are much more abundant in Phanerozoic orogens and cratonic covered areas. In order to apply the methodology to areas that are more typically outside of the Canadian Shield, the discovery potential for the following deposit types need to be assessed:

A: Copper ± molybdenum ± gold porphyry systems
B: Skarn deposits
C: Low- and high-sulfidation epithermal deposits
D: Mississippi-Valley Pb-Zn deposits
E: Granite-hosted tin deposits

3: Make the software developed for this assessment process more user-friendly.

References

Davenport, P., Boisvert, E., Quat, M., Okulitch, A., Brodaric, B., Colman-Sadd, S., Nolan, L., Struik, B., MacIntyre, D., Tzeng, P., Scott, D., Gilbert, C., Abbott, G., Andrea B., Journeay, M., Francis, J., and Houlahan, T., 2002. A Scalable, Digital Map Database of Bedrock Geology for Canada: A Progress Report. Digital Mapping Techniques '02 -- Workshop Proceedings, 2002, 33 p.

Eckstrand, O. R., Sinclair, W. D., and Thorpe, R. I., 1995. Geology of Canadian Mineral Deposit Types, *in* Decade of North American Geology, P -1: Ottawa, Geological Survey of Canada Series no. 8, 640 p.

Franklin, J. M., Gibson, H. G., Galley, A. G., and Jonasson, I. R., 2005. Volcanogenic Massive Sulfide Deposits, *in* Hedenquist, J. W., Thompson, J. F. H., Goldfarb, R. J., and Richards, J. P., eds., Economic Geology, 100th Anniversary Volume, Society of Economic Geologists, p. 523-560.

Franklin, J. M., Sangster, D. M., and Lydon, J. W., 1981. Volcanic-associated massive sulfide deposits, *in* Skinner Brian, J., ed., Economic geology; Seventy-fifth anniversary volume; 1905-1980, Society of Economic Geologists, p. 485-627.

Frith, R. A., 1987. Precambrian geology of the Hackett River area, District of MacKenzie, N.W.T., Geological Survey of Canada Memoir 417.

Goodfellow, W., D., 2007. Mineral deposits of Canada: A synthesis of major deposit types, district metallogeny, and evolution of geological provinces and exploration methods, Geological Association of Canada, 1061p. plus CD.

Hannington, M.D., de Ronde, C.E.J.; Petersen, S. 2005. Sea-floor tectonics and submarine hydrothermal systems. *in* Hedenquist, J.W.; Thompson, J.F.H.; Goldfarb, R.J.; Richards, J.P. eds., Economic Geology : One Hundredth Anniversary Volume : 1905 - 2005. Society of Economic Geologists, p. 111-141.

Hedenquist, J. W., Thompson, J. F. H., Goldfarb, R. J., and Richards, J., 2005. One Hundredth Anniversary Volume, Economic Geology, Society of Economic Geologists, 1136 p. plus CD.

Leech, G. B., 2007. Operation September 1972: http://gsc.nrcan.gc.ca/hist/friends_e.php HSCHIS-A009.pdf, Geological Survey of Canada, 17p.

Lydon, J. W., 1984. Volcanogenic massive sulphide deposits Part 1: A descriptive model: Geoscience Canada, v. 11, p. 195-202.

McKelvey, V. E., 1972. Mineral Resource Estimates and Public Policy: American Scientist, v. 60, p. 32-40.

Sangster, D. F., 2007. Notes on Operation September: http://gsc.nrcan.gc.ca/hist/friends_e.php http://gsc.nrcan.gc.ca/hist/friends_e.php Ottawa, Geological Survey of Canada, p. 10.

Sangster, D. F., and Scott, S. D., 1976. Precambrian stratabound massive Cu-Zn-Pb sulfide ores of North America, *in* Wolf, K. H., ed., Handbook of strata-bound and stratiform ore deposits, Elsevier, p. 129-222.

Seyfried, W. E. B. M. E., and Seewald, J. S., 1988. Hydrothermal alteration processes at mid-ocean ridges: constraints from diabase alteration experiments, hot-spring fluids and composition of the oceanic crust: *in:* Martin, R. F. ed., Seafloor hydrothermal mineralization, Canadian Mineralogist, 26, p. 787-804.

Singer, D. A., and Kouda, R., 2003. Typing mineral deposits using their grades and tonnages in an artificial neural network, *in* Singer, Donald, A., and Kouda, R., eds., Special issue on Neural networks., Kluwer Academic/Plenum Publishers. New York.

Stubley, M.P., 2005. Slave Craton: Interpretive bedrock compilation; Northwest Territories Geoscience Office, NWT-NU Open File 2005-01. Digital files and 2 maps.

Vervoort, J. D., White, W. M., Thorpe, R. I., and Franklin, J. M., 1993. Postmagmatic thermal activity in the Abitibi greenstone belt, Noranda and Matagami districts; evidence from whole-rock Pb isotope data, *in* Spooner Edward, T. C., and Barrie, C. T., eds., A special issue devoted to Abitibi ore deposits in a modern context., . Economic Geology and the Bulletin of the Society of Economic Geologists: v. 88, no. 6, p. 1598-1614.

Zaleski, E., and Pehrsson, S., 2005. Geology, Halfway Hills and Whitehills Lake area, Nunavut, *in* Canada, Geological Survey of Canada, Open File Map Series 2069A, Digital Map.